

AREA  
TX  
GTHM  
Balcones

REGIONAL ASSESSMENT OF GEOTHERMAL  
POTENTIAL ALONG THE BALCONES  
AND LULING-MEXIA-TALCO FAULT ZONES,  
CENTRAL TEXAS

Final Report

by

C. M. Woodruff, Jr. and Mary W. McBride

Assisted by

Lisa E. Craig, James P. Immitt,  
Rebecca M. Russo, and David R. Wuerch

Consulting services by

O. T. Hayward, R. G. Font, M. S. Brigham, W. A. Charvat,  
R. V. Corwin, R. H. Hazelwood, R. M. Knapp,  
and C. S. McKnight of Waco, Texas

Prepared for

United States Department of Energy, Division of Geothermal Energy

Under Contract No. DE-AS05-78ET28375

(formerly ET-78-S-05-5864)

May 1979

Bureau of Economic Geology  
The University of Texas at Austin

W. L. Fisher, Director

**UNIVERSITY OF UTAH  
RESEARCH INSTITUTE  
EARTH SCIENCE LAB.**

## Table of Contents

Executive Summary . . . . .	1
Overview . . . . .	3
General . . . . .	3
Purpose and Scope . . . . .	6
Data Base . . . . .	8
Regional Physiography and Climate. . . . .	12
Regional Structural Geology. . . . .	14
Regional Stratigraphy. . . . .	23
Pre-Cretaceous Surface . . . . .	62
General . . . . .	62
Structural Configuration of the Pre-Cretaceous Surface . . . . .	63
Hosston and Trinity Sands Undifferentiated . . . . .	67
General . . . . .	67
Net-Sand Distribution of the Hosston/Trinity. . . . .	67
Structural Configuration of the Hosston/Trinity . . . . .	72
General Aquifer Properties of the Hosston/Trinity . . . . .	75
Water Level of the Hosston/Trinity . . . . .	76
Water Quality of the Hosston/Trinity . . . . .	78
Water Temperature of the Hosston/Trinity . . . . .	80
Geothermal Potential of the Hosston/Trinity . . . . .	84
Hensel Sand . . . . .	92
General . . . . .	92
Thickness of the Hensel . . . . .	92
Structural Configuration of the Hensel. . . . .	94
General Aquifer Properties of the Hensel . . . . .	94
Paluxy Sand . . . . .	98
General . . . . .	98
Net-Sand Distribution of the Paluxy. . . . .	98
Structural Configuration of the Paluxy. . . . .	101
General Aquifer Properties of the Paluxy . . . . .	103
Water Level of the Paluxy . . . . .	103
Water Quality and Water Temperature of the Paluxy. . . . .	105
Geothermal Potential of the Paluxy. . . . .	107
Edwards Limestone . . . . .	115
General . . . . .	115
Structural Configuration of the Edwards . . . . .	115
Thickness of the Edwards . . . . .	117
General Aquifer Properties of the Edwards . . . . .	118
Woodbine Sand . . . . .	124
General . . . . .	124
Net-Sand Distribution of the Woodbine. . . . .	124
Structural Configuration of the Woodbine . . . . .	127
General Aquifer Properties of the Woodbine . . . . .	129
Water Level of the Woodbine . . . . .	129
Water Quality of the Woodbine . . . . .	131
Water Temperature of the Woodbine . . . . .	133
Geothermal Potential of the Woodbine . . . . .	133
Conclusions . . . . .	142
References . . . . .	144
Appendix . . . . .	separate volume

## Figures

- Figure 1. Location of study region in Central Texas.
- Figure 2. Major facilities within study region.
- Figure 3. Counties included within geologic data base and hydrologic data base; also approximate limits of Paleozoic and Tertiary aquifers that yield warm water.
- Figure 4. Geologic data base—location of well-control and cross-section lines.
- Figure 5. Physiographic provinces of study region.
- Figure 6. Mean annual air temperature and January mean minimum temperature.
- Figure 7. Mean annual freeze period of study region.
- Figure 8. Regional structural elements.
- Figure 9. Regional tectonic features.
- Figure 10. Geothermal gradient of region.
- Figure 11. Schematic dip section showing facies and nomenclatural changes of selected Cretaceous units in Central Texas.
- Figure 12. Schematic strike section showing facies and nomenclatural changes of Cretaceous units from Central Texas to North-Central Texas.
- Figure 13. Map showing outcrop of warm-water-bearing Cretaceous strata with respect to Balcones and Luling-Mexia-Talco Fault Zones.
- Figure 14. Strike-oriented cross section A-A'.
- Figure 15. Strike-oriented cross section B-B'.
- Figure 16. Strike-oriented cross section C-C'.
- Figure 17. Strike-oriented cross section D-D'.
- Figure 18. Strike-oriented cross section E-E'.
- Figure 19. Strike-oriented cross section F-F'.
- Figure 20. Strike-oriented cross section G-G'.
- Figure 21. Strike-oriented cross section H-H'.
- Figure 22. Strike-oriented cross section I-I'.
- Figure 23. Strike-oriented cross section J-J'.

- Figure 24. Dip-oriented cross section 1-1'.
- Figure 25. Dip-oriented cross section 2-2'.
- Figure 26. Dip-oriented cross section 3-3'.
- Figure 27. Dip-oriented cross section 4-4'.
- Figure 28. Dip-oriented cross section 5-5'.
- Figure 29. Dip-oriented cross section 6-6'.
- Figure 30. Dip-oriented cross section 7-7'.
- Figure 31. Dip-oriented cross section 8-8'.
- Figure 32. Dip-oriented cross section 9-9'.
- Figure 33. Dip-oriented cross section 10-10'.
- Figure 34. Dip-oriented cross section 11-11'.
- Figure 35. Dip-oriented cross section 12-12'.
- Figure 36. Dip-oriented cross section 13-13'.
- Figure 37. Dip-oriented cross section 14-14'.
- Figure 38. Dip-oriented cross section 15-15'.
- Figure 39. Dip-oriented cross section 16-16'.
- Figure 40. Dip-oriented cross section 17-17'.
- Figure 41. Dip-oriented cross section 18-18'.
- Figure 42. Dip-oriented cross section 19-19'.
- Figure 43. Dip-oriented cross section 20-20'.
- Figure 44. Dip-oriented cross section 21-21'.
- Figure 45. Dip-oriented cross section 22-22'.
- Figure 46. Dip-oriented cross section 23-23'.
- Figure 47. Dip-oriented cross section 24-24'.
- Figure 48. Typical electric logs of geologic units in Travis and Dallas Counties.
- Figure 49. Structural map of pre-Cretaceous surface.
- Figure 50. Net sand thicknesses of the Hosston/Trinity.

- Figure 51. Schematic Hosston/Trinity paleogeographic map.
- Figure 52. Structural configuration of the Hosston/Trinity.
- Figure 53. Water level contours for the Hosston/Trinity aquifer.
- Figure 54. Total dissolved solids contours for Hosston/Trinity ground water.
- Figure 55. Piper diagram for Hosston ground water—McLennan County.
- Figure 56. Piper diagram for Hosston ground water—Travis County.
- Figure 57. Water temperature contours for Hosston/Trinity aquifer.
- Figure 58. Temperature/depth scattergram for Hosston ground water.
- Figure 59. Total dissolved solids/depth scattergram for Hosston ground water.
- Figure 60. Temperature/total dissolved solids scattergram for Hosston ground water.
- Figure 61. Municipalities using Hosston/Trinity ground water compared to areas of optimum geothermal potential.
- Figure 62. Isopach map of Hensel Sand.
- Figure 63. Structural configuration of Hensel Sand.
- Figure 64. Water temperature contours for Hensel Sand.
- Figure 65. Net-sand thicknesses of the Paluxy.
- Figure 66. Schematic Paluxy paleogeographic map.
- Figure 67. Structural configuration of the Paluxy.
- Figure 68. Water level contours for the Paluxy.
- Figure 69. Total dissolved solids contours for Paluxy ground water.
- Figure 70. Water temperature contours for the Paluxy.
- Figure 71. Temperature/depth scattergram for the Paluxy.
- Figure 72. Total dissolved solids/depth scattergram for the Paluxy.
- Figure 73. Temperature/total dissolved solids scattergram for the Paluxy.
- Figure 74. Municipalities using Paluxy ground water compared to areas of optimum geothermal potential.
- Figure 75. Structural configuration of Edwards Limestone.
- Figure 76. Isopach map of Edwards Limestone.

- Figure 77. Water level contours for the Edwards.
- Figure 78. Water temperature contours for the Edwards.
- Figure 79. Total dissolved solids contours for the Edwards ("bad-water zone").
- Figure 80. Net-sand thicknesses of the Woodbine.
- Figure 81. Schematic Woodbine paleogeographic map.
- Figure 82. Structural configuration of the Woodbine.
- Figure 83. Water level contours for the Woodbine.
- Figure 84. Total dissolved solids contours for Woodbine ground water.
- Figure 85. Total dissolved solids/depth scattergram for the Woodbine.
- Figure 86. Temperature/total dissolved solids scattergram for the Woodbine.
- Figure 87. Water temperature contours for the Woodbine.
- Figure 88. Temperature/depth scattergram for the Woodbine.
- Figure 89. Municipalities using Woodbine ground water compared to areas of optimum geothermal potential.
- Figure A-1. State well numbering convention (see appendix).

#### Tables

- Table 1. Municipal water use--Hosston/Trinity aquifer.
- Table 2. Municipal water use--Paluxy aquifer.
- Table 3. Municipal water use--Woodbine aquifer.

## EXECUTIVE SUMMARY

The Balcones and Luling-Mexia-Talco Fault Zones delineate a belt that stretches across the central part of Texas from the Rio Grande to the Red River. The fault zones are denoted by broken and displaced strata, and juxtaposition of diverse bedrock types has had a marked effect on natural resources both at the earth's surface and below ground. There have also been demographic responses to the abrupt changes in natural features; many of the major Texas cities, including Austin, Dallas, Fort Worth, San Antonio, and Waco, occur along this trend.

Several Cretaceous aquifers along this belt provide ground water for municipal, industrial, and domestic users; in general, the waters obtained from these aquifers have low temperatures and low concentrations of dissolved solids. However, in some areas the only available water supply occurs in the deepest, downdip parts of the aquifer, and there, water temperature values are anomalously high--locally as much as 60 ° C (140 ° F). For many years these warm and locally mineralized waters have supplied municipal and domestic needs, but the heat content was considered a nuisance or an oddity. Warm waters have supplied a few health spas and swimming pools, but in general, the heat content of these waters has been wasted.

This report presents a region-wide inventory and assessment of aquifers known to yield warm water (greater than 90° F; 32 ° C). We have conducted this study to ascertain the potential for obtaining geothermal energy for space heating and water heating needs. The aquifers investigated include the Hosston/Trinity Sands, the Hensel Sand, the Paluxy Sand, the Edwards Limestone, and the Woodbine Sand. We have examined each aquifer in terms of its stratigraphic and structural framework and its hydrogeological properties.

Of the aquifers studied, three possess the greatest potential as sources of geothermal energy. They are the Hosston/Trinity, the Paluxy, and the Woodbine. All three provide local municipalities with potable water having elevated temperature. The Edwards and the Hensel, on the other hand, have either adverse water quality, low sustainable yields, or insufficient caloric content.

The Hosston/Trinity aquifer has the greatest geothermal potential of the aquifers studied. That is, the Hosston/Trinity (1) covers the largest area, (2) provides more towns across that area with water, (3) is the deepest (hence, hottest) of the aquifers studied, and (4) has generally moderate dissolved solids content through the area in which it is currently tapped. Our data on well yields are insufficient to project

aquifer capabilities for future ground-water withdrawals, but previous workers (Klemt and others, 1975, p. 55) have indicated a potential for future increased pumpage from the downdip parts of the Hosston Sand in Central Texas.

The Woodbine and Paluxy Sands have a moderate geothermal potential in North-Central and northeast Texas, but both aquifer systems have a smaller geographic extent compared with the Hosston/Trinity; also ground water from the Woodbine and Paluxy generally has lower temperatures and higher concentrations of dissolved solids.

If the water obtained from the deep, geothermal parts of the aquifers does not have to be potable, (that is, if it does not have to serve multiple needs), the geothermal resource base will be expanded. Thus, the potential resource will include hot brines that are known to occur in parts of the Edwards Limestone and high-salinity waters that occur within the deeper parts of the various sand aquifers. In fact, current projects to obtain heat from ground water from the Hosston (in Falls County) and the Woodbine (in Navarro County) have selected the parts of the aquifers in which water quality precludes the use of these aquifers as a potable water supply. Geologic conditions in deep parts of the Hosston/Trinity, the Paluxy, and the Woodbine seem favorable for large amounts of hot (but probably saline) waters. These are the deep deltaic deposits that occur in Bowie, Red River, Lamar, Delta, Hopkins, Franklin, and Titus Counties in northeast Texas, but since these deep sands have not been tapped as aquifers, their hydrologic properties are conjectural.

Probably the greatest known geothermal potential along the Balcones and Luling-Mexia-Talco Fault Zones occurs in those areas where warm waters are now being extracted and consumed without regard for the heat value. The rate of pumpage and the difference between prevailing winter air temperature and the ground-water temperature show the magnitude of this resource that is being wasted. Taylor, Texas, for example, pumps enough water at 116° F (47° C) that during winter months approximately  $2.07 \times 10^{10}$  Btu ( $5.2 \times 10^9$  kg-cal.) is wasted. Part of this heat can probably be extracted economically, because those Btu's dissipated during an average January have a value of as much as \$52,000. The retrieval of this heat would entail designation of a recipient, modification of water distribution, and the installation of a heat exchange device. The geologic resource exists, therefore, but its utilization is an engineering and economic problem.



## OVERVIEW

### General

For more than 80 years, warm waters with temperatures of up to 60° C (140° F) have been produced from several aquifers located along a belt that bisects Texas from the Rio Grande to the Red River. This trend, which is broadly delimited by the Balcones Fault Zone on the west and the Luling-Mexia-Talco Fault Zones on the east (fig. 1), constitutes a low-grade geothermal resource. Waters from aquifers in this region have long supplied municipal and domestic needs, but except at local spas and health resorts, the heat content of these waters has been considered a nuisance and thus wasted. Today, however, because of increased costs of fossil fuels, low-grade energy sources are attracting new attention. The waters produced along this belt provide a potential supply for hot water and space-heating needs, and projects are currently underway to tap this heat source for the Torbett-Hutchings-Smith Memorial Hospital at Marlin and the Navarro Junior College at Corsicana.

Although the heat content of these waters is low, the warm-water-bearing aquifers constitute an appealing potential resource because of the convergence of social and geologic attributes within the region. The belt from which the warm waters are obtained is one of the most heavily populated and intensively used regions in Texas. Total population of the region is more than 5 million with a maximum population density in Dallas County of 1,616 people/mi<sup>2</sup> (624 people/km<sup>2</sup>). There are six Standard Metropolitan Statistical Areas and numerous large industrial, military, educational, and institutional facilities that might efficiently use this "alternative energy source" (fig. 2). Perhaps more important than the sheer number and size of potential users of this resource is the aforementioned fact that many communities already tap the warm waters for their municipal water supplies. Thus, the costs of drilling a well and pumping the water have already been borne. In these instances, all that is necessary for using the heat is the designation of a recipient (a local school or other public building, for example) and installation of the necessary heat exchange systems.

However, a water resource of the type studied here--that is, one that provides potable water and caloric energy--is an anomaly. In general, aquifers of moderately shallow depth (up to several hundred feet deep) yield dependable amounts of water of low, constant temperature and low total dissolved solids. But in the deeper parts of

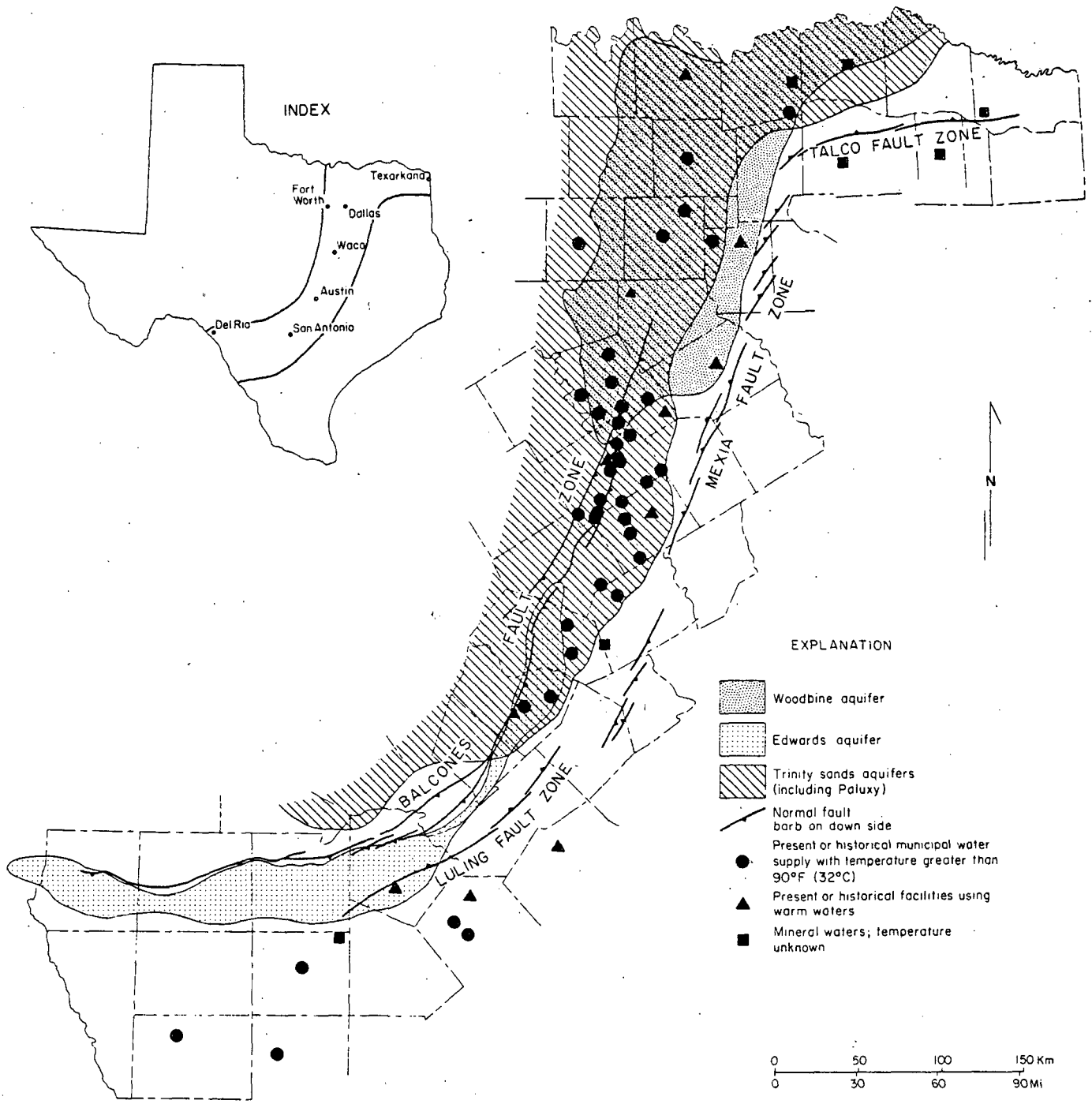


Figure 1. Location of study region in Central Texas; note localities historically producing or using warm (or mineral) waters.

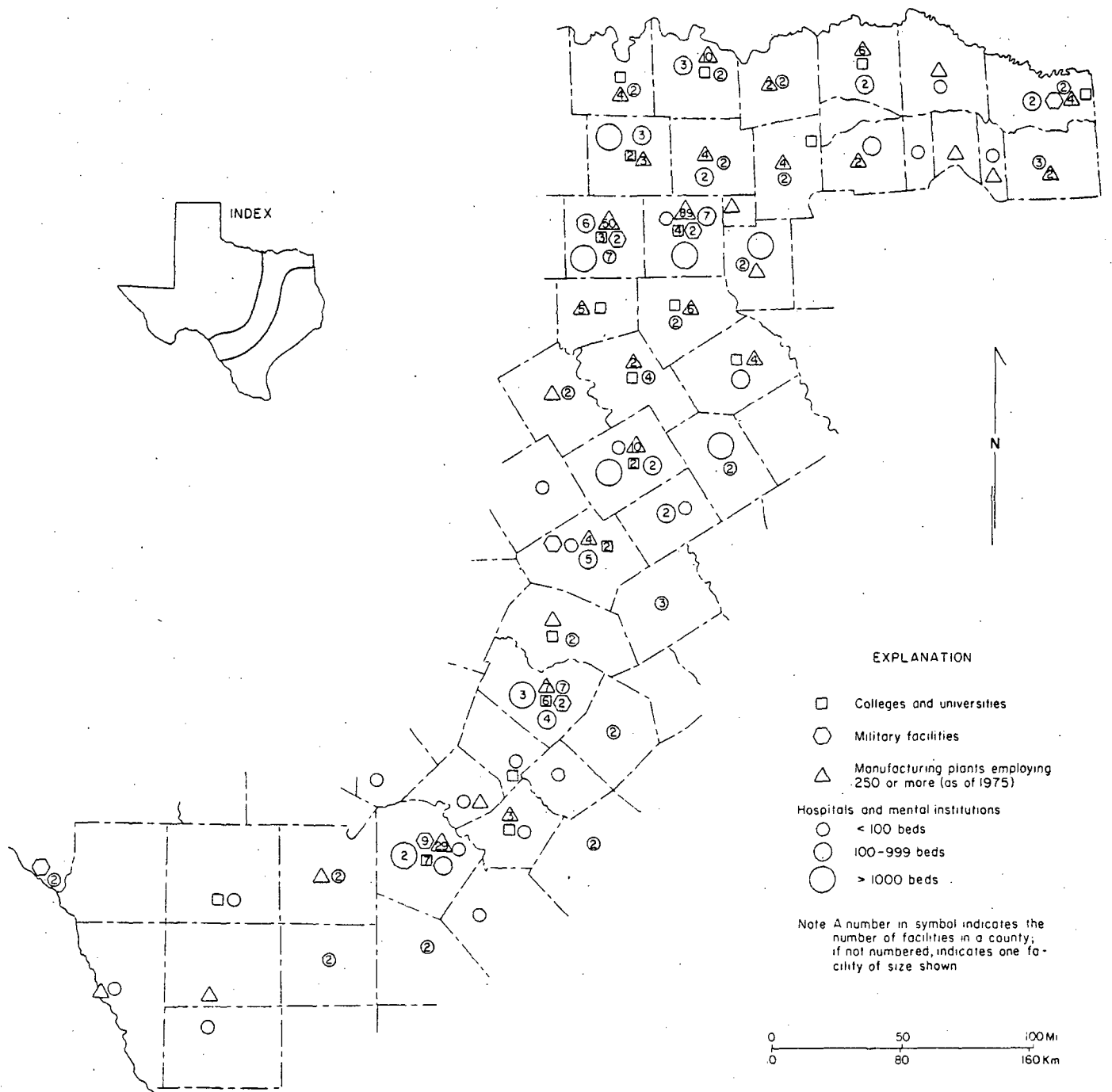


Figure 2. Major facilities within study region (from Arbingast and others, 1976).

aquifers, porosity and permeability commonly decrease with an associated decline in well yields. Also, water quality declines with increasing depth as a result of poor circulation and either chemical equilibrium between deep ground water and minerals composing the host rocks or a mixing of meteoric waters and pre-existing fluids within the aquifer. This increase in dissolved constituents is further abetted by the increase in earth temperature with depth; the hotter the ground water, the greater the capacity of the water to retain salts in solution. Given these expected relations, plus the cost of drilling a well, it is no mystery why wells usually tap the shallowest dependable source of ground water in an area. People naturally seek the best quality water at the lowest cost, and in the past, a hot-water well was considered unsatisfactory for domestic or municipal supply. Many such wells may have been abandoned leaving no record; hence, data on these waters are sometimes sparse.

Clearly, there are several constraints on the widespread use of warm potable water; these constraints include geographic variations in quality, quantity, and heat content of geothermal ground-water reservoirs. These factors combined affect the technical and economic feasibility of tapping the waters either for drinking supply or for heat extraction.

#### Purpose and Scope

This investigation is a regional inventory and overview. Its purpose is to assess areal and stratigraphic extent and capabilities of aquifers that yield warm waters within the Balcones and Luling-Mexia-Talco Fault Zones. The study involves a state-of-knowledge evaluation of multiple-use potential (potable water and heat content) on the basis of geologic, climatic, and demographic factors. Because multiple use is so important to the viability of this potential energy resource, we have focused our attention mainly on areas of known ground-water production. Thus, our major questions are, "Where are there warm potable waters, and what are their geochemical and hydrologic attributes?" However, we have also delineated as potential targets untested areas that might yield potable geothermal waters. Finally, we have defined possible future research tasks for further assessment of these resources.

The geographic scope of study included a region of more than 50,000 mi<sup>2</sup> (approximately 137,000 km<sup>2</sup>) within 65 Texas counties (fig. 3). This study region was defined on the basis of the location of Cretaceous aquifers in Central Texas that are known to yield warm water locally. We purposely excluded areas in which warm waters are confirmed from Tertiary strata in the Gulf Coast Basin in South Texas, and from Paleozoic strata farther west; the Tertiary and Paleozoic aquifers differ from

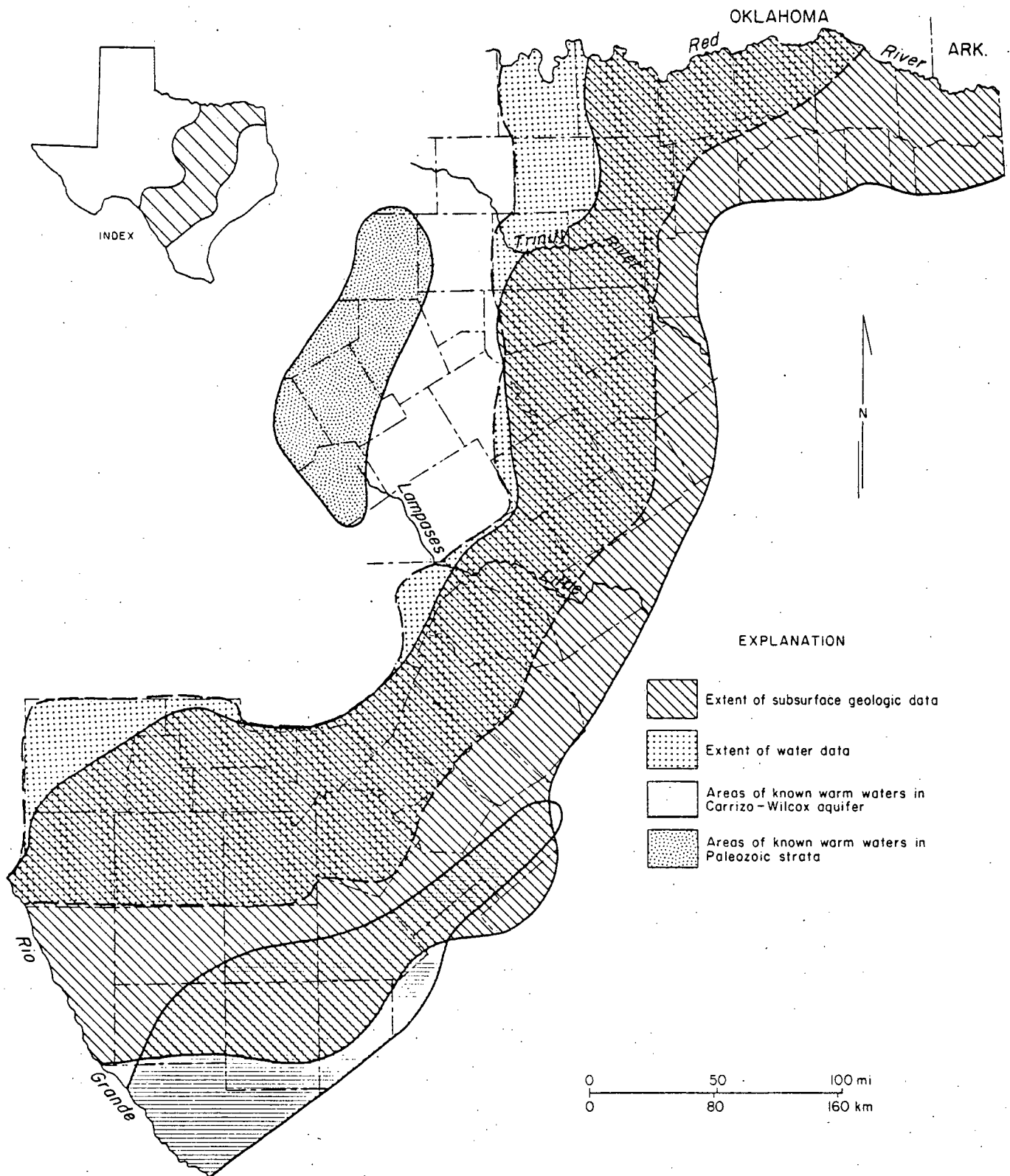


Figure 3. Counties included within geologic data base and hydrologic data base; also approximate limits of Paleozoic and Tertiary aquifers that yield warm water.

the Cretaceous strata in geologic age, in mode of origin, and in areal extent. Time constraints during this one-year project did not allow expansion of the study region to include these adjacent geothermal provinces.

The conceptual scope of study involved two major avenues of inquiry, one dealing with the stratigraphic and structural framework of the aquifers identified, and the other addressing the hydrologic, geochemical, and thermal aspects. Both avenues of investigation, however, were limited by extant data, whether it was information on subsurface lithic control, water quality, or historical well yield. Limited water data especially constrained the scope of study; no ground-water data exist for the rock units studied where they are not used as aquifers. There, aquifer potential must be inferred from our interpretations of the geologic setting. Our interpretations of the regional geologic framework were similarly constrained by uneven distribution and quality of subsurface data. In many areas there has been little petroleum exploration activity, and in several instances where exploration wells do occur, the wells are often cased through the water-bearing units, and thus the formations of interest in this study do not appear on electric logs. The scope of follow-up investigations could be expanded by the acquisition of a more complete data base within selected areas.

Because of the size and complexity of the study region, it has been subdivided into three subareas (fig. 3). The Lampasas and Little Rivers separate the southern area from the central part of the region, and the Trinity River separates the central from the northern sections. The northern and southern areas were studied by scientists at the Bureau of Economic Geology. The central segment was studied under a contractual agreement with a team of consultants led by Drs. O. T. Hayward and Robert G. Font of Baylor University at Waco, Texas. In addition to contributing data and interpretations to the regional assessment, these consultants also completed a state-of-knowledge assessment of the geologic and hydrologic settings in Falls County. The Falls County study provided technical support for drilling a well to supply warm water for the Memorial Hospital at Marlin funded mainly by the U.S. Department of Energy. Maps and reports by these consultants--both on the entire central study area and on Falls County--are on file at the Bureau of Economic Geology.

#### Data Base

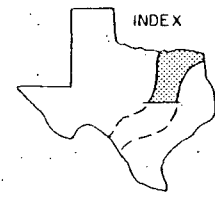
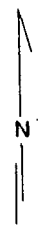
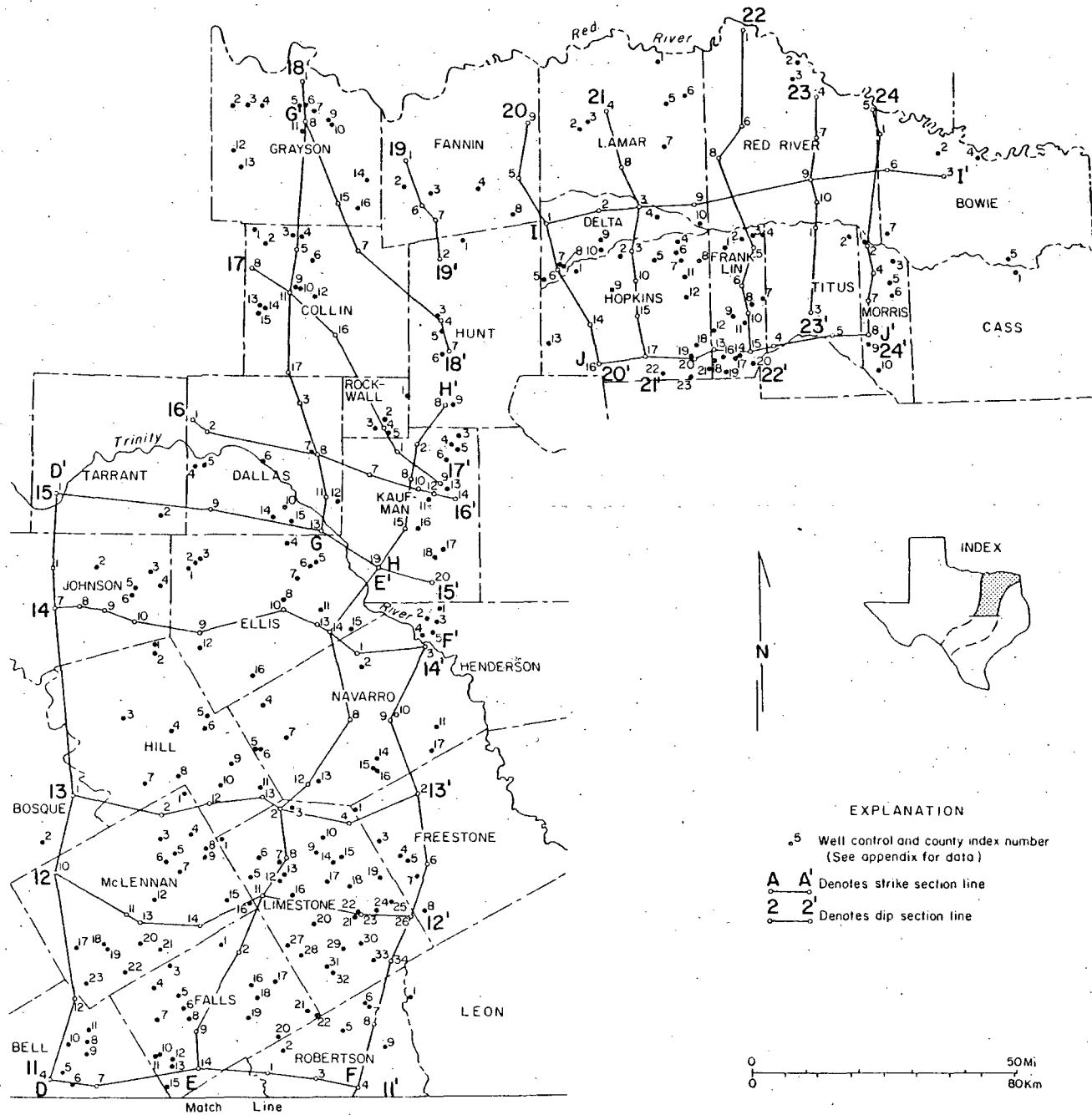
Two types of data were used in this inventory. One type is applied to the geologic framework; the other is used in assaying hydrology, water chemistry, and historical use patterns of the aquifers delineated. In all instances, mapping was done at a scale of 1:250,000. The work maps for all three study areas were then compiled

into a single base at a scale of 1:1,000,000. These compilation maps are on file at the Bureau of Economic Geology.

The geologic interpretations were based mainly on electric logs of wells occurring across the region, although we also examined some cuttings and cores to substantiate stratigraphic horizons in problem areas. Our well control consists of 724 data points in 63 counties (fig. 4). We used these data to construct 24 dip-oriented and 10 strike-oriented cross sections, as well as a series of 11 maps that present the structural framework of various stratigraphic horizons and the isopachous or isolith geometry of the aquifers studied. Bottom-hole temperature values from these electric logs were also used to construct a map showing the geothermal gradient across the region.

Our subsurface geologic data base was computer indexed and is presented in the appendix to this report. This appendix contains selected information obtained from the electric log heading or from other sources, and it also contains our lithic interpretations. Each data point is located by county numbers (fig. 4) and each well has a unique number code that is compatible with the State well numbering system of the Texas Department of Water Resources. Of the two numbering systems, the county-by-county convention shown in figure 4 is more important in using this report because our interpretative maps and cross sections use this system. Hence, if anyone wants to retrieve data used in any interpretation here, he or she may do so by referring to the appendix by county and number of the well in question.

Most of the geohydrologic data used in this report were obtained from the computer files of the Texas Department of Water Resources, although some data on dissolved solids and temperature were obtained from published reports. Computerized data include several thousand values of water level measurements, water quality and temperature, and municipal ground-water withdrawals. For each aquifer system deemed potentially important as a geothermal resource, the data were treated in two main types of operations. One of these operations was to plot representative points on maps to provide depictions of regional geographic variations in water level, water chemistry, water temperature, and municipal water use. This procedure resulted in the construction of 16 maps. The other operation was to treat the water quality information for each aquifer in the aggregate--that is, in a non-site-specific manner. This entailed running computer programs to plot scattergrams showing the relations among dissolved solids, temperature, and well depth. Finally, water quality data were programmed to show major anion and cation relations using piper diagrams. This was mainly done in an individual county format in order to denote a characteristic



EXPLANATION

- .5 Well control and county index number  
(See appendix for data)
- A A' Denotes strike section line
- 2 2' Denotes dip section line





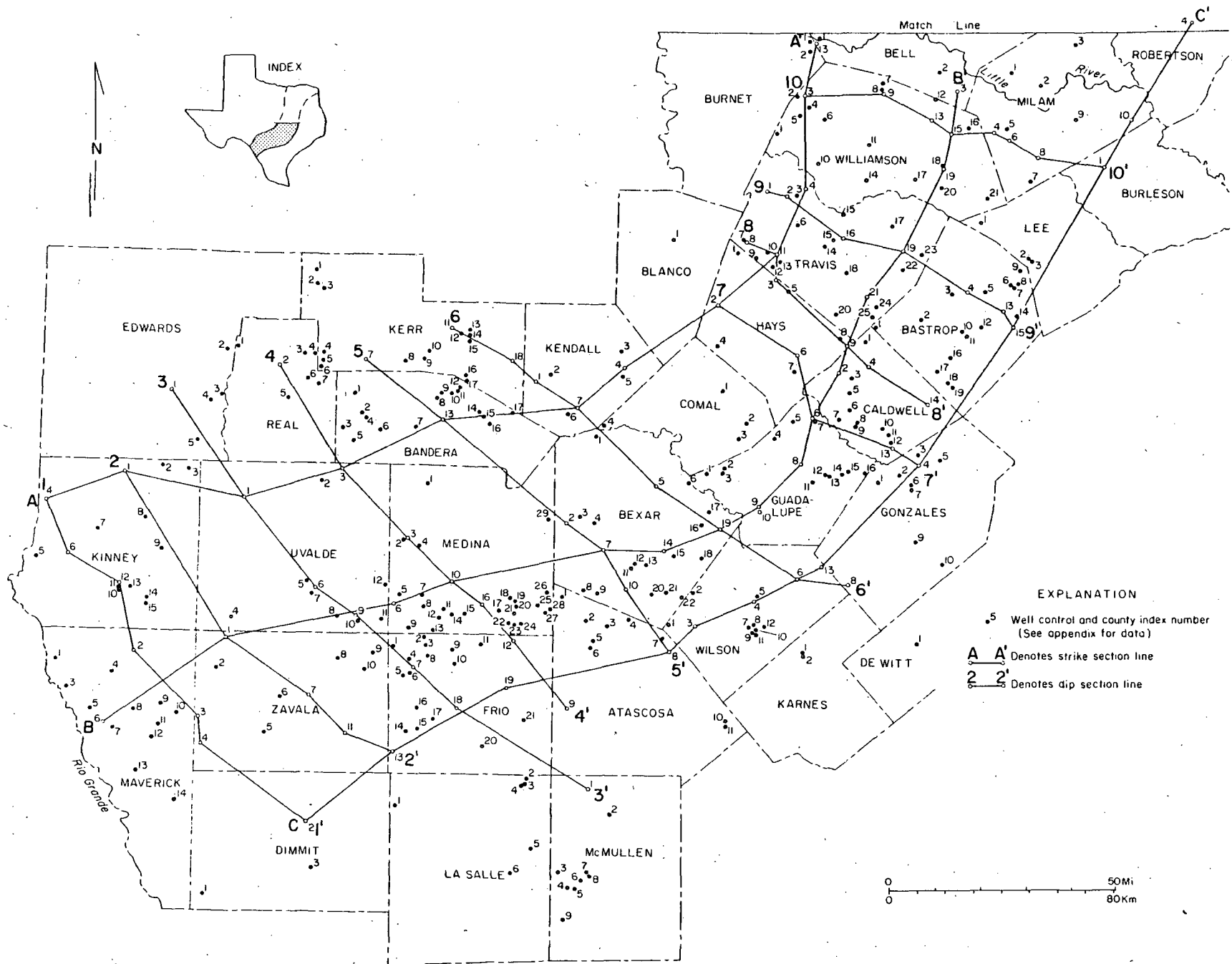


Figure 4. Geologic data base--location of well control and cross-section lines (on facing pages).

geochemical "thumbprint" of a given aquifer, or to show strike-oriented or dip-oriented changes in anion-cation balance within an aquifer.

The data on water quality and water level are not indexed in this report because of the massive repetition of information that is readily obtainable from computer files of the Texas Department of Water Resources. The location-specific information for hydrologic data used in contouring maps presented in this report is retained on the open-file work maps at the Bureau of Economic Geology. These work maps present the water-quality and water-level data base from which the interpretations were drawn. These data are coded by county, by aquifer, and by State well number.

In this report we first present general discussions of regional physiography, climate, structural geology, and stratigraphy. Then we focus on each of the horizons that were mapped in detail, beginning with the pre-Cretaceous "basement complex" and including each of the major Cretaceous aquifers that yield low-temperature geothermal waters. These aquifers are addressed from oldest to youngest.

### Regional Physiography and Climate

Most of the large facilities that might potentially use the low-temperature geothermal waters lie along the Blackland Prairie physiographic province (fig. 5). The intensive human use of the Blackland belt is due to several factors. The terrain is gently rolling, and the soils are fertile, so that the area constitutes prime agricultural land. Moreover, especially in the south-central part of the Blackland belt, geologic changes across the Balcones Fault Zone have resulted in marked demographic responses. Most notable are the changes in terrain from the Hill Country and its dominant ranching economy to the inner coastal plain and its cotton-based farming economy. Also, the Balcones Fault Zone delineates the Edwards artesian aquifer system that constitutes a major supply of fresh water in south-central Texas.

Other physiographic provinces that warrant special notice are the Western Cross Timbers and the Eastern Cross Timbers because they generally delimit the recharge areas for the various warm-water-bearing aquifers in Central and North-Central Texas. The Western Cross Timbers receives recharge for all the basal Cretaceous sand units, including the Hosston, the Hensel, the "Trinity Undifferentiated" sand units, and part of the Paluxy Sand. The Eastern Cross Timbers is the recharge zone for the Woodbine Sand.

Climatic factors that are important in evaluating low-temperature geothermal water resources include mean annual air temperature, seasonal (winter) deviations

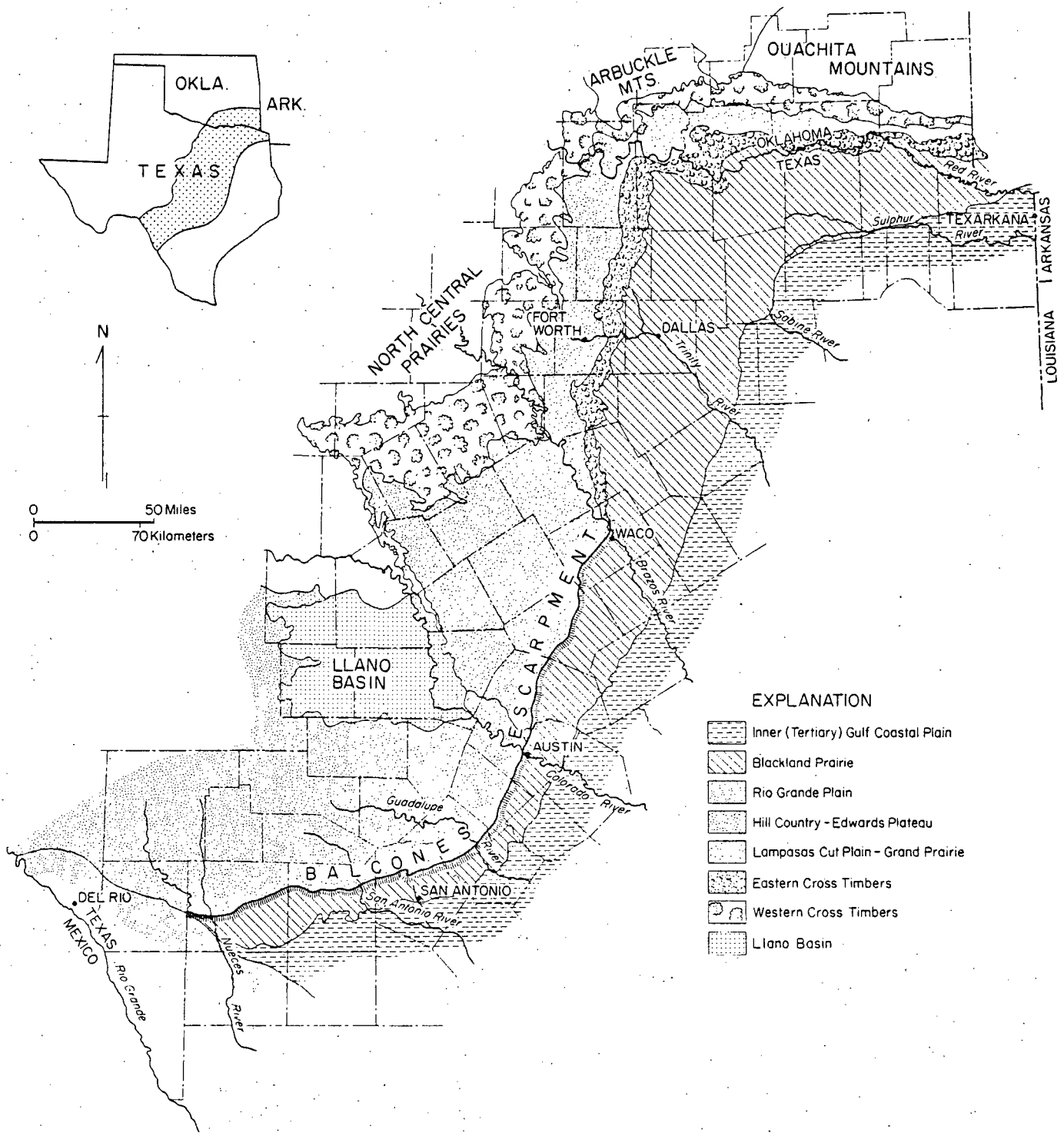


Figure 5. Physiographic provinces of study region.

from this mean, and average length of seasons that are subject to freezing temperature.

Mean annual air temperature (fig. 6) provides a basis for approximating the temperature of water entering the aquifers; in other words, initial aquifer temperature should be close to the mean annual air temperature across the respective recharge areas. Moreover, mean annual air temperature represents a reasonable estimate for near-surface ground temperature, and this value is used as a baseline for computing geothermal gradients.

Mean temperature values for winter months provide a way to compute the effective caloric value of warm waters for space heating needs. Hence, the difference between January mean minimum temperatures (fig. 6) and the temperature of the local ground water provides an approximate maximum figure for available heat, even though the actual usable heat will be somewhat less than this differential, because of heat-exchange efficiencies and other factors. The most conservative estimate of available heat may be obtained by computing the difference between temperatures of geothermal waters and the local mean annual air temperatures, as this value should approximate the difference between temperatures of recharging waters and the waters at depth in the same ground-water system.

The map showing mean length of freeze periods (fig. 7) provides a rough estimate of the length of time during which space-heating needs are greatest. However, in most of Texas there are many warm interludes within this freeze period. Also at other times temperatures may be above freezing but below the range of comfort, so that for a detailed, site-specific analysis the climatic parameter needed is the "annual heating degree days," which is available from National Weather Service data files but is not presented here. The map depicting freeze period does illustrate the brief part of the year in which space heating is needed. But for water-heating needs, the caloric value of the water does not depend on seasonal air temperature, and the demand for hot water implies a year-round need for geothermal water. Yet warm water in storage tanks loses heat, and for this reason hot-water heaters powered by fossil fuels are widely used even in homes that directly tap the geothermal aquifers.

### Regional Structural Geology

The study region lies along a major structural hinge that separates the Texas Craton from the embayments of the Gulf coastal province (fig. 8). The hinge occupies a zone as much as 40 mi (64 km) wide that shows evidence of structural activity over an expanse of geologic time. The major tectonic features delimiting the hinge zone

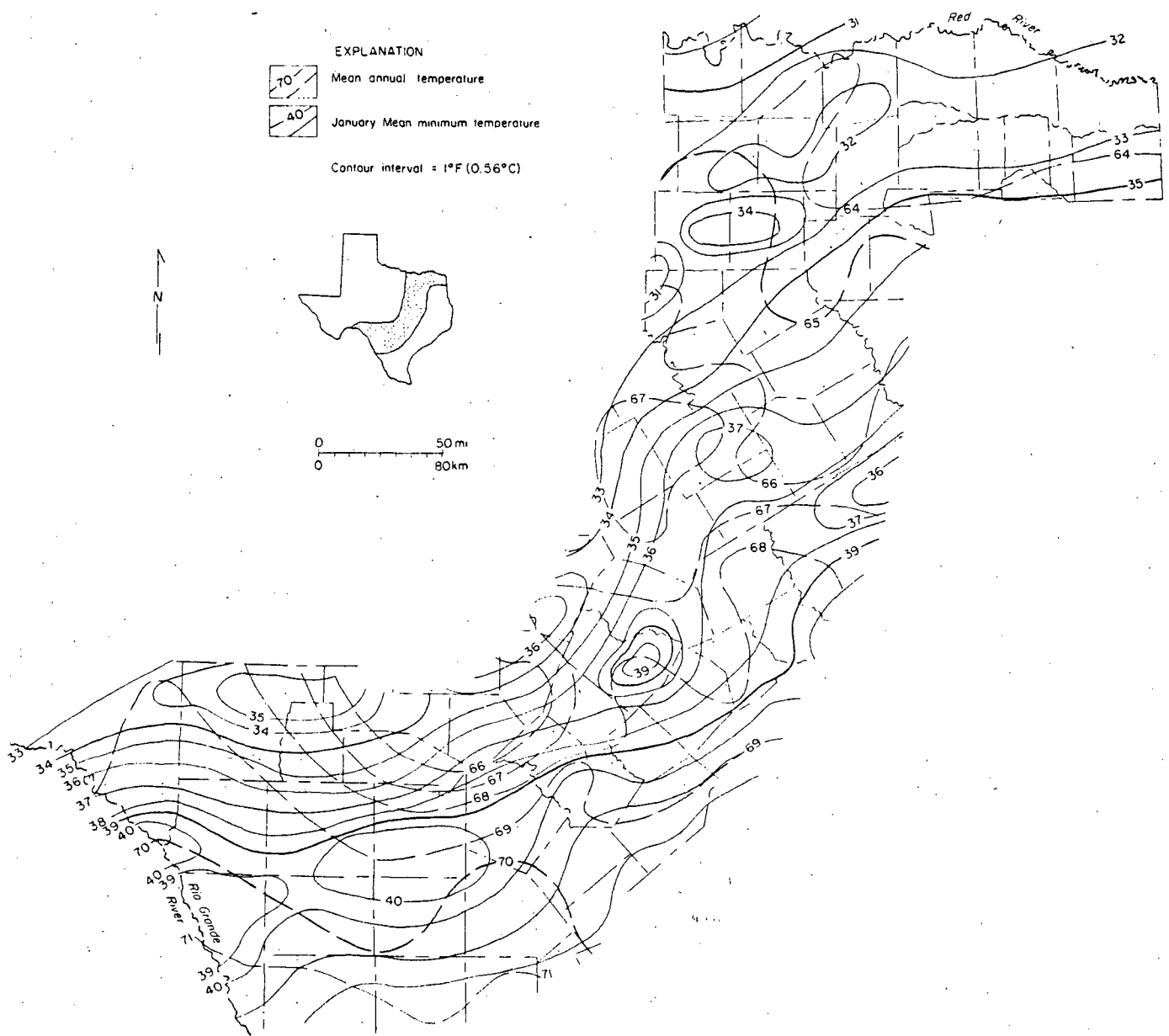


Figure 6. Mean annual air temperature and January mean minimum temperature of study region (data from Texas Natural Resources Information System).

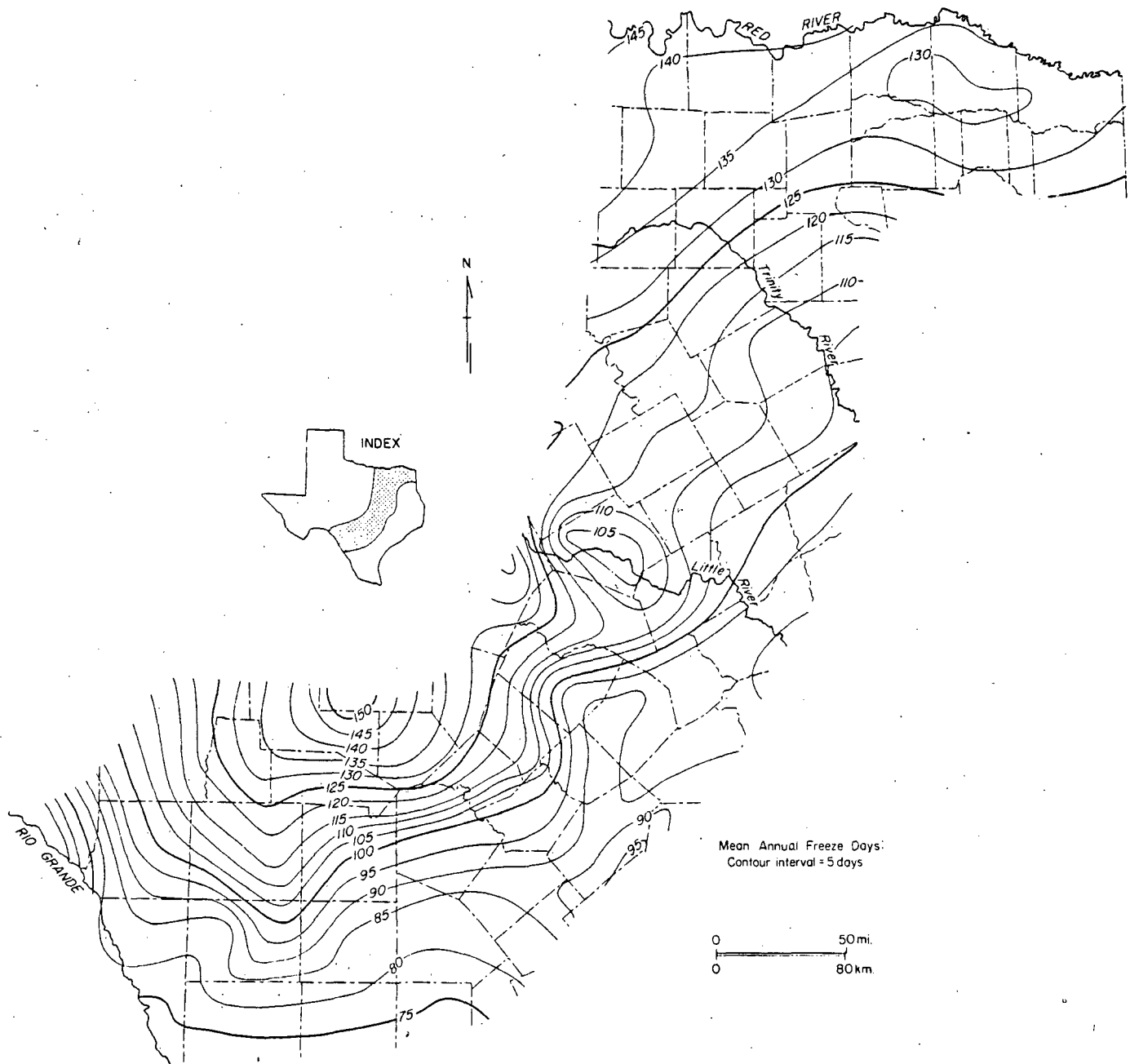


Figure 7. Mean annual freeze period of study region (data from Texas Natural Resources Information System).

are the surface faults of the Balcones and Luling-Mexia-Talco systems and the buried Ouachita structural belt (fig. 9). Other features that lie along this trend are the updip subcrop of Jurassic strata, Cretaceous igneous plugs, and the updip outcrop of Tertiary rocks. Detailed stratigraphic and structural analyses demonstrate facies changes, abrupt thickening and rapid changes in the rate of dips of strata, complex faulting, and anomalously high geothermal gradients. The time of structural deformation spans more than 200 million years from the late Paleozoic during Ouachita deformation to Miocene time when the major events of Balcones faulting occurred. The foundered Ouachita structural belt and the proximity of the Jurassic subcrop suggest that this hinge line was the locus of rifting during the opening of the ancestral Gulf of Mexico at the beginning of the Mesozoic Era. Subsequently, the Balcones and Luling-Mexia-Talco fault systems formed in response to tensional stresses, perhaps related to this rifting. The Balcones Fault System shows displacement mainly down-to-the-coast, whereas the Luling-Mexia-Talco system is displaced both up-to-the-coast and down-to-the-coast, but in many areas a graben occurs superjacent to the Ouachita belt between the Balcones and Luling-Mexia-Talco Fault Zones.

The dominant features that affected the depositional framework of Cretaceous rock units along this hinge zone are the various positive and negative structural features within the region (fig. 8). The three positive elements that were most influential in determining the composition and depositional aspects of Cretaceous sandstone units are the Llano Uplift, the Arbuckle Mountains, and the Ouachita Mountains. All three of these features provided sediment for the basal Cretaceous terrigenous clastic deposits, the downdip areas of which are the major geothermal aquifers. Other positive features of more limited areal extent are the Devil's River Uplift and the Chittim Anticline, both of which are especially denoted by their effects on the structural configuration of the Edwards Limestone in South Texas. In Central Texas, the San Marcos Platform is a major salient extending southeastward from the Llano Uplift. This platform is the locus of several facies changes with concomitant effects on aquifer properties of the Hosston and Hensel sand units. The Muenster Arch and the Preston Anticline affected the sand trends of several units in north Texas. The Sligo Reef Trend delineates the Cretaceous (Comanchean) shelf edge, and the pre-Cretaceous shelf edge is inferred from the location of the updip Jurassic line.

The major negative structural features are the Maverick Basin, the East Texas Basin, and the Gulf Coast Basin. Both the Maverick and the East Texas Basins are delineated on figure 9, but the Gulf Coast Basin is shown only on the index map because overall it is interpreted to be a super-province encompassing the entire region

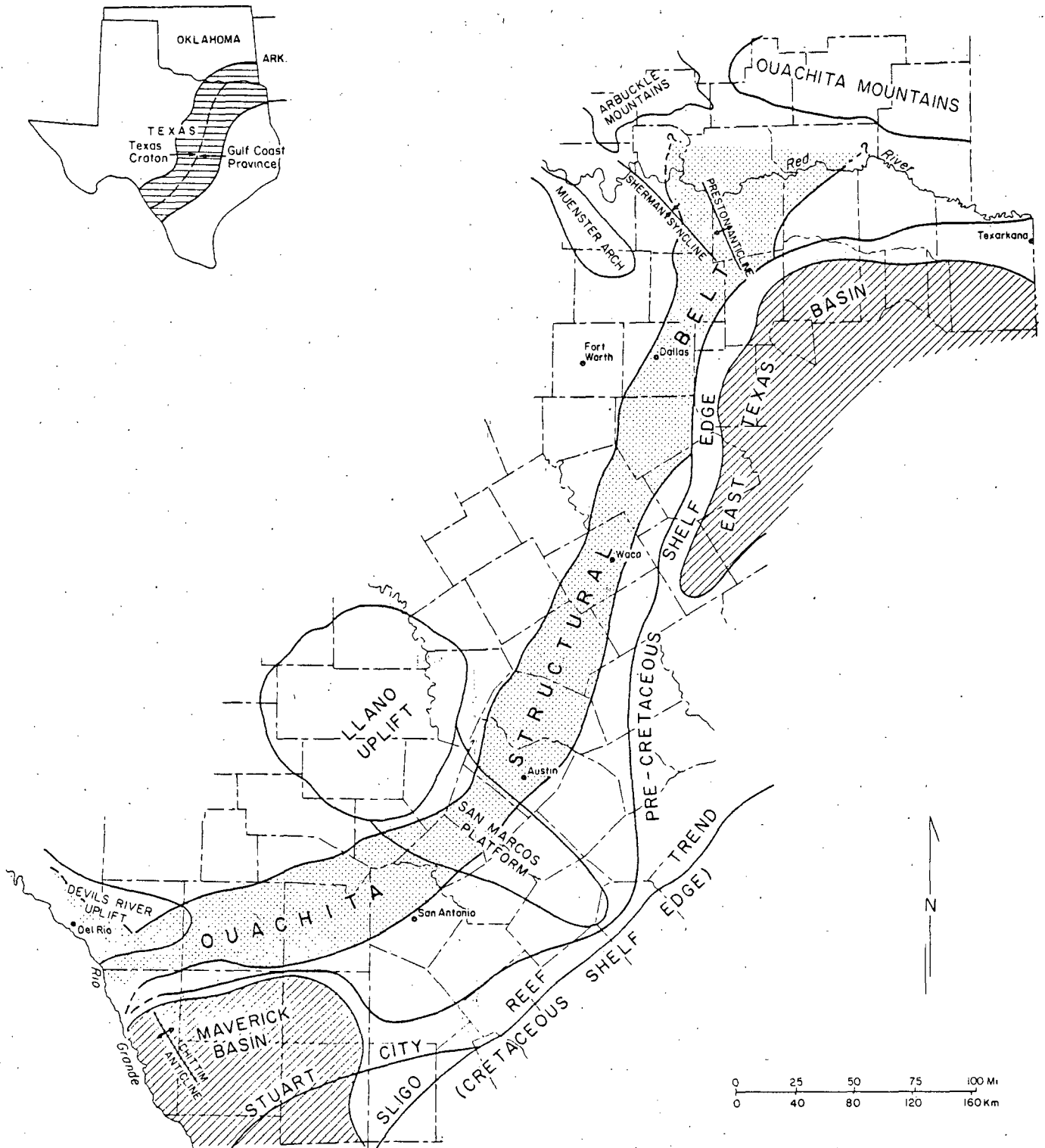


Figure 8. Regional structural elements.



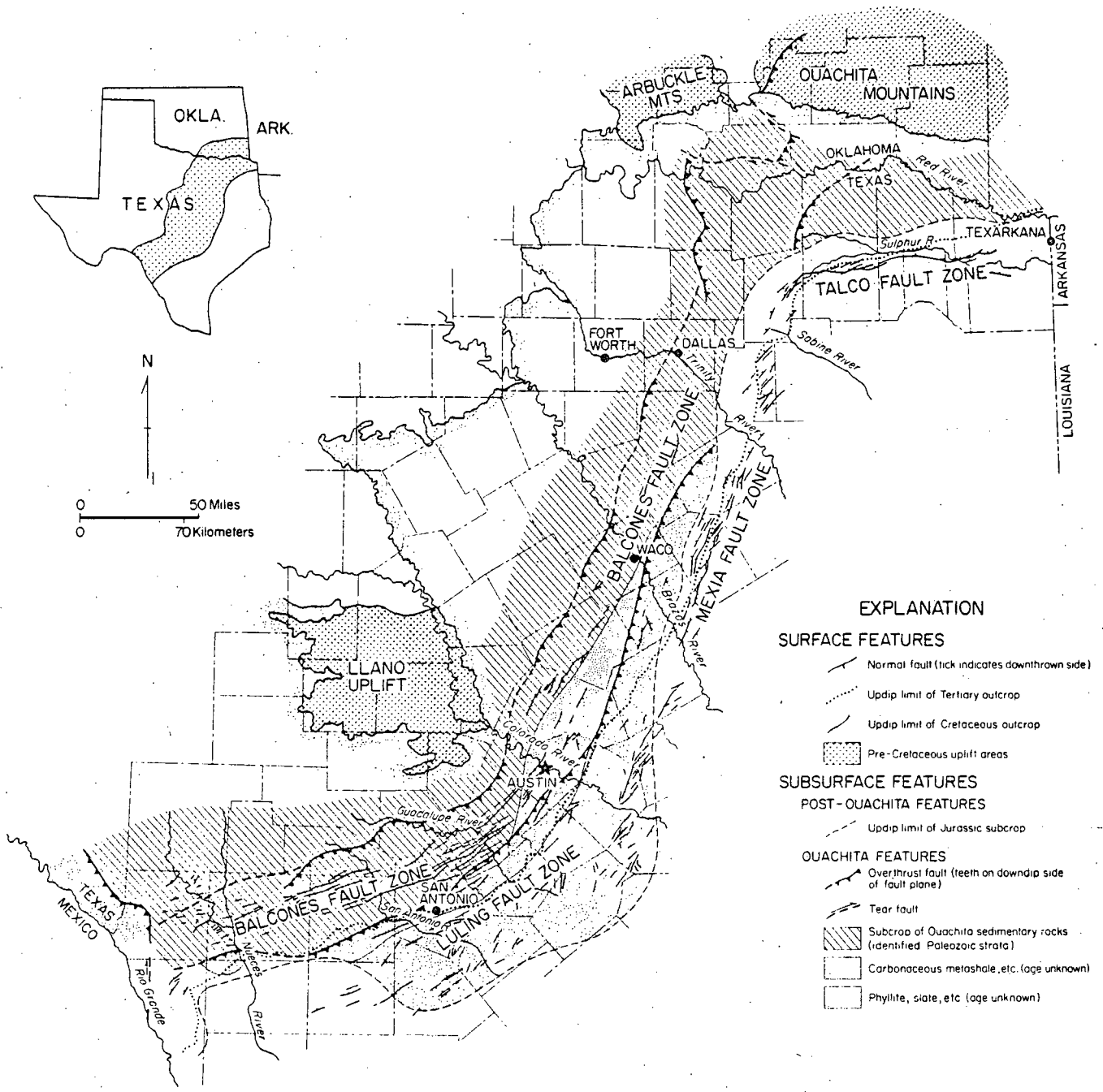


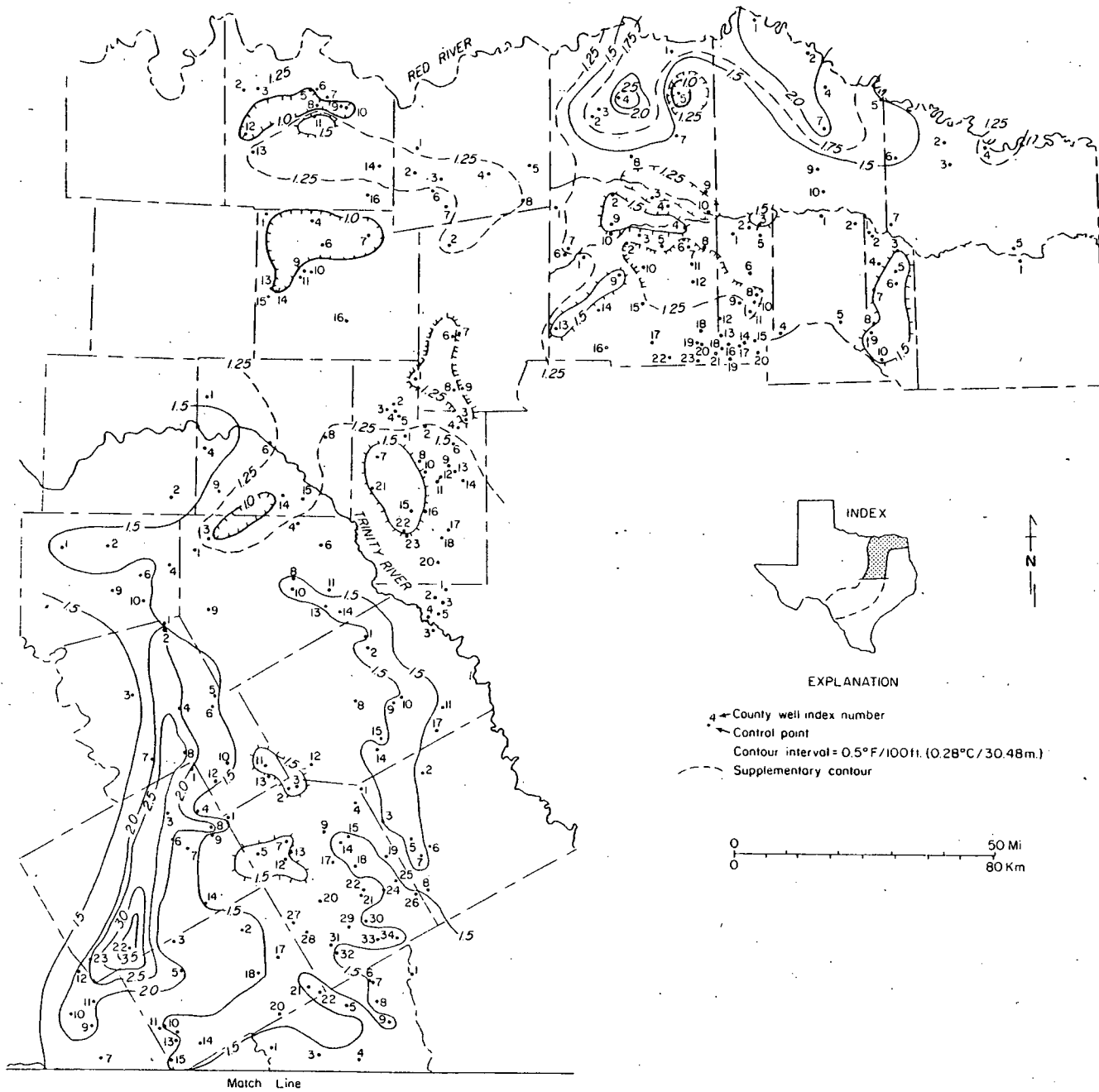
Figure 9. Regional tectonic features (modified from Flawn and others, 1961, and Sellards and Hendricks, 1946).

east of the Texas Craton. An initial boundary might have been the southeastern edge of the Ouachita structural belt. As the basin was filled with sediment during the early Mesozoic, the shelf edge migrated eastward. During deposition of the Edwards Group the shelf edge apparently stabilized along the Stuart City Reef Trend. Later, during the Tertiary and Quaternary periods, the basin continued to regress with only minor transgressions.

The map showing geothermal gradient (fig. 10) reflects some of the regional structural and tectonic features. Most of the gradient values show an increase ranging from  $1.0^{\circ}$  to  $1.5^{\circ}$  F for every 100 ft ( $18^{\circ}$  to  $27^{\circ}$  C/km) of depth. However, there are anomalies with closures of more than  $3.0^{\circ}$  F/100 ft ( $55^{\circ}$  C/km). These high anomalies lie mostly along the main zones of normal faulting in the Balcones system, which is also superjacent to Ouachita structural belt and its zones of thrust faulting and different degrees of metamorphism (Flawn and others, 1961).

Geothermal anomalies may be due to structural setting or to hydrologic factors. Clearly, there appears to be a relation between the location of faults and the abnormal gradients. This may be due to two divergent mechanisms; the faults may be conduits for upwelling fluids (i.e. hot brines), or the faults might retard fluid flow, thus resulting in a stagnating hydrologic system and a long-term increase in temperature. The local sources of the heat either trapped or conveyed by faults include (1) exothermic chemical reactions among deep-seated fluids, (2) buried plutons that are still cooling, (3) the presence of radiogenic rocks at depth, and (4) zones of rock possessing relatively high thermal conductivity properties. As noted by Plummer and Sargent (1931), these and other factors might act singularly or in concert to contribute to abnormal geothermal gradients in the Gulf Coast region.

It is beyond the scope of this report to address fully the problem of geothermal heat sources. Nevertheless, convergence of high geothermal gradients, locus of faulting, major deep-seated structural elements, and the occurrence of warm groundwaters pose many potentially fruitful lines of inquiry for further study. No doubt a combination of factors has affected the geothermal setting in this study region. The geothermal gradients as reported here are conservative (low) values based on bottom-hole temperatures as recorded on electric logs. These logs are generally run immediately after a well is drilled, yet the bottom-hole temperature is usually mediated by the circulation of drilling muds. A long-term monitoring of thermal conditions in this region might show even greater temperature anomalies.



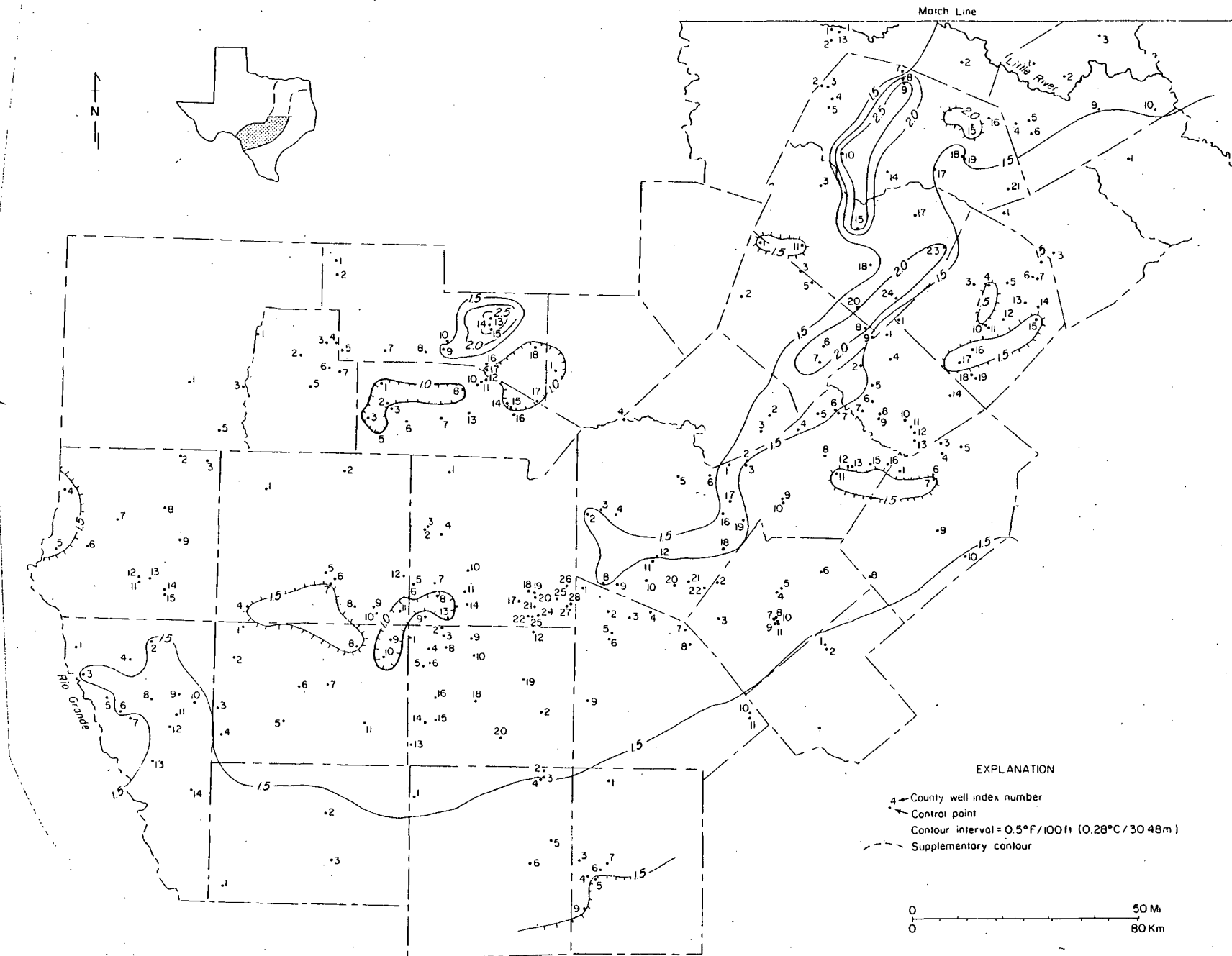


Figure 10. Geothermal gradient of region (on facing pages).

## Regional Stratigraphy

The geothermal aquifers are mostly Lower Cretaceous sandstone units that are superjacent to the Ouachita structural belt. Of these, the most notable potential geothermal resource occurs in the basal Cretaceous sands--the strata that rest directly on the Ouachita rocks. However, in South Texas, the Edwards Limestone also yields warm waters, as does the Carrizo Sand of Tertiary (Eocene) age farther east in the Gulf Coast Basin. In northeast Texas, the Upper Cretaceous Woodbine Sand is also a notable source of warm water. The geographic and stratigraphic distribution of the warm-water-bearing rock units indicates that near this structural hinge zone the deepest stratum that maintains hydrologic communication with meteoric waters (and thus is part of a viable aquifer system) exhibits abnormally high temperatures in its downdip reaches. The aquifers apparently serve as a natural heat exchange and heat storage system in response to the anomalous geothermal gradients along the Ouachita-Balcones trend. Because of the functioning of aquifers in this way progressively younger stratigraphic units serve as geothermal water-bearing units from the Texas Craton to the Gulf Coast Basin.

The regional stratigraphic picture is complex, partly because of structural framework and resulting changes in depositional processes across this region, but mostly because of nomenclatural inconsistencies. For example, the basal Cretaceous (Trinity) sands aquifer systems--that is, the initial terrigenous sands that were deposited on the Paleozoic surface--has no less than nine stratigraphic units cited in the literature for sands of (probably) equivalent age and of similar depositional environments. There are nomenclatural changes from outcrop into the subsurface, as noted in Central Texas (fig. 11), and there are nomenclatural changes along strike (fig. 12).

Of the various basal Cretaceous sandstone units, eight of these and their permutations are listed as aquifers in the data files of the Texas Department of Water Resources. For the sake of simplicity, we have considered only three or four of these units. In Central Texas we have focused on the Hosston Sand and the Hensel Sand, thus discriminating these two "members" from what has previously been termed the Travis Peak Formation (Klemt and others, 1975). Farther north, near the Trinity River, we have combined Travis Peak, Trinity, Twin Mountains, Antlers, and the updip part of the Paluxy all under the rubric "Trinity Sands Undifferentiated." Hence, we consider only six units region-wide: the Hosston, the Hensel, the Trinity Undifferentiated, the Paluxy, the Woodbine Sands, and the Edwards Limestone. Of these, the most important in terms of geothermal potential are three major aquifer systems:

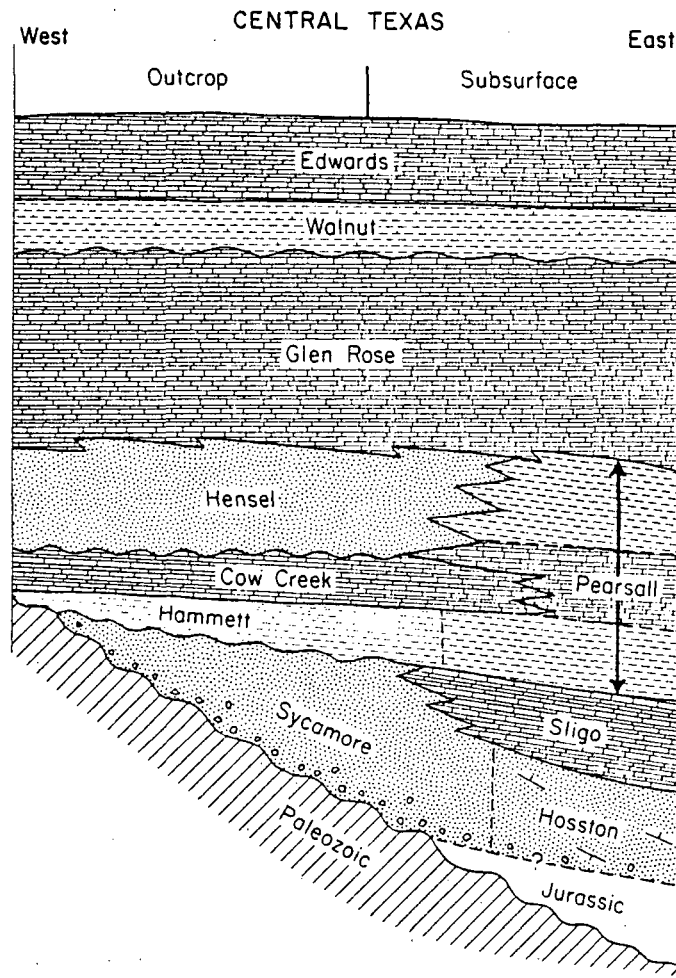


Figure 11. Schematic dip section showing facies and nomenclatural changes of selected Cretaceous units in Central Texas.

SOUTH

NORTH

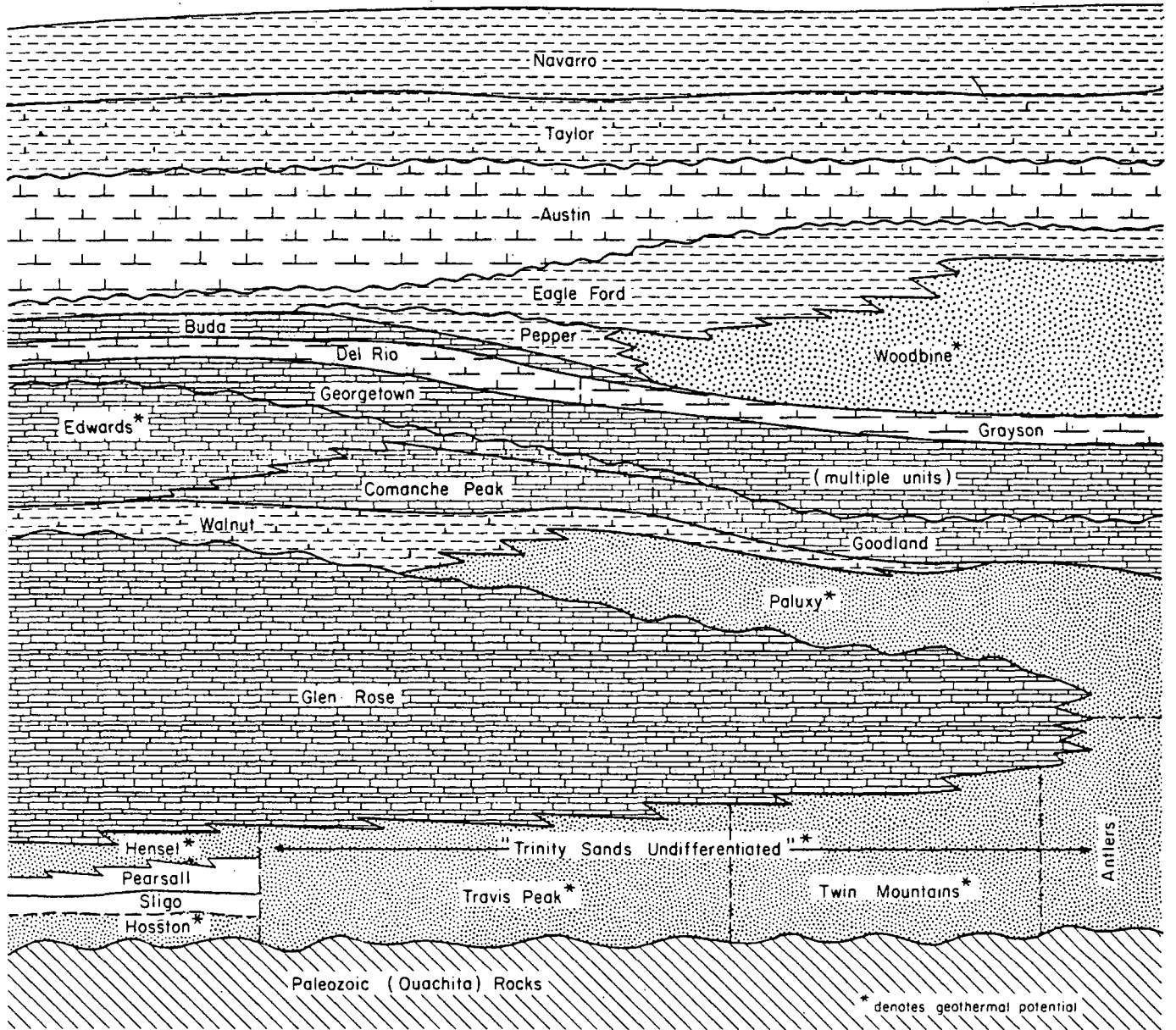


Figure 12. Schematic strike section showing facies and nomenclatural changes of Cretaceous units from Central Texas to North-Central Texas (modified from Fisher and Rodda, 1967).

(1) the Hosston/Trinity Undifferentiated, (2) the Paluxy, and (3) the Woodbine. Outcrop patterns of these units show the geographic distribution of their recharge zone (fig. 13); their configuration at depth is shown on both subsurface geologic maps and cross sections. The series of cross sections (figs. 14-47) shows the geographic location and thickness of rock units that are considered as potential geothermal aquifers; these sections extend beyond the areas in which the strata are tapped as aquifers, so that many downdip and lateral facies changes that limit aquifer capabilities may be seen on the electric log signatures.

Two typical electric logs--one from Travis County and one from Dallas County-- illustrate actual lithic variations from south to north (fig. 48) and provide a basis for recognizing diagnostic log signatures for use of the cross sections presented here. Marked changes also occur in a downdip direction; downdip changes generally militate against aquifer capability at depth owing to either adverse water quality or insufficient well yield. Furthermore, in many instances facies boundaries result in extreme changes in lithic properties of an aquifer host rock. This happens where the Hensel Sand changes downdip into the shales and limestones of the Pearsall Formation in south-central Texas (Loucks, 1977). Such changes result from different environments of deposition--a dip-oriented terrigenous sand system for the Hensel, a strike-oriented carbonate marine shelf system for the Pearsall. Similar changes from a dip-oriented terrigenous sand to a strike-oriented carbonate sand (Bebout, 1977) cause the Hosston Sand to terminate as a viable aquifer in many of its downdip reaches.



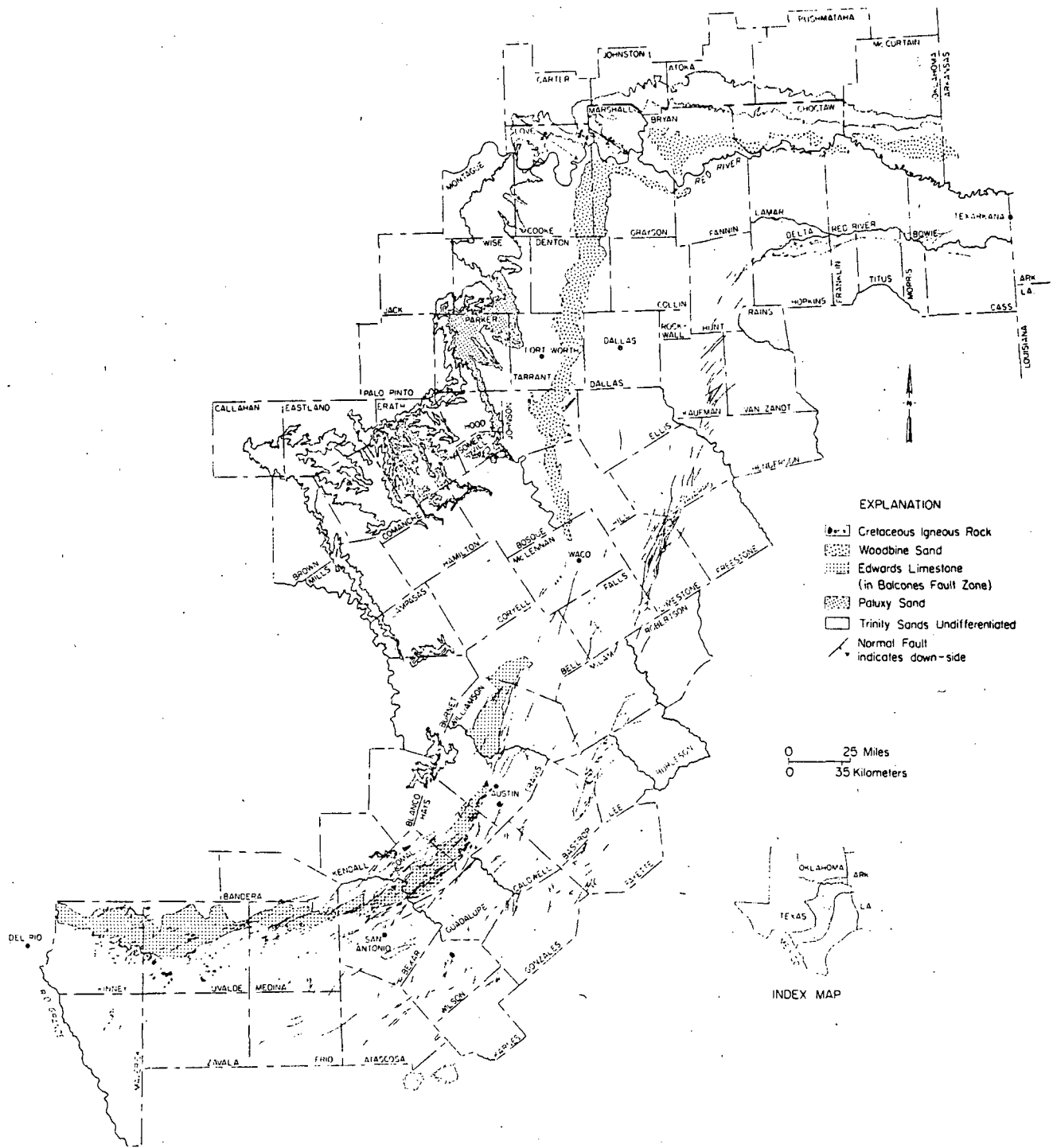


Figure 13. Map showing outcrop of warm-water-bearing Cretaceous strata with respect to Balcones and Luling-Mexia-Talco Fault Zones.

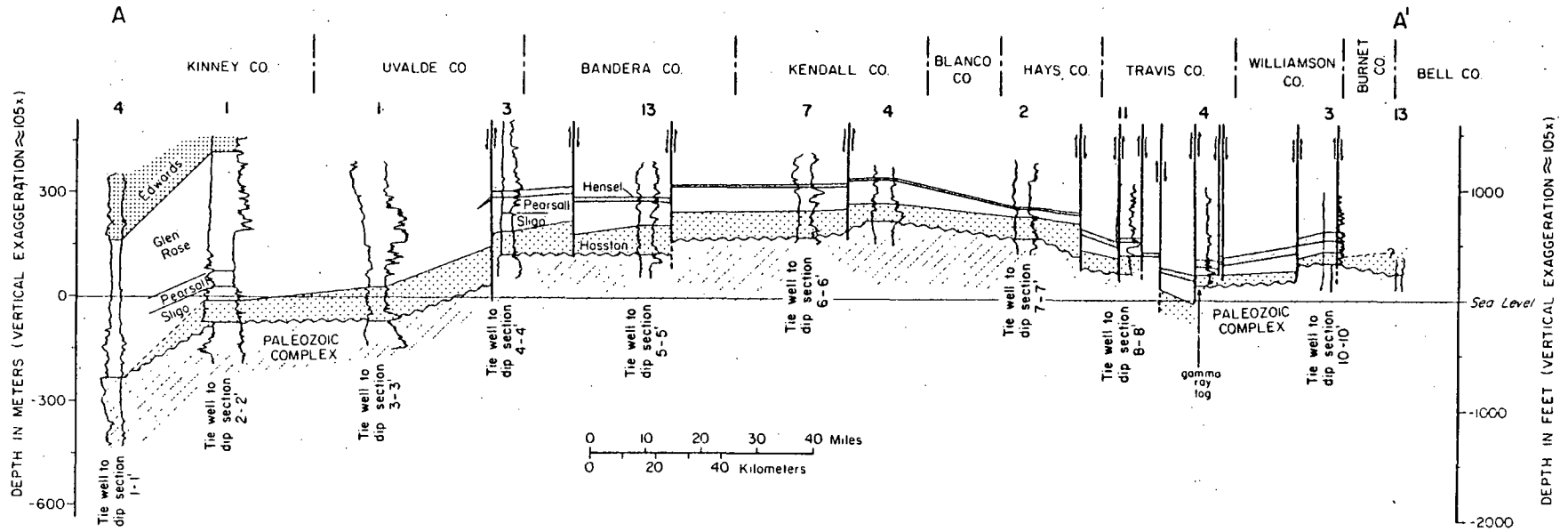


Figure 14. Strike-oriented cross section A-A' (see figure 4 for location; see appendix for individual well data).

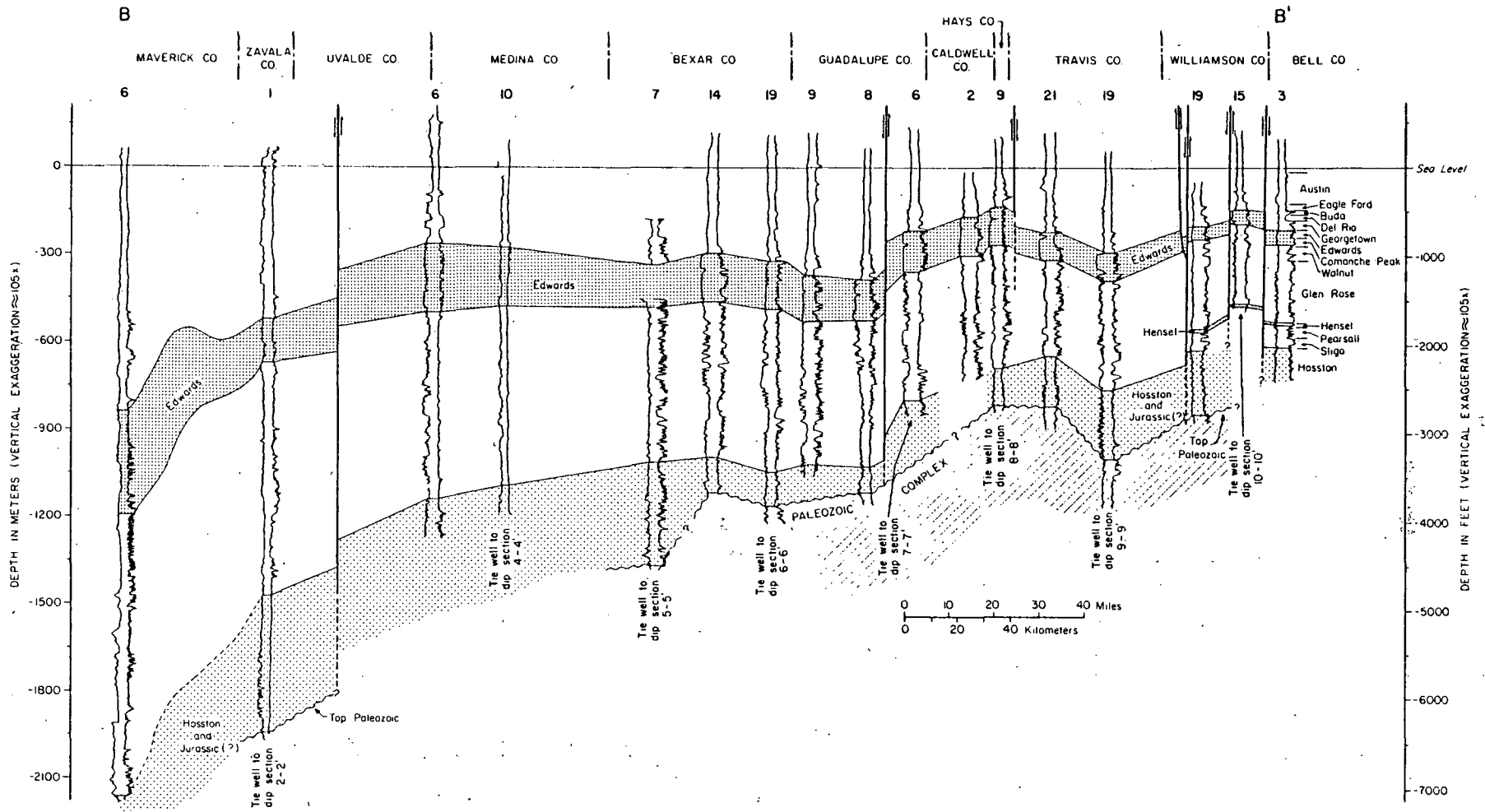
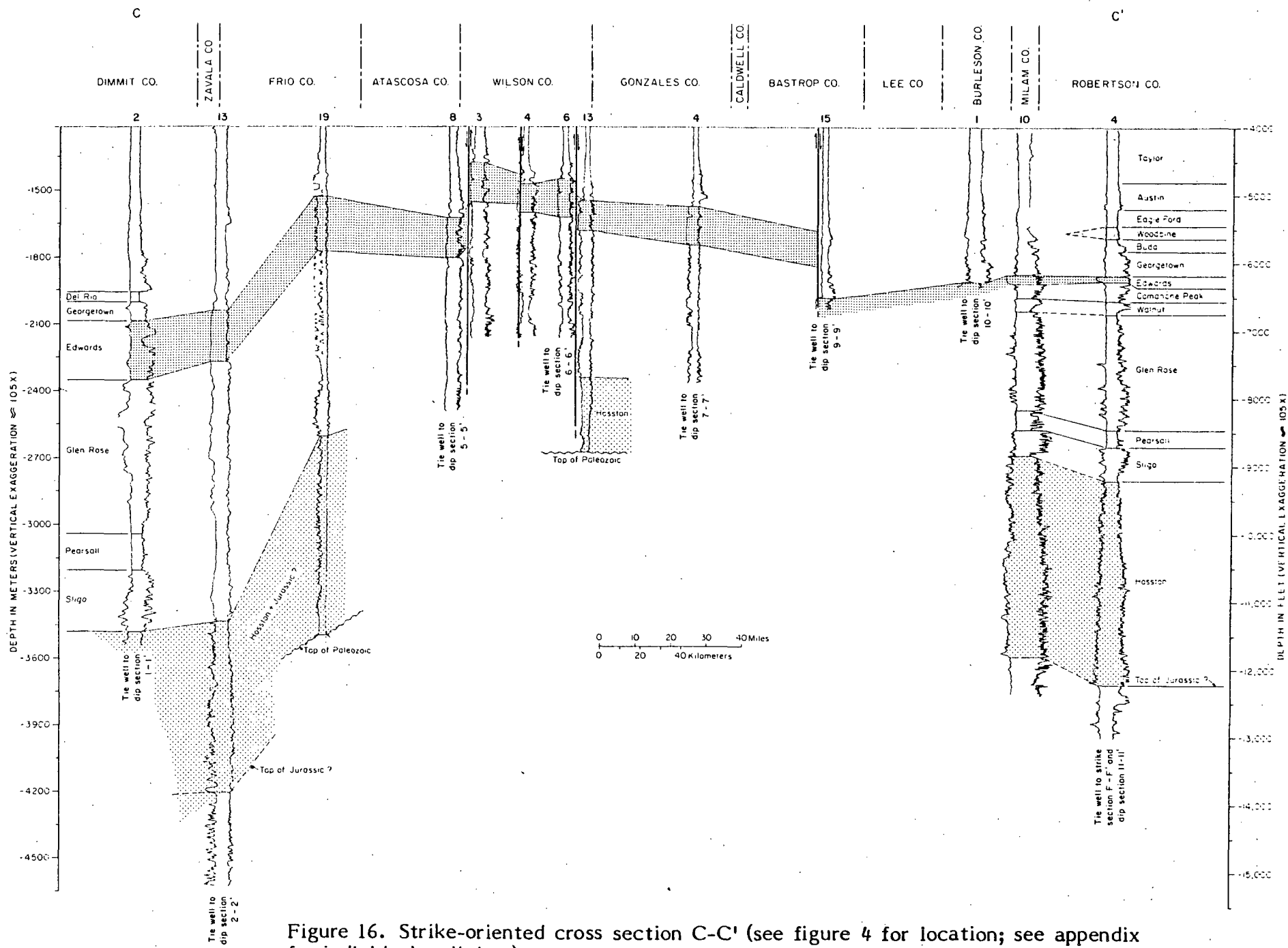


Figure 15. Strike-oriented cross section B-B' (see figure 4 for location; see appendix for individual well data).



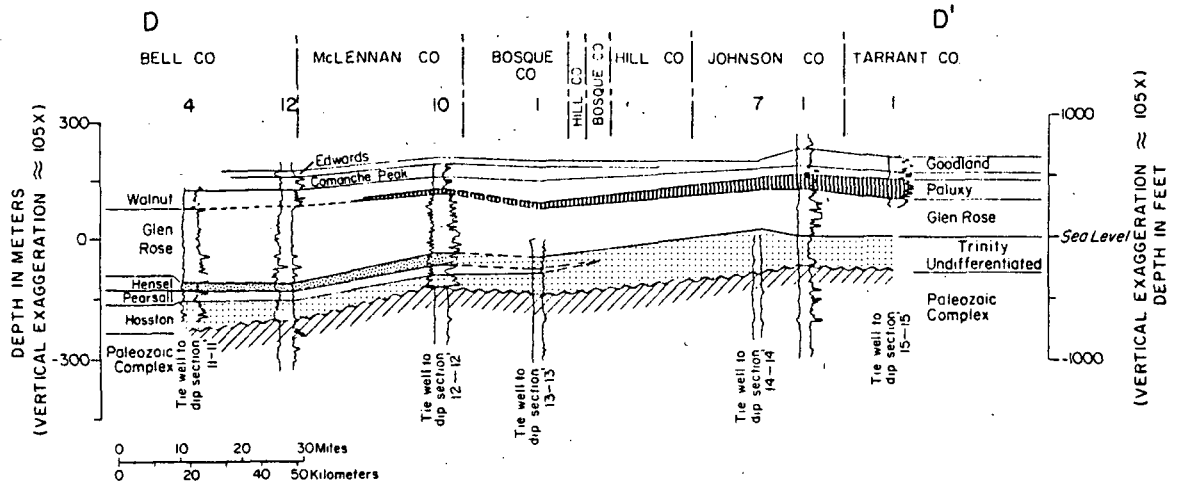


Figure 17. Strike-oriented cross section D-D' (see figure 4 for location; see appendix for individual well data).

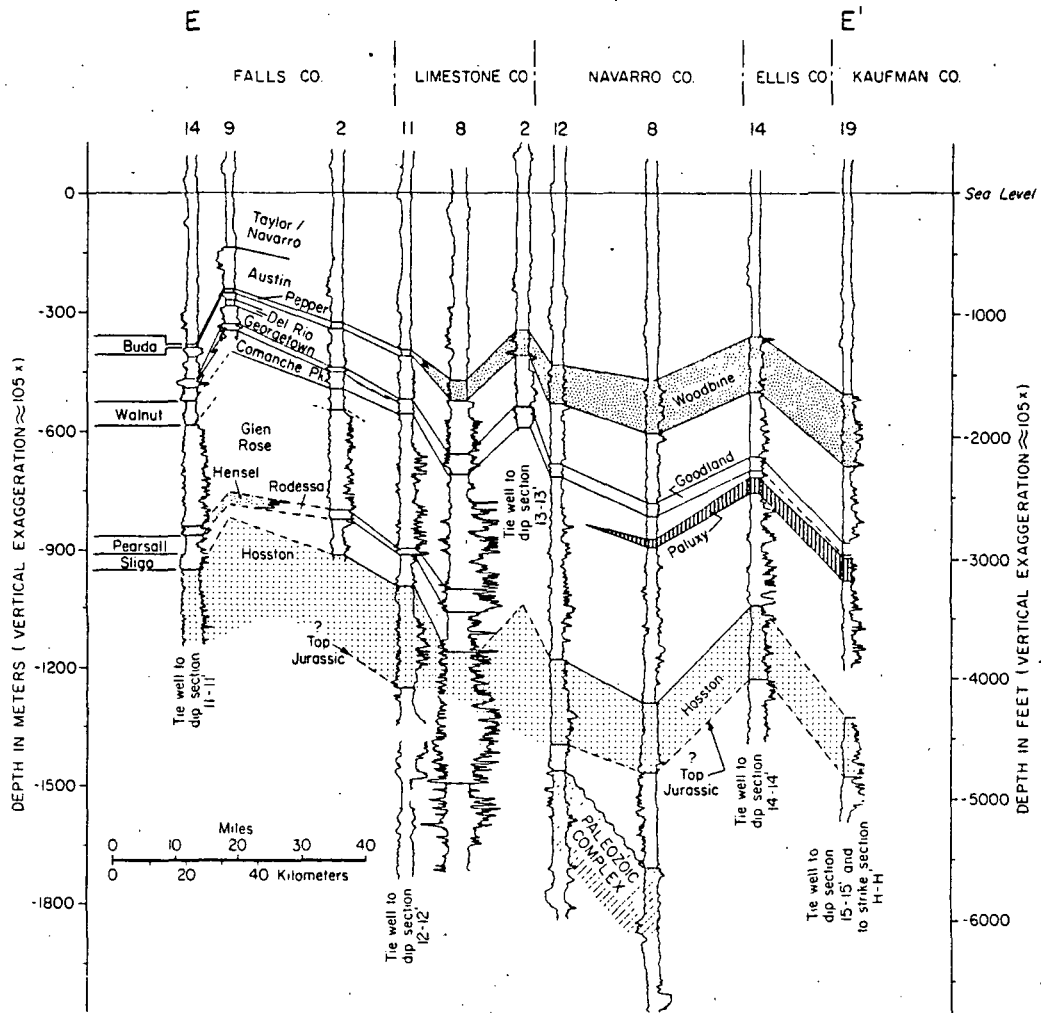


Figure 18. Strike-oriented cross section E-E' (see figure 4 for location; see appendix for individual well data).

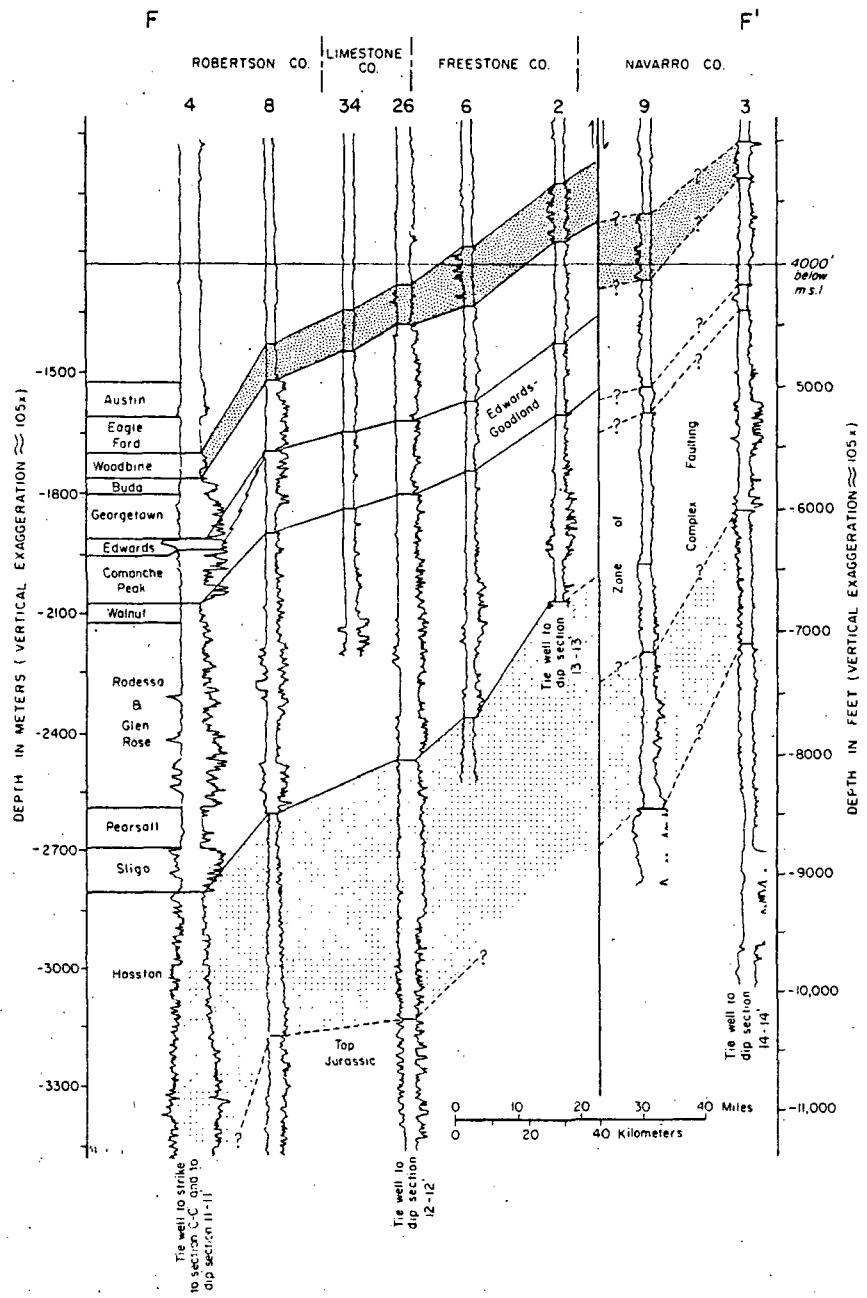


Figure 19. Strike-oriented cross section F-F' (see figure 4 for location; see appendix for individual well data).

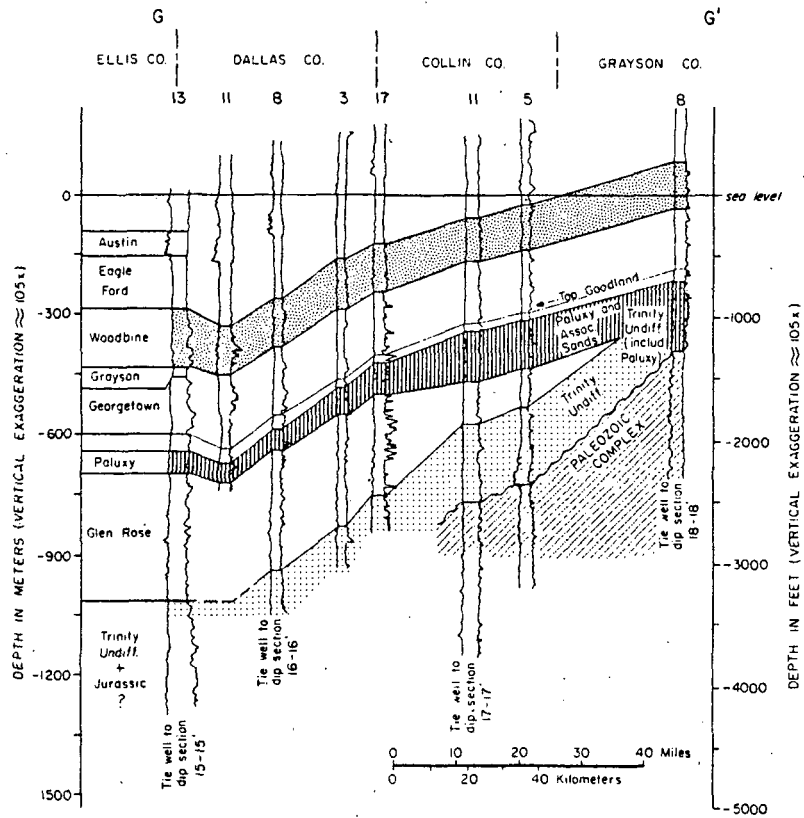


Figure 20. Strike-oriented cross section G-G' (see figure 4 for location; see appendix for individual well data).

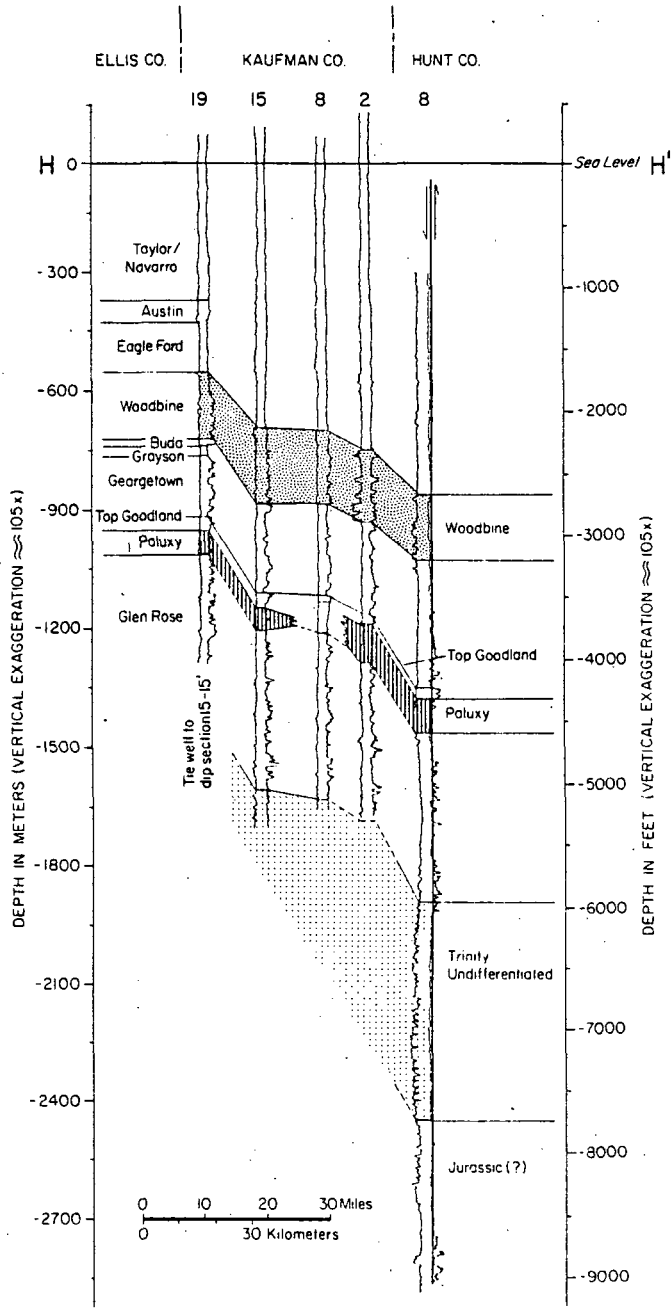


Figure 21. Strike-oriented cross section H-H' (see figure 4 for location; see appendix for individual well data).



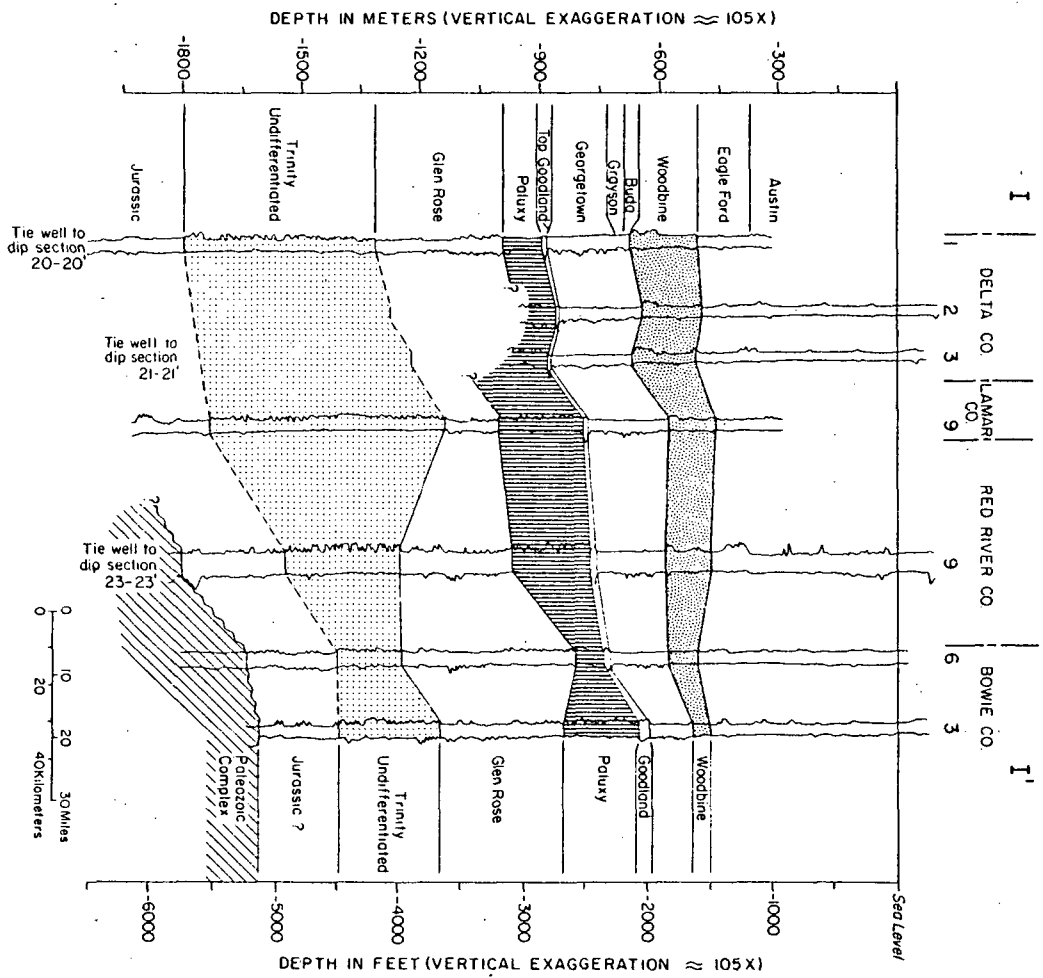


Figure 22. Strike-oriented cross section I-I' (see figure 4 for location; see appendix for individual well data).

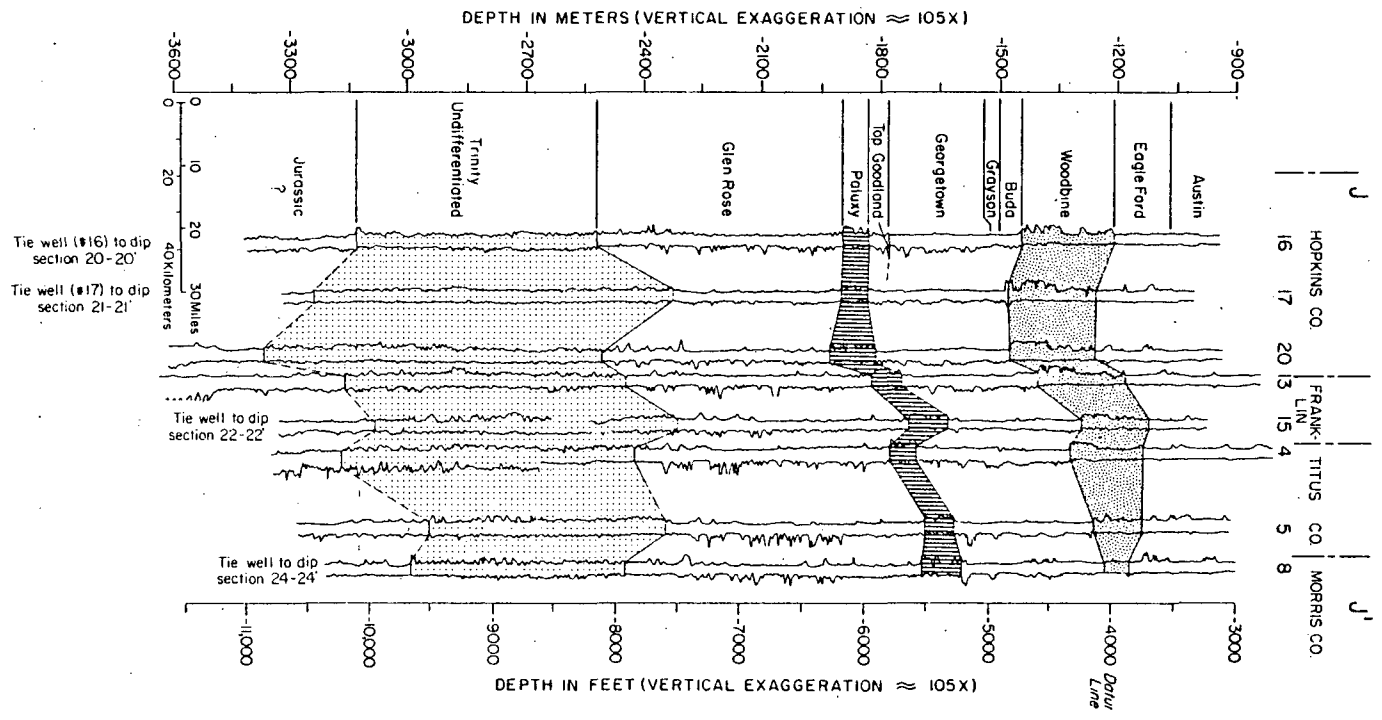


Figure 23. Strike-oriented cross section J-J' (see figure 4 for location; see appendix for individual well data).

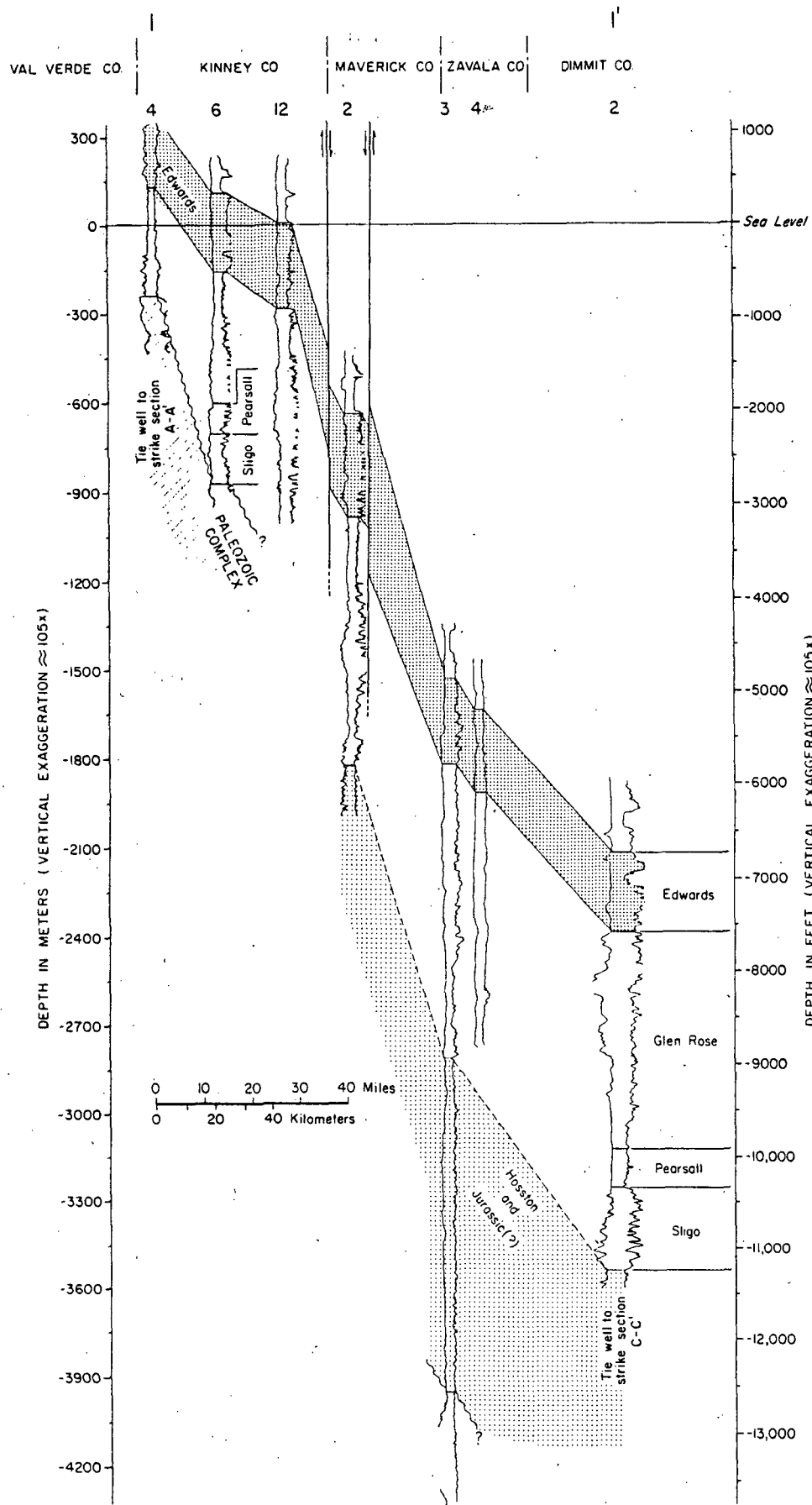


Figure 24. Dip-oriented cross section 1-1' (see figure 4 for location; see appendix for individual well data).

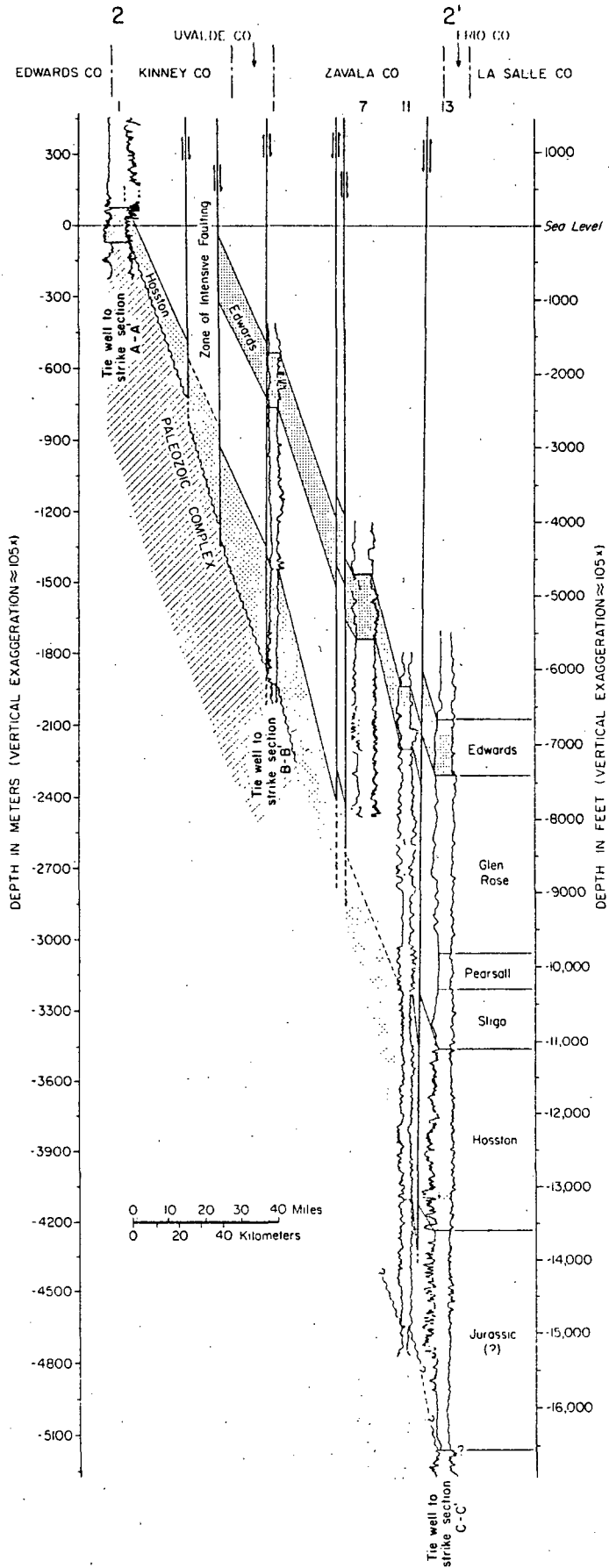


Figure 25. Dip-oriented cross section 2-2' (see figure 4 for location; see appendix for individual well data).

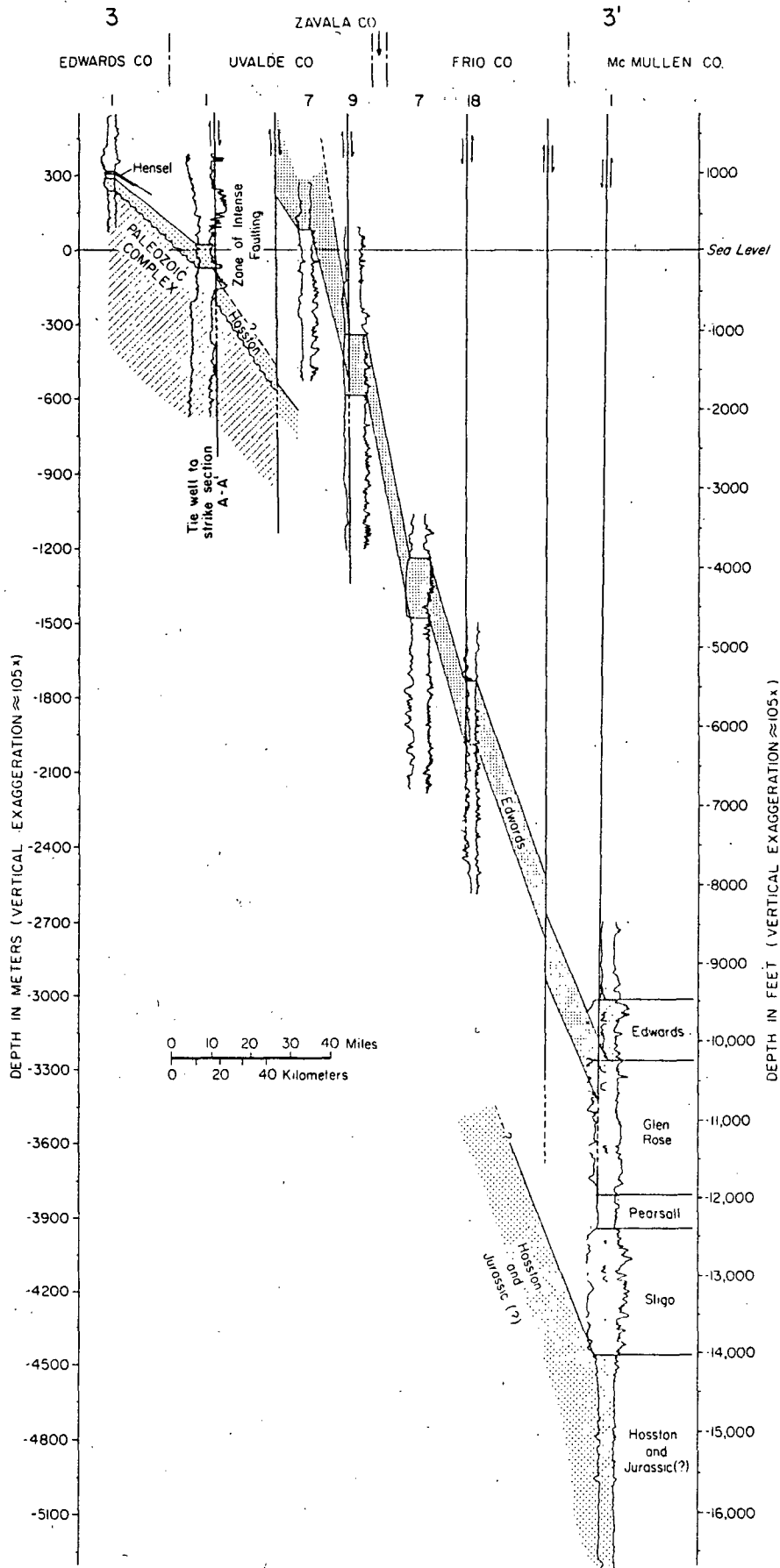


Figure 26. Dip-oriented cross section 3-3' (see figure 4 for location; see appendix for individual well data).

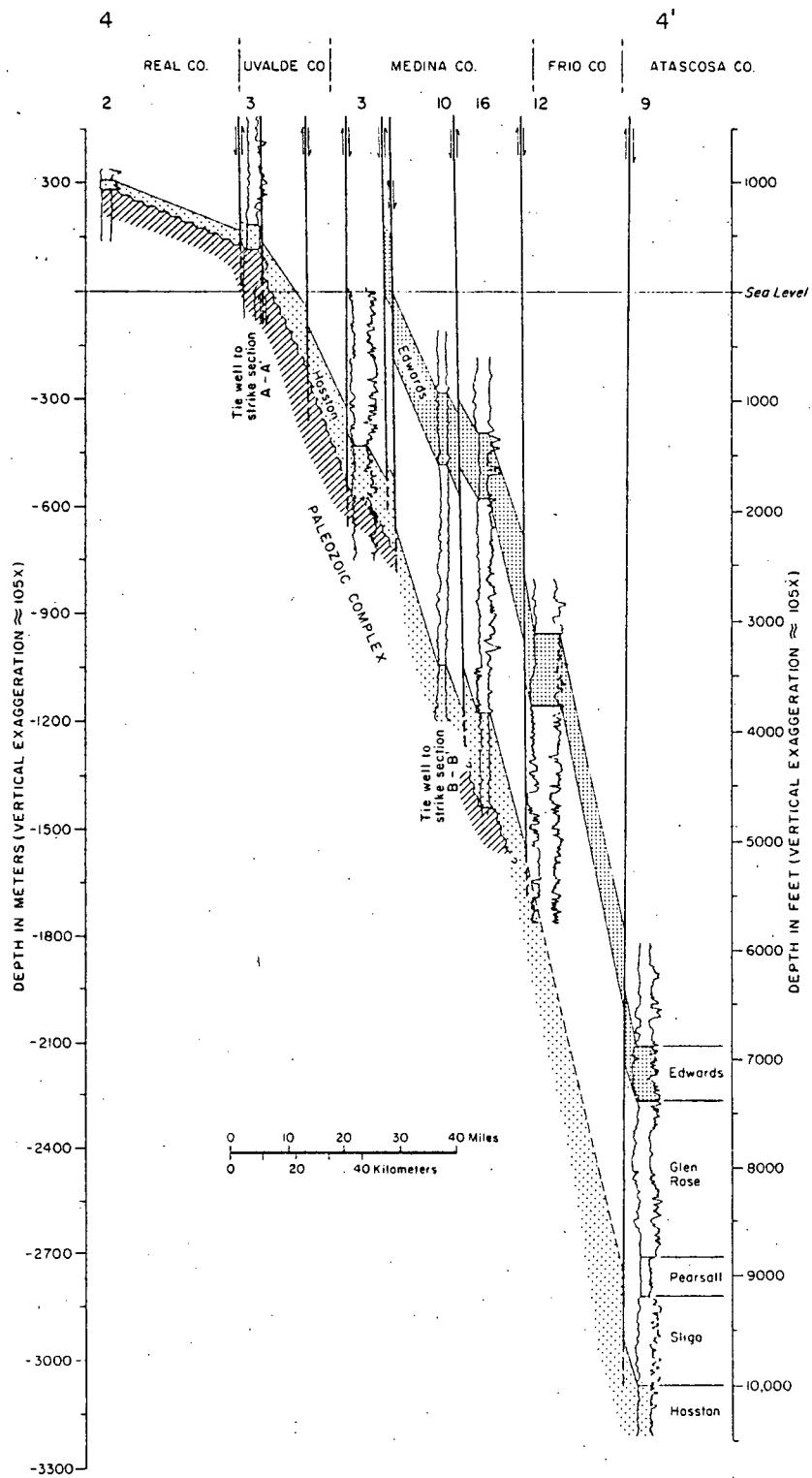


Figure 27. Dip-oriented cross section 4-4' (see figure 4 for location; see appendix for individual well data).

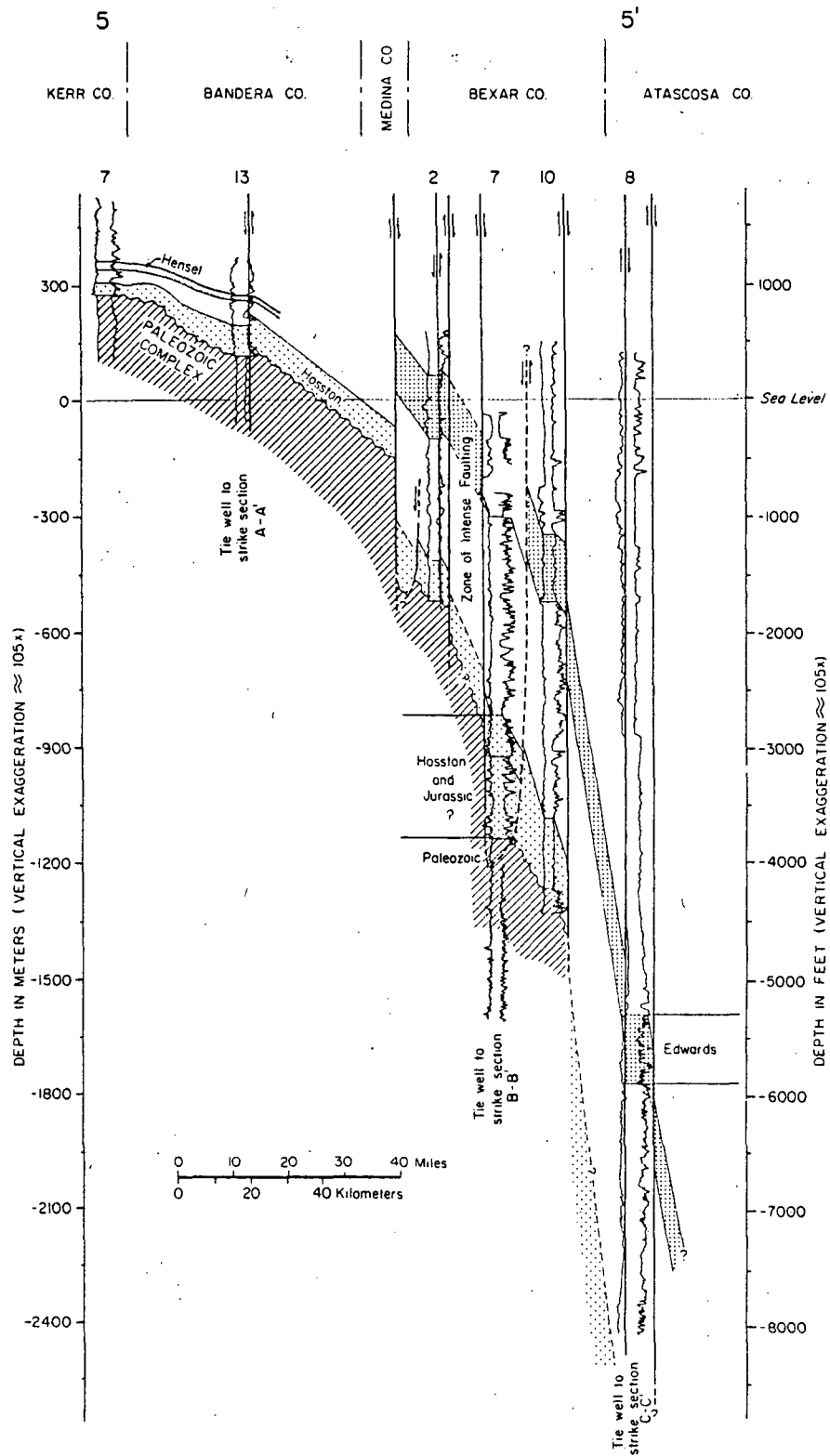


Figure 28. Dip-oriented cross section 5-5' (see figure 4 for location; see appendix for individual well data).

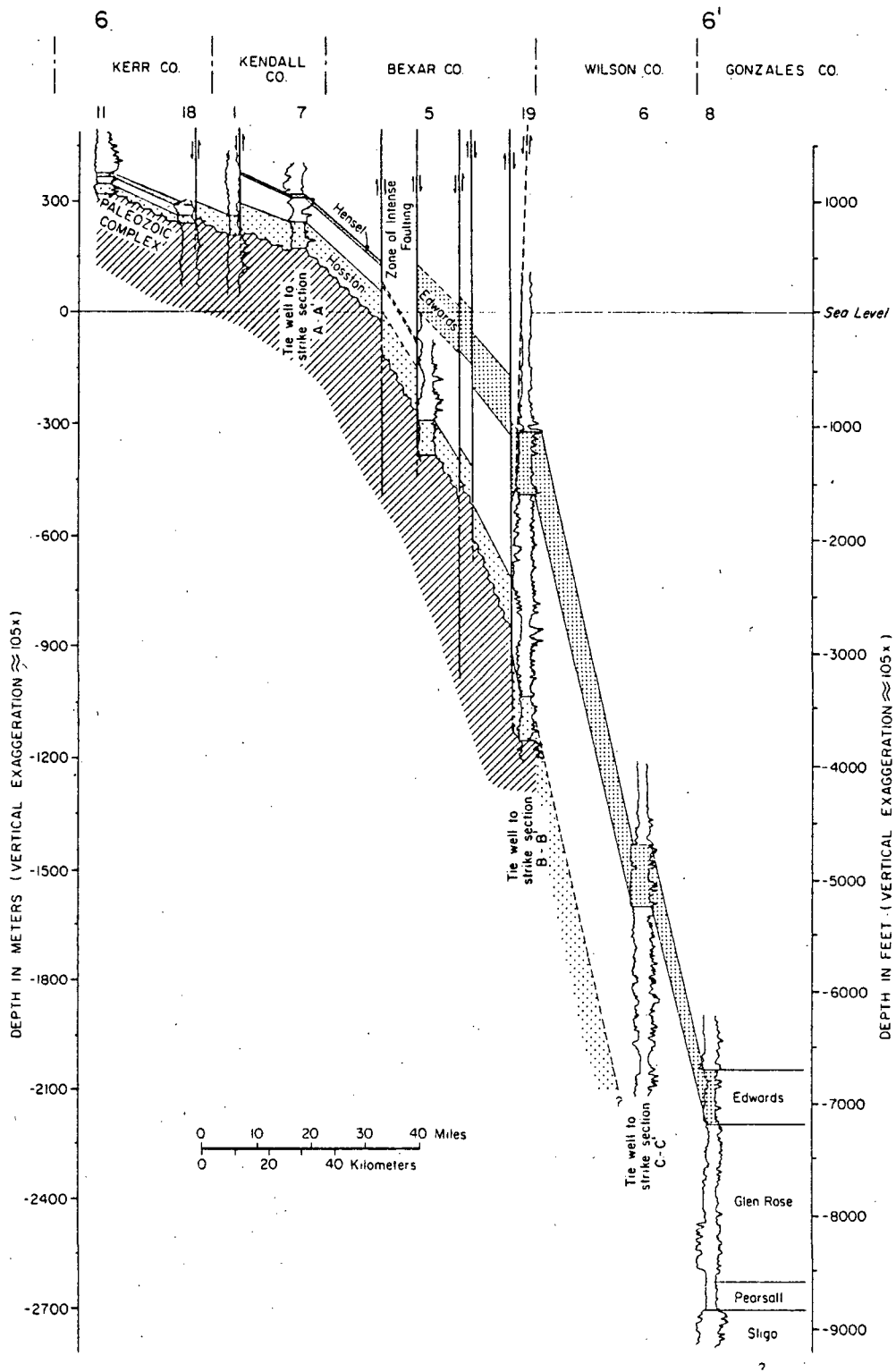


Figure 29. Dip-oriented cross section 6-6' (see figure 4 for location; see appendix for individual well data).



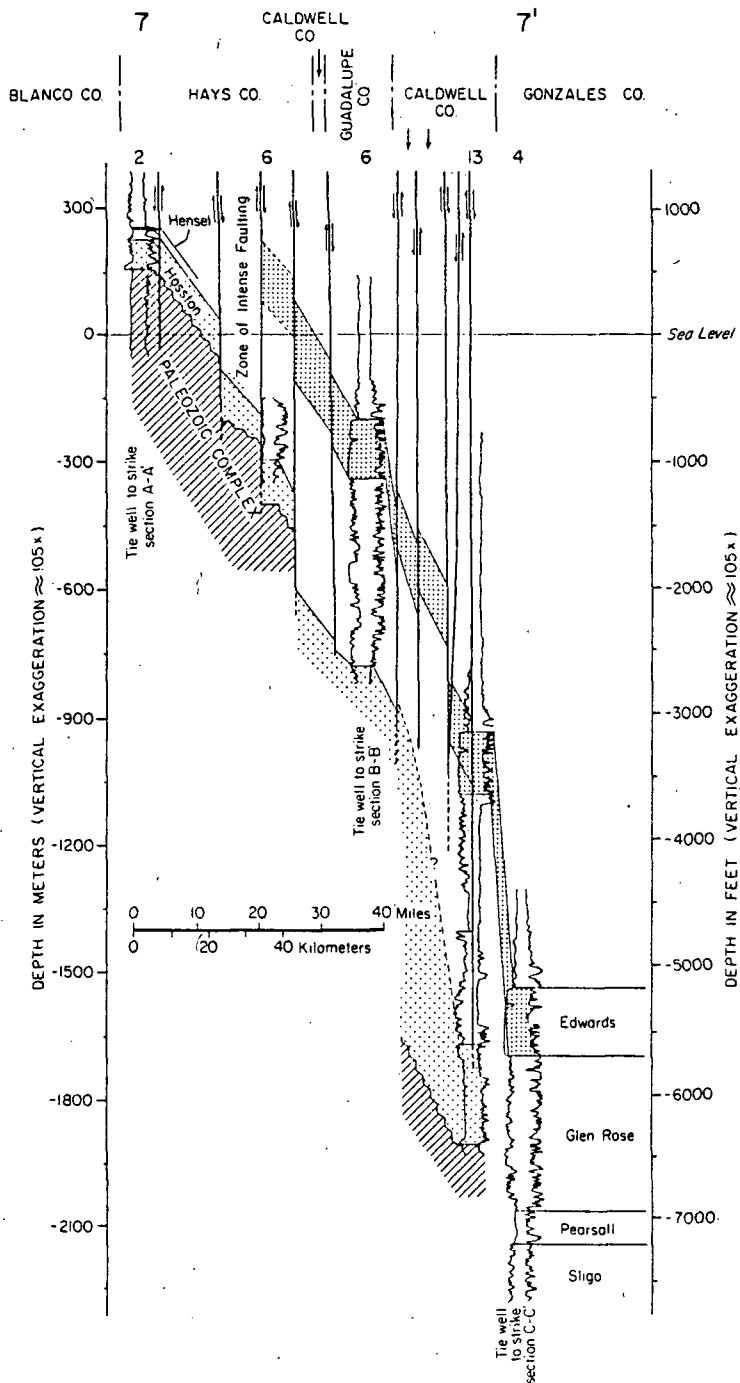


Figure 30. Dip-oriented cross section 7-7' (see figure 4 for location; see appendix for individual well data).

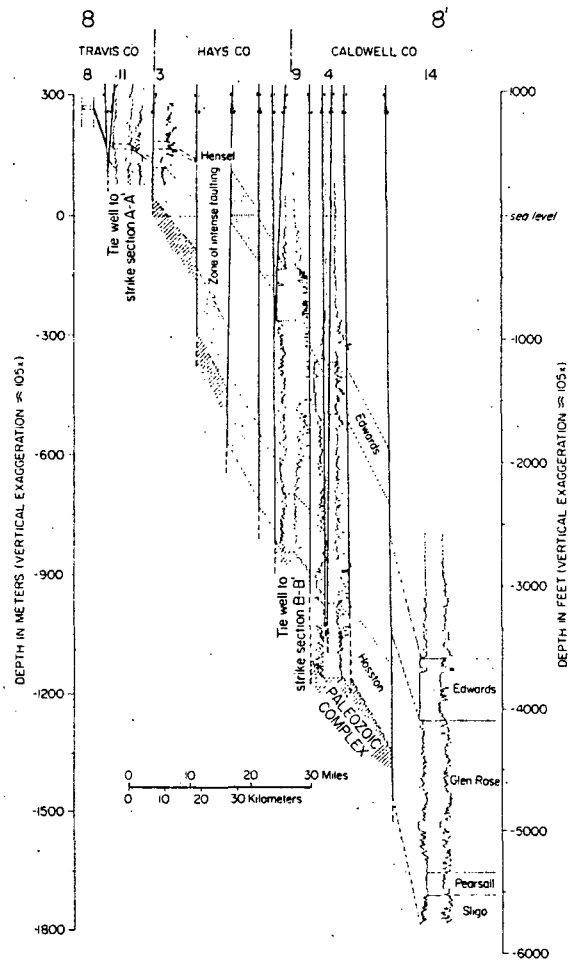


Figure 31. Dip-oriented cross section 8-8' (see figure 4 for location; see appendix for individual well data).

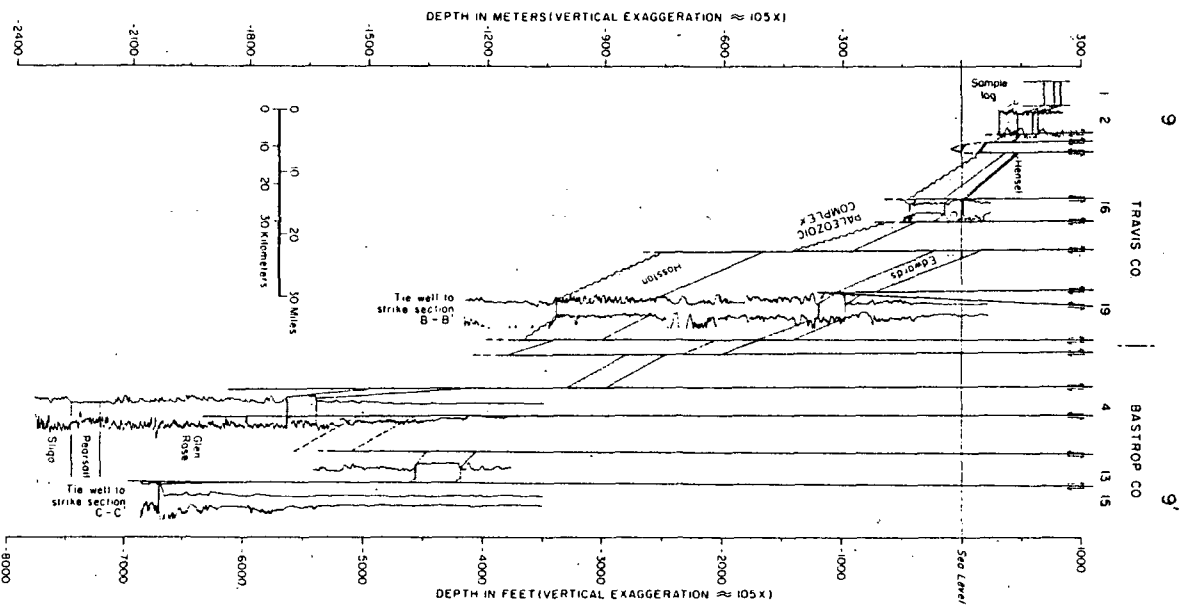


Figure 32. Dip-oriented cross section 9-9' (see figure 4 for location; see appendix for individual well data).

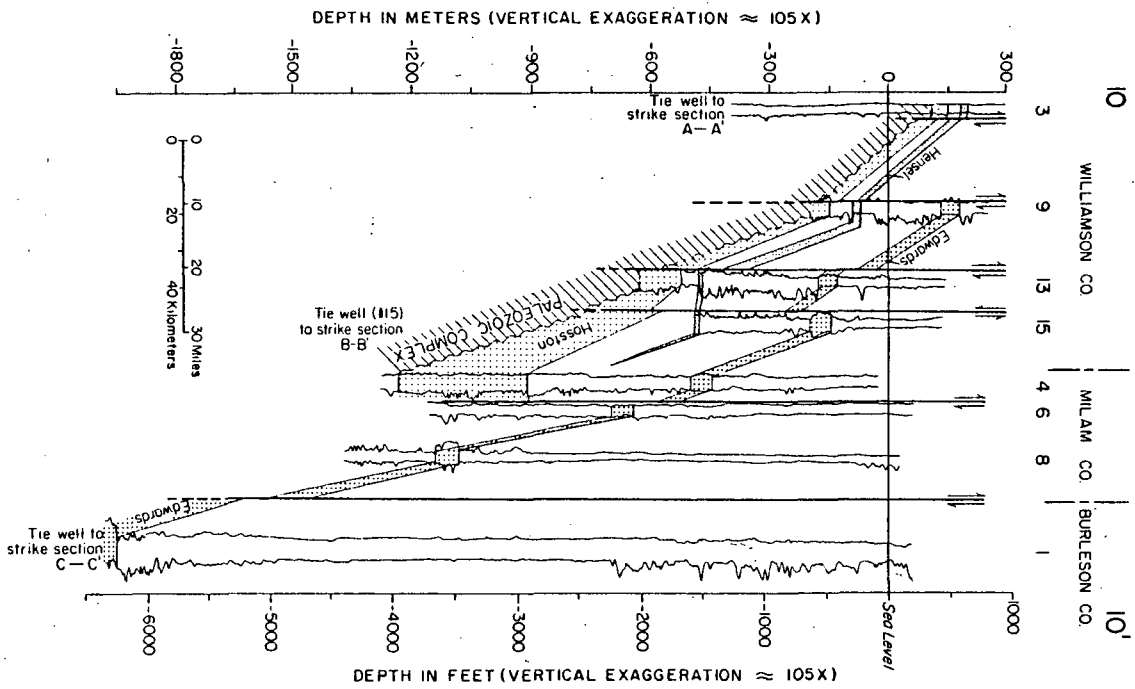


Figure 33. Dip-oriented cross section 10-10' (see figure 4 for location; see appendix for individual well data).

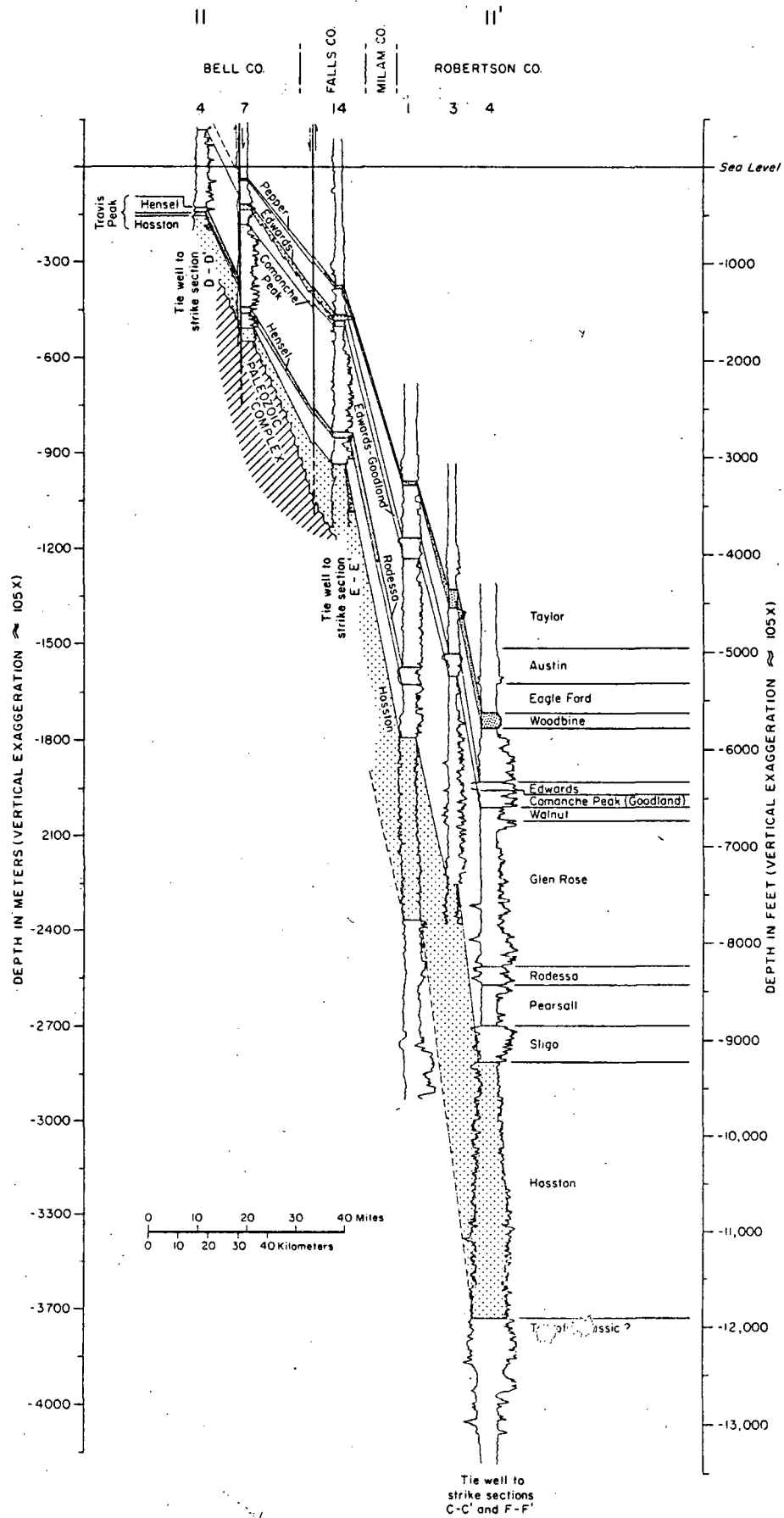


Figure 34. Dip-oriented cross section 11-11' (see figure 4 for location; see appendix for individual well data).

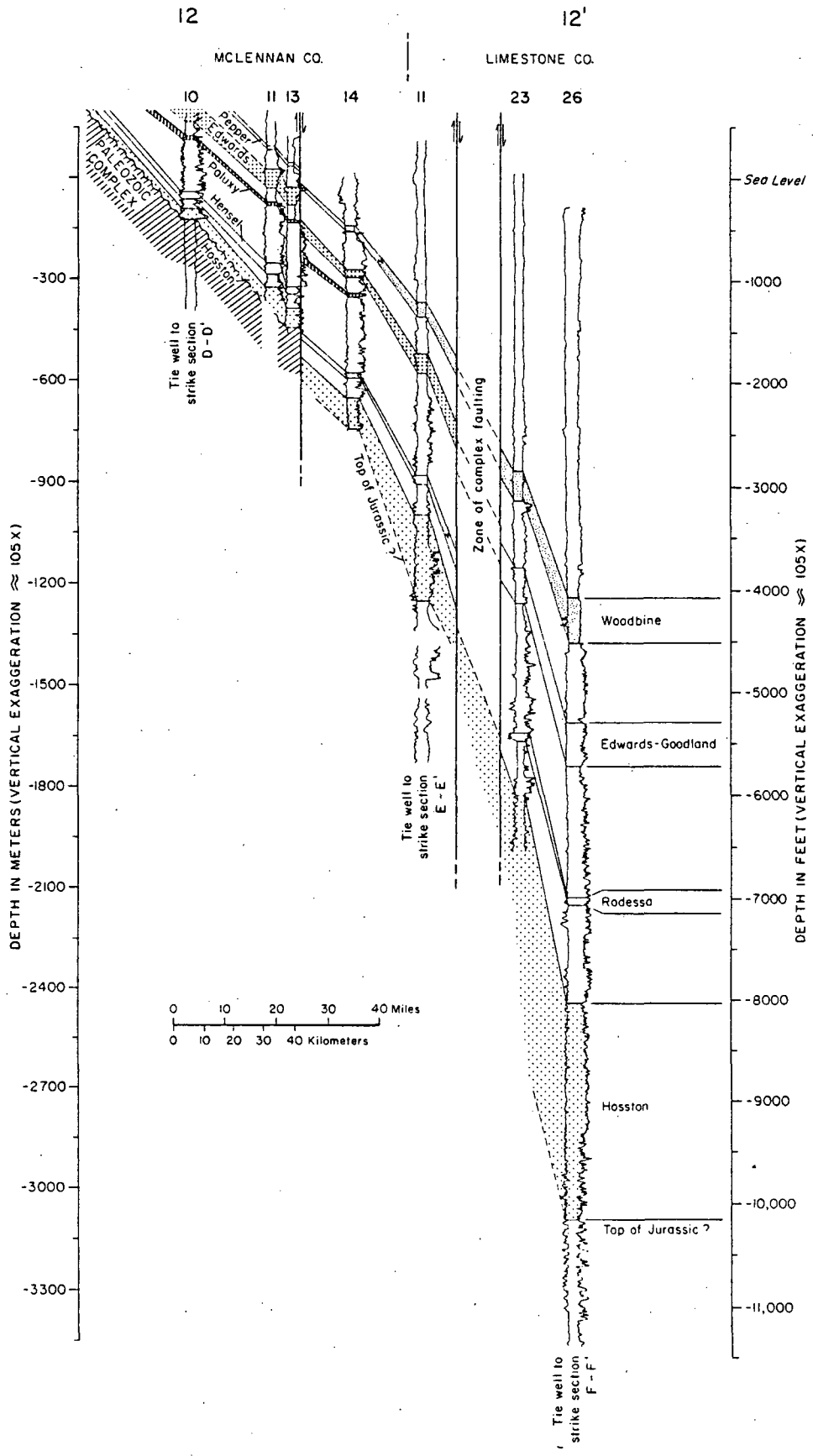


Figure 35. Dip-oriented cross section 12-12' (see figure 4 for location; see appendix for individual well data).

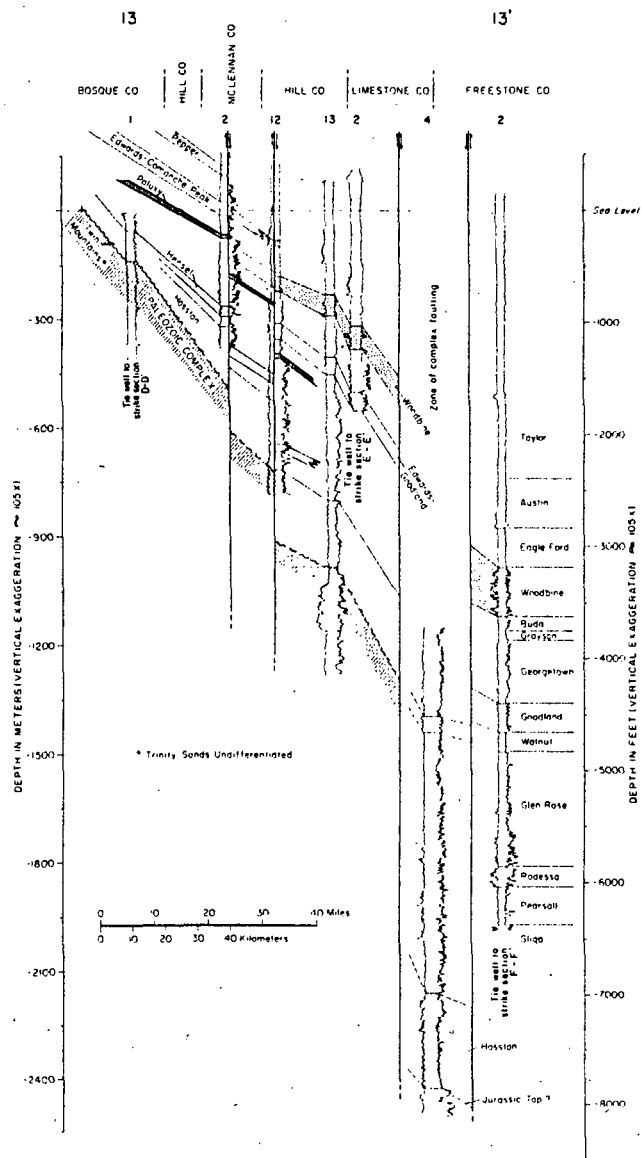


Figure 36. Dip-oriented cross section 13-13' (see figure 4 for location; see appendix for individual well data).

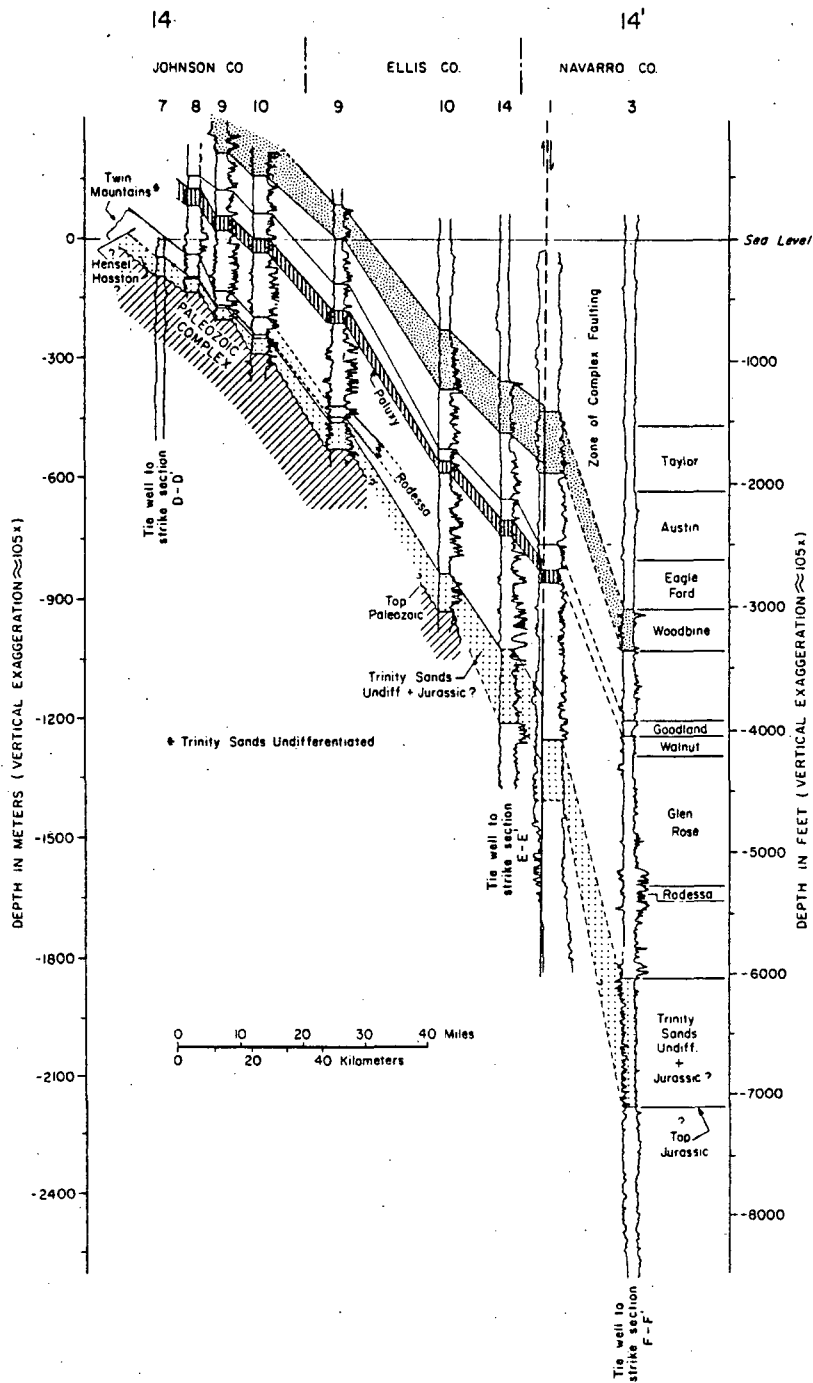


Figure 37. Dip-oriented cross section 14-14' (see figure 4 for location; see appendix for individual well data).



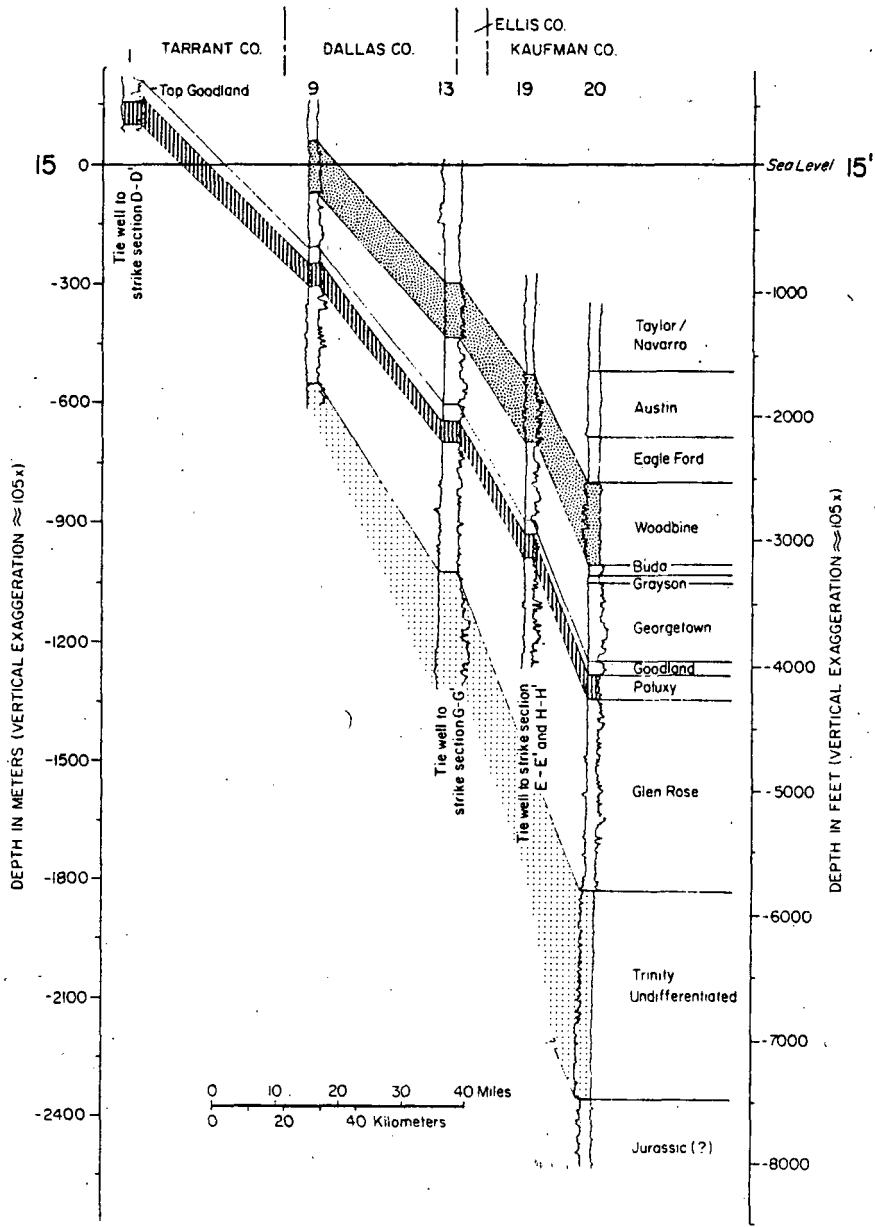


Figure 38. Dip-oriented cross section 15-15' (see figure 4 for location; see appendix for individual well data).

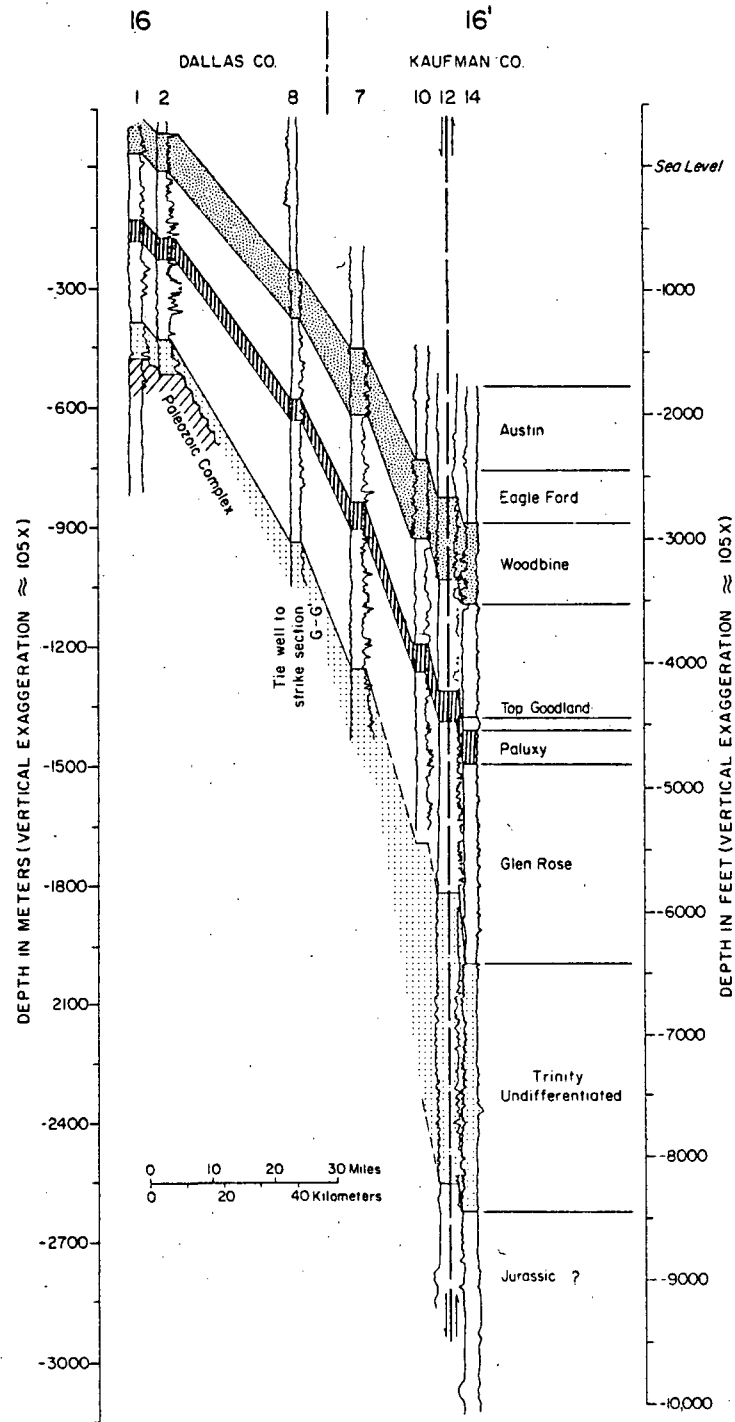


Figure 39. Dip-oriented cross section 16-16' (see figure 4 for location; see appendix for individual well data).

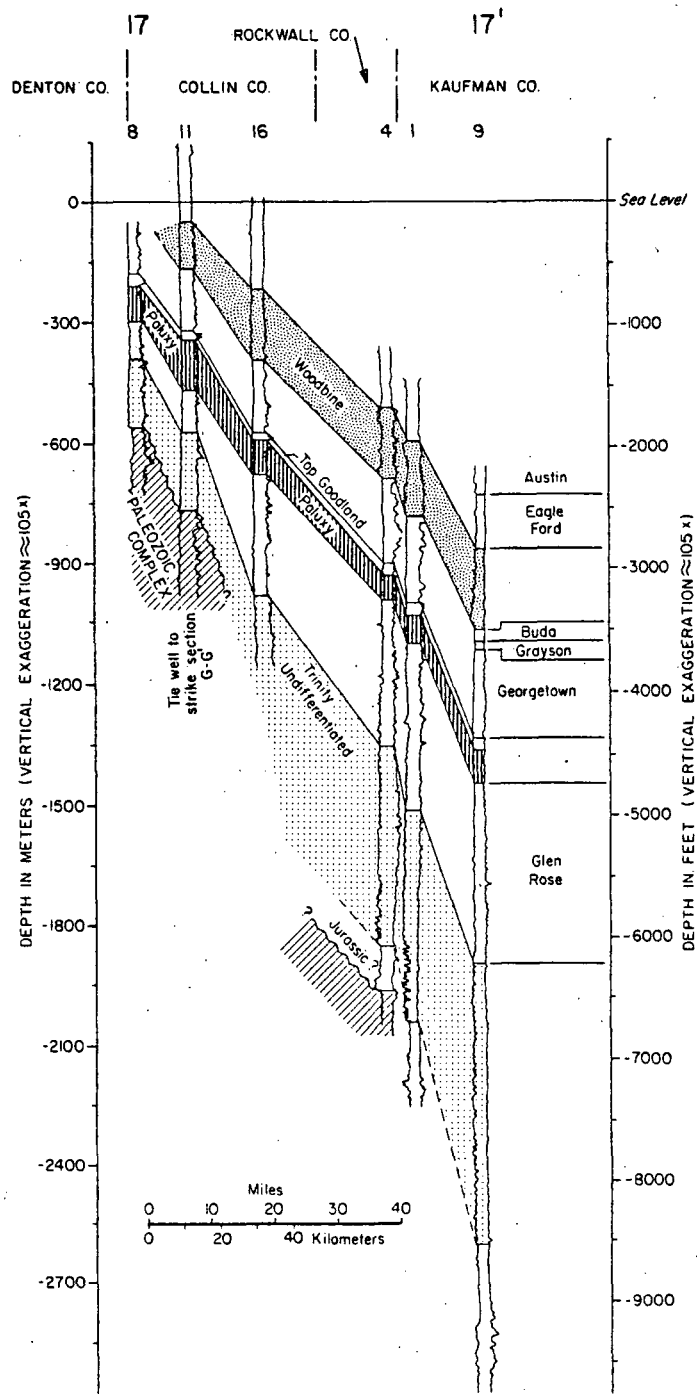


Figure 40. Dip-oriented cross section 17-17' (see figure 4 for location; see appendix for individual well data).

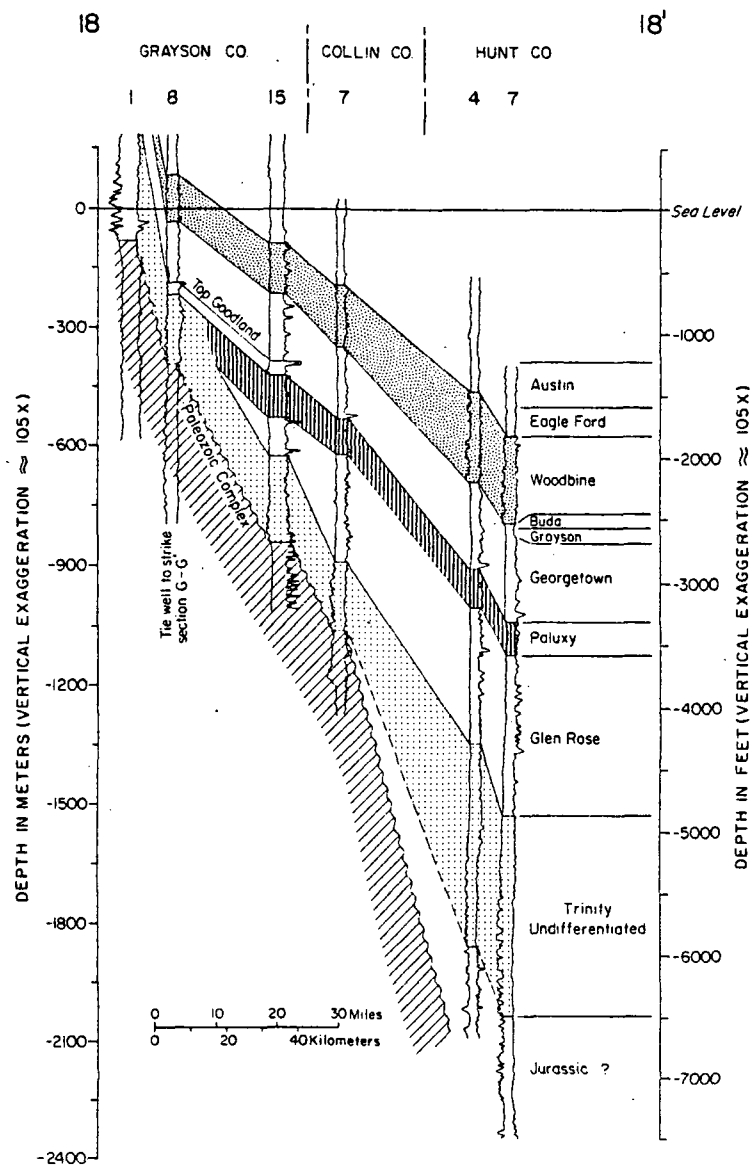


Figure 41. Dip-oriented cross section 18-18' (see figure 4 for location; see appendix for individual well data).

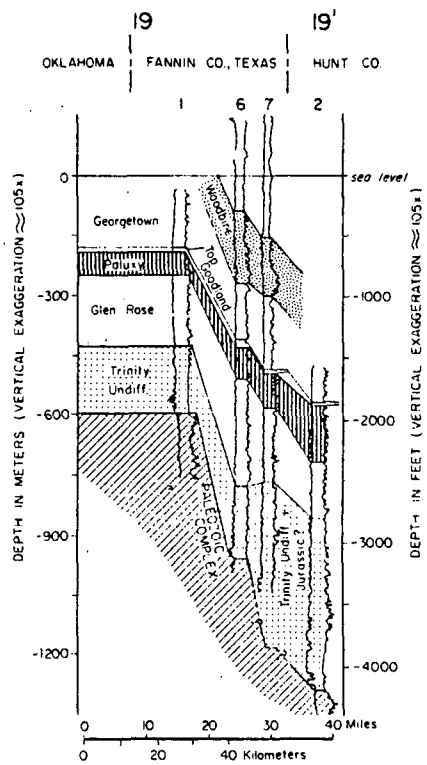


Figure 42. Dip-oriented cross section 19-19' (see figure 4 for location; see appendix for individual well data).

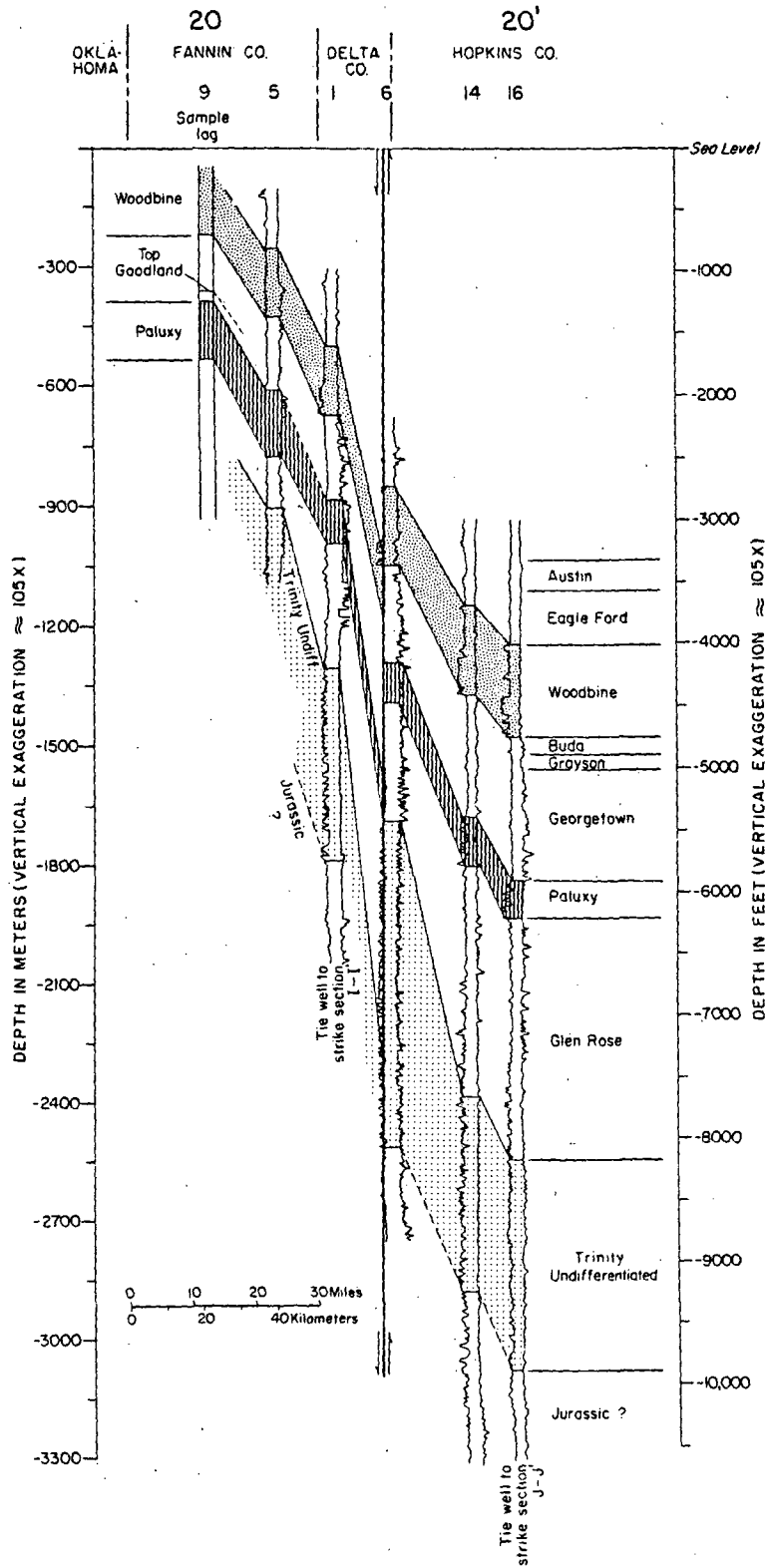


Figure 43. Dip-oriented cross section 20-20' (see figure 4 for location; see appendix for individual well data).

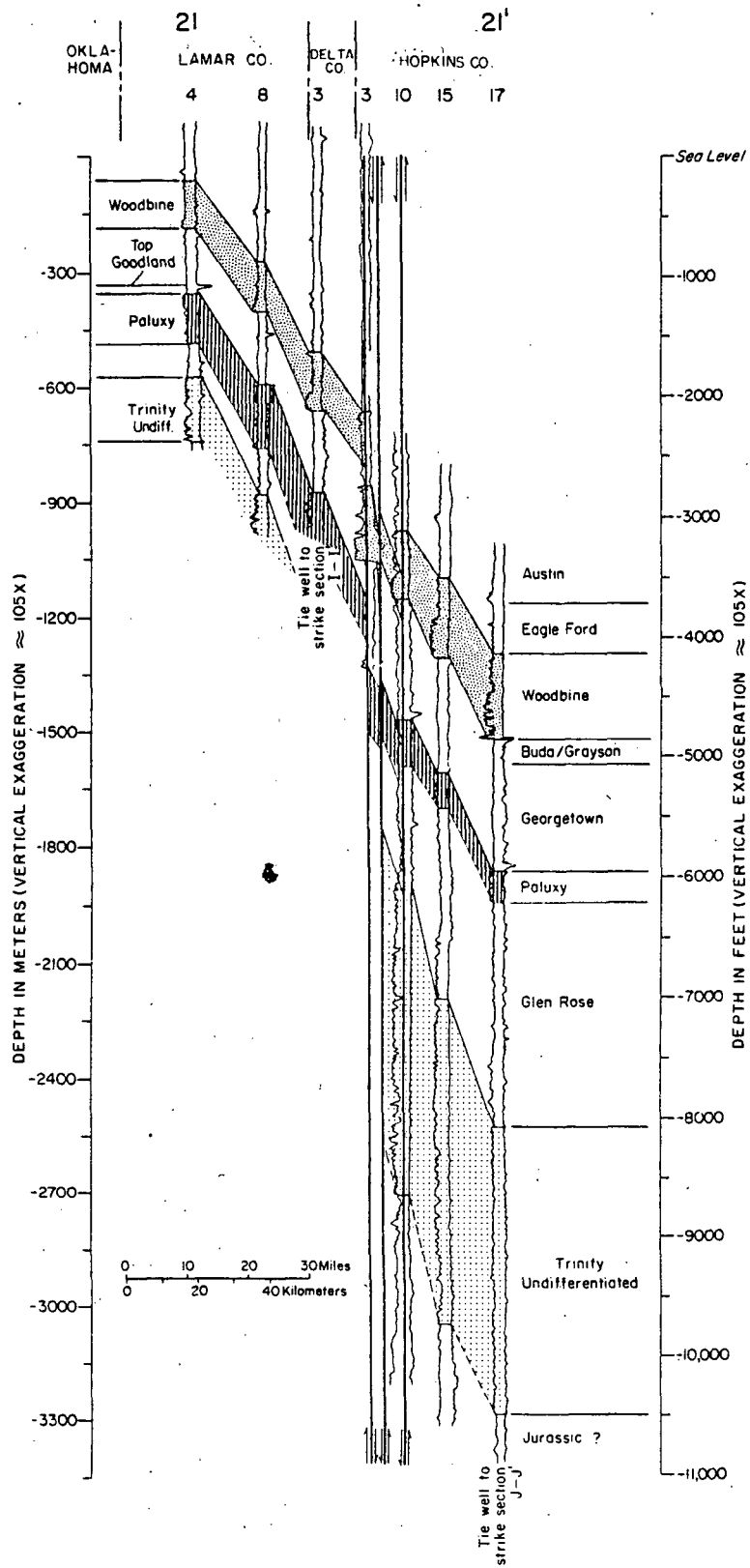


Figure 44. Dip-oriented cross section 21-21' (see figure 4 for location; see appendix for individual well data).

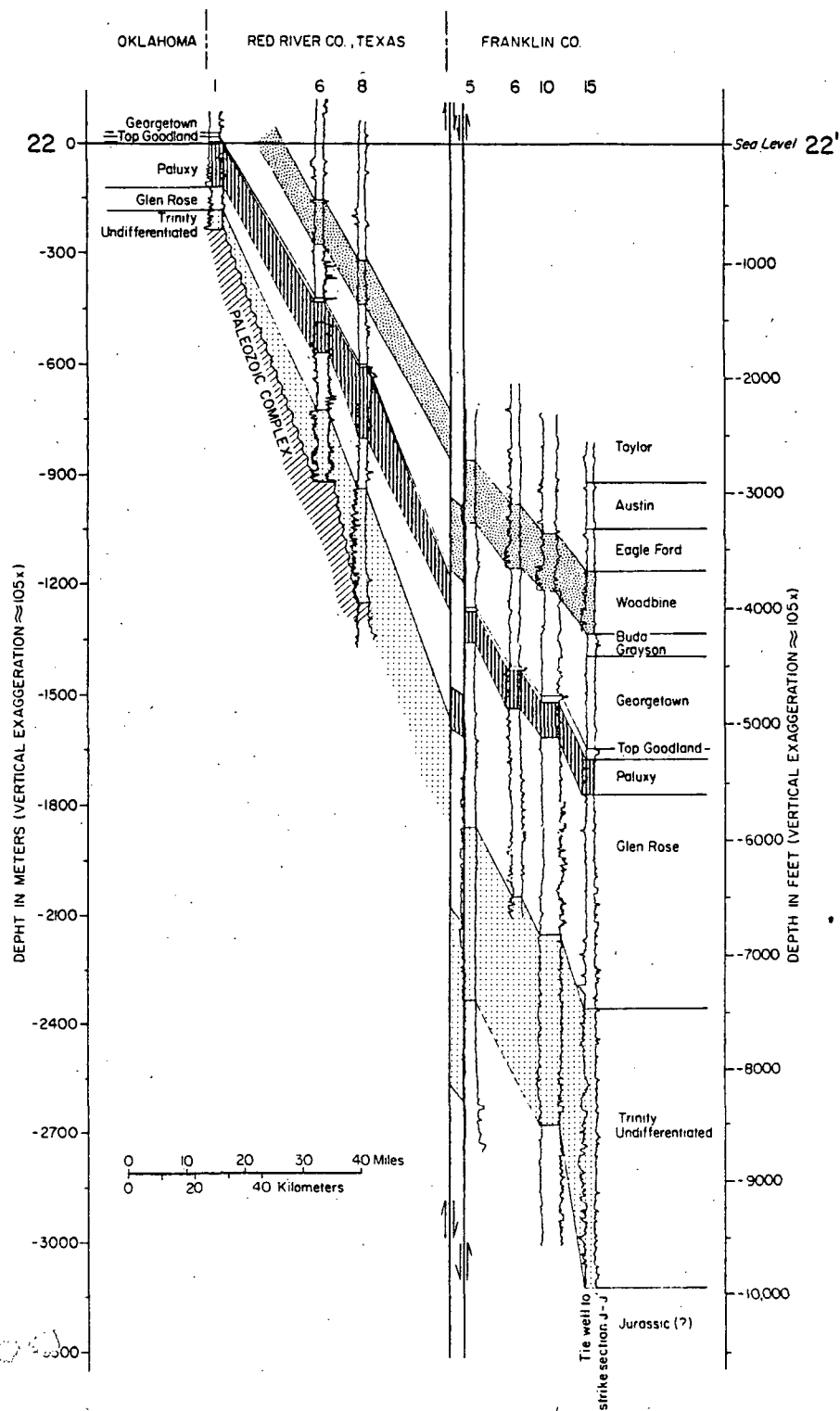


Figure 45. Dip-oriented cross section 22-22' (see figure 4 for location; see appendix for individual well data).





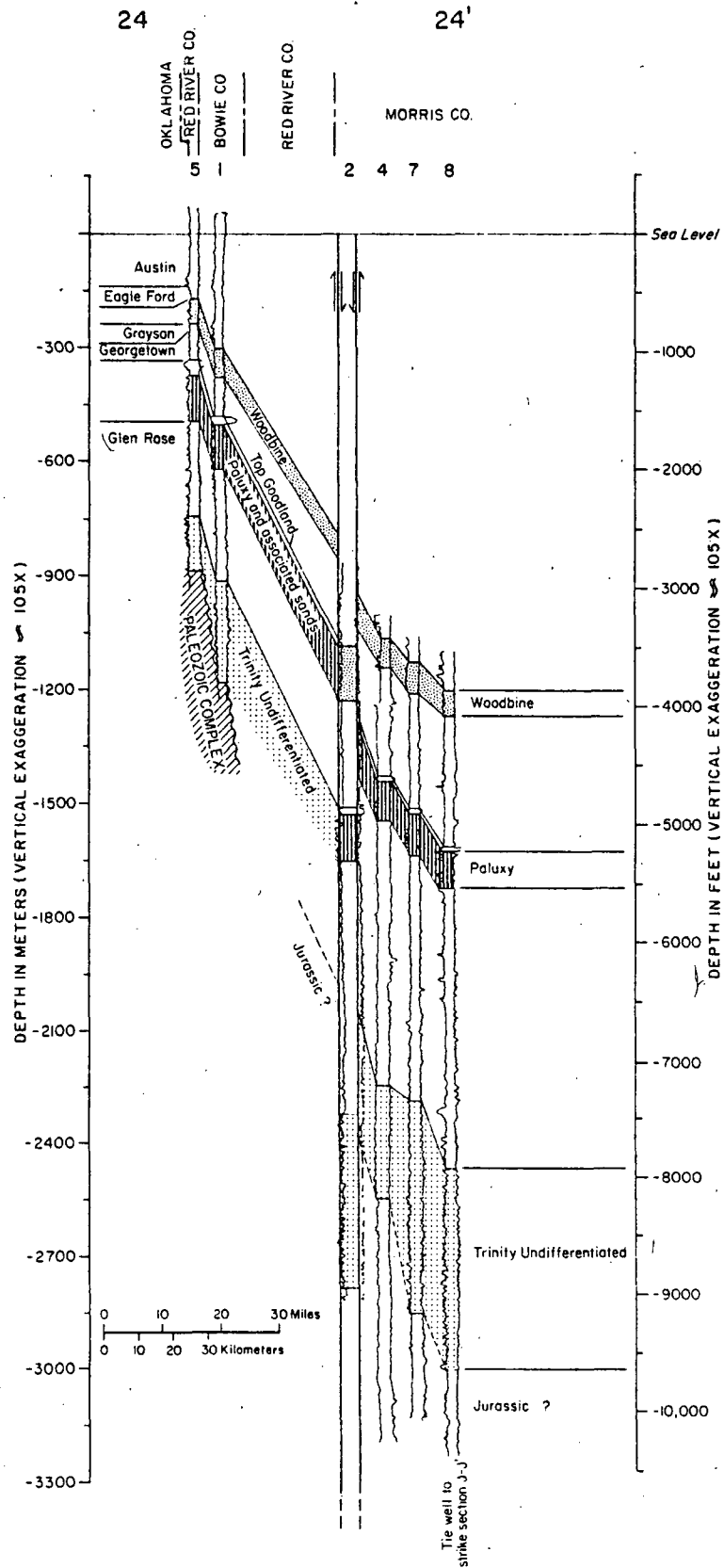


Figure 47. Dip-oriented cross section 24-24' (see figure 4 for location; see appendix for individual well data).

TRAVIS CO.

Woodward

I-Nelson

DALLAS CO.

Guiberson & Lucy

I-Moyer

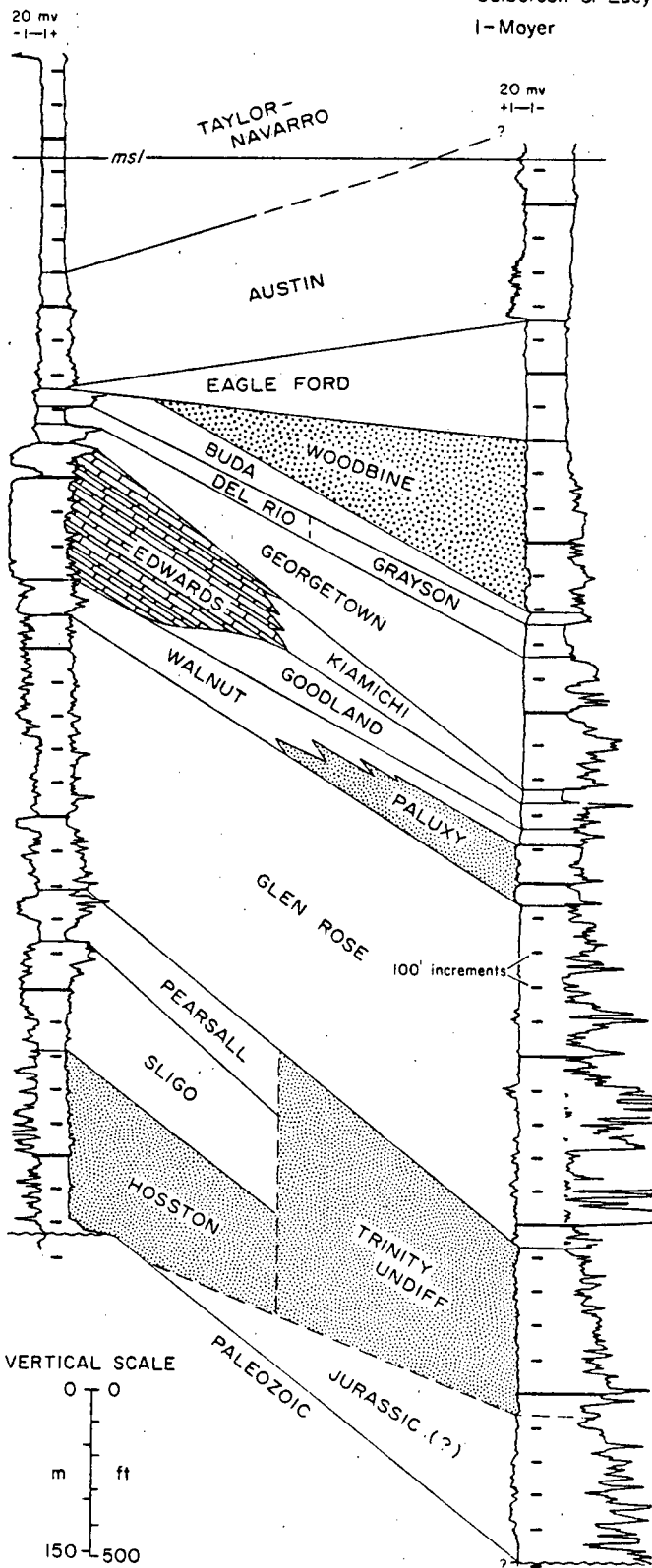


Figure 48. Typical electric logs showing geologic units in Travis County and Dallas County.

## PRE-CRETACEOUS SURFACE

### General

Pre-Cretaceous rocks exposed in the study region consist of Precambrian igneous and metamorphic rocks that crop out in the Llano area, and the unmetamorphosed Paleozoic "foreland facies" strata (Flawn and others, 1961) that crop out in the Llano area and that occur beneath the Cretaceous strata west of the Balcones Fault Zone. Farther east, in the subsurface, the Ouachita complex becomes progressively more highly deformed and metamorphosed, and dips of the Ouachita rocks become progressively steeper. At the eastern margin of control on the Ouachita complex, there are thick terrigenous and evaporitic (?) strata of presumed Jurassic age.

Pre-Cretaceous rocks have affected both composition and geometry of the Cretaceous aquifers in the region investigated. This is because the pre-Cretaceous rocks constituted source materials for many of the overlying clastic sediments, and the late Paleozoic erosion surface composed the substrate on which the updip parts of the basal Cretaceous sandstone units were deposited. Moreover, pre-Cretaceous physiographic and structural conditions affected areal extent of the depositional environments that resulted in the various facies of Cretaceous strata. For example, the structural hinge defined by the eastern margin of the steeply dipping Ouachita belt marked the locus of change from predominantly terrestrial sedimentation to a marine depositional regime during early Cretaceous time. Although numerous transgressive and regressive migrations of the marine environment occurred throughout the early Cretaceous (Stricklin and others, 1971), the hinge line persisted as a zone of major changes between depositional environments. Examples along this trend include the updip subcrop limit of Jurassic strata and facies changes from terrestrial to marine strata for both the Hosston and Hensel sand units in Central Texas. Moreover, it is along this trend that many of the terrigenous rock units change from being dominantly dip-oriented to being mainly strike-oriented, as the depositional environments changed from fluvial and deltaic systems to lagoonal or marine systems. Commonly, there are also drastic compositional changes in rocks representing the different environments of deposition. The dip-oriented systems are dominantly composed of quartzose sand, whereas the strike-oriented units are made up mainly of carbonate rocks, evaporites, or mud. Because of both compositional effects and geometry of rock bodies, the dip-oriented parts of the various rock units have superior aquifer properties. Porosity and

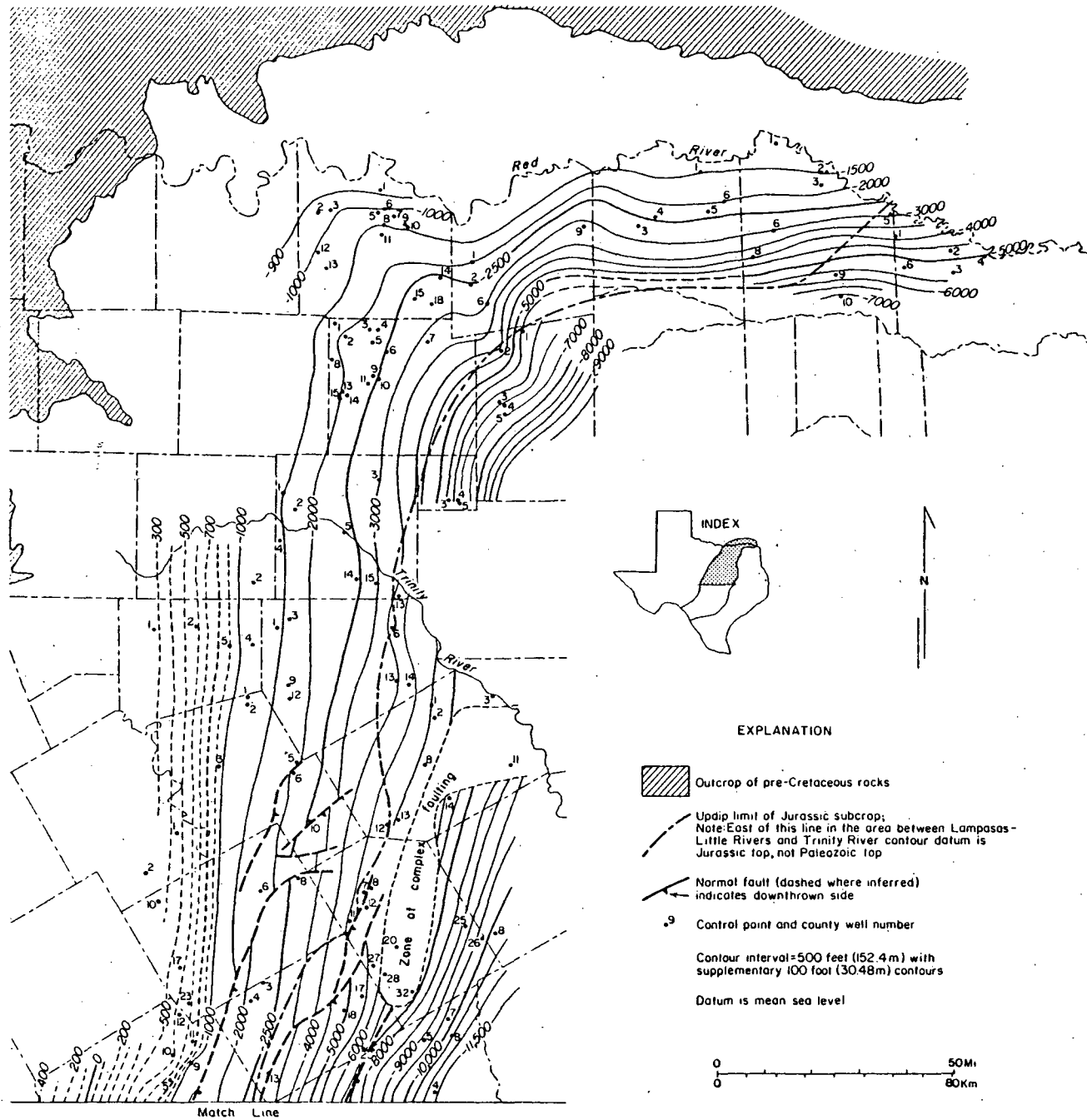
permeability are generally higher for these rocks, hence, expected well yields are greater than for other depositional systems. Also, the dip-oriented geometry ensures adequate hydrologic communication with the outcrop (recharge) area, and this mediates both well yield and water quality aspects.

### Structural Configuration of the Pre-Cretaceous Surface

The hinge zone separating the Texas Craton from the Gulf coastal province is noted on the structural map of the top of the pre-Cretaceous surface (fig. 49) by a marked steepening of dip. West of the hinge zone, dips are less than 70 ft/mi (13m/km), and are commonly less than 20 ft/mi (4m/km) farther inland. East of the hinge, dips of more than 200 ft/mi (38m/km) are common. The hinge also coincides with the main locus of Balcones faulting, which happens to be a zone of sparse well data in south-central Texas; within this area, paucity of well data prevented our extrapolating contours on various maps. Moreover, there is an abrupt compositional change across the hinge; as denoted by Flawn and others (1961), slightly metamorphosed Ouachita strata of recognizable age abut more intensively metamorphic rocks of unknown age.

When viewed in plan, the pre-Cretaceous surface also shows marked changes in strike. A major structural salient occurs at about the location of the San Marcos Platform, where strike changes from approximately northeast-southwest to nearly east-west. A major embayment occurs along an axis that parallels the Preston Anticline in north Texas; there strike changes from a northeast trend to an approximately east-west orientation. It is in this area that the Arbuckle and Ouachita structural trends converge; also this embayment occurs near where the Ouachita structural belt dips beneath the ground surface. These combine to produce a locally complicated subsurface geologic setting.

On the Texas Craton, erosional topographic features on the pre-Cretaceous surface (the Washita Paleoplain of Hill, 1901, p. 363) determined composition, texture, and overall geometry of subsequent Cretaceous rocks. Topographic relief of more than 200 ft (61 m) is mapped in Kerr County. High-relief areas were local sources of sediments during Cretaceous time, and low-topographic areas determined the major sites of early Cretaceous fluvial deposition (Hall, 1976). Across the hinge zone, in the Gulf coastal province, structural downwarping was more important than initial erosional topographic irregularities on the pre-Cretaceous surface in controlling subsequent Cretaceous sedimentation.



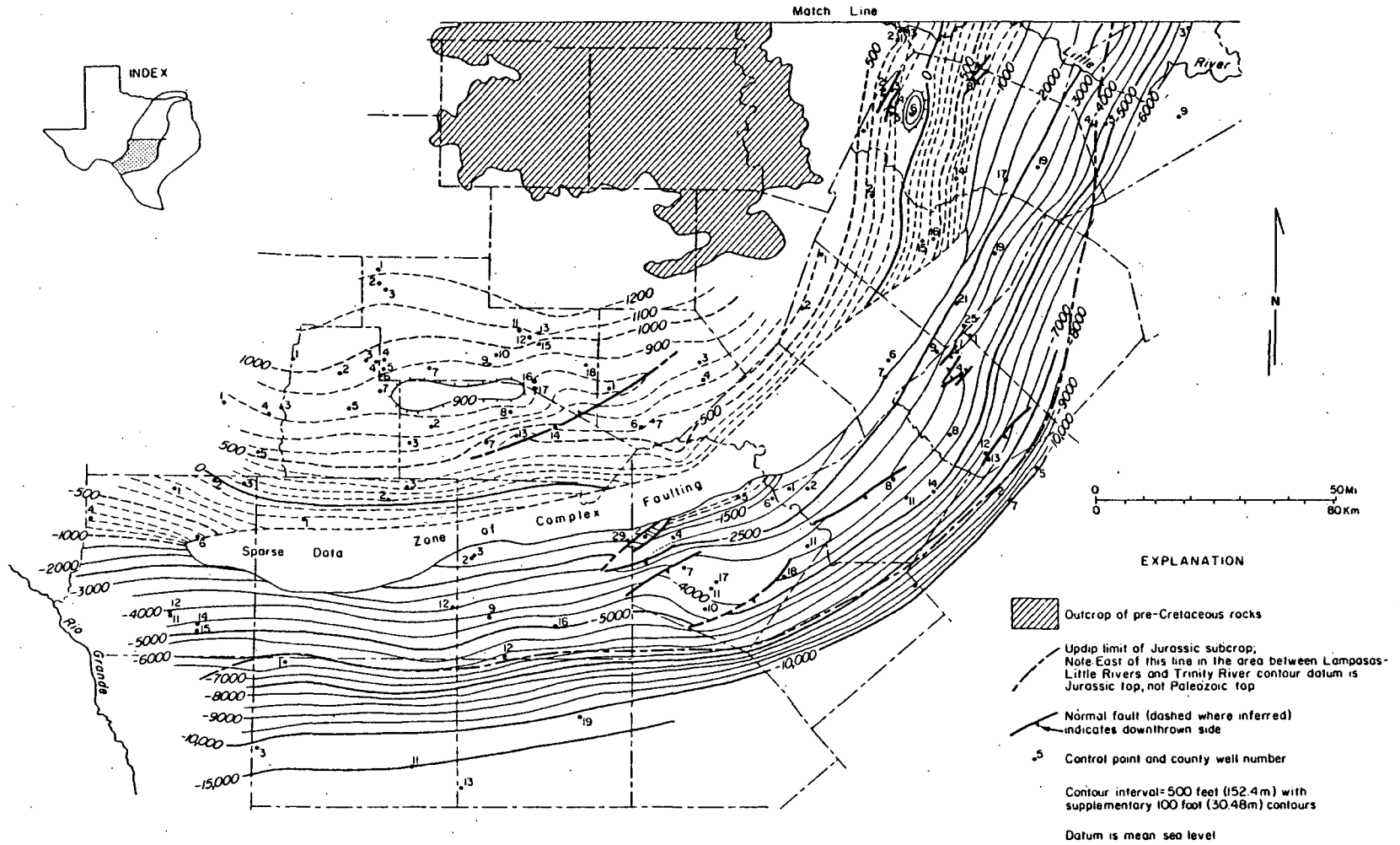


Figure 49. Structural map of pre-Cretaceous surface (on facing pages).

The structural hinge zone marks one of the probable loci of initial rifting of the Gulf of Mexico, as evidenced by the abrupt occurrence of thick sequences of interbedded evaporites and terrigenous clastic sediments composing the presumed Jurassic subcrop (figs. 25, 35, 37, 47). Furthermore, there are very few localities identified where Jurassic(?) strata overlie the Paleozoic basement complex. This relation suggests that during initial rifting, Jurassic strata were formed in a series of periodically subsiding grabens that received terrigenous detritus and that acted as salt flats. Initially, the Ouachita complex was both sediment source and substrate for these Jurassic rocks, but as rifting continued, formation of new (oceanic?) crust and possible local crustal thinning resulted in continued downwarping in the sediment-receiving basins. Tensional forces associated with rifting, coupled perhaps with crustal thinning, resulted in the foundering of the Ouachita Mountains throughout Texas.

The structural scenario presented here is conjectural, but it does affect our formulating hypotheses that explain the origin of anomalous geothermal gradients within the study region. A rift zone is denoted by high heat flow values. Even a "fossil rift" might continue as an area of high heat flow, and given a blanket of insulating sediments (Jurassic[?] and Cretaceous strata), a long-term anomalous geothermal gradient might be the result. Thus, one hypothesis for the source of heat for the warm waters along the Balcones and Luling-Mexia-Talco Fault Zones is that the basement complex there is a relict analogue to the Salton Sea.

Faults provide another explanation of the observed geothermal anomalies. There are numerous normal faults depicted on the structural map of the pre-Cretaceous surface; there are also zones of thrust faulting mapped by Flawn and others (1961). Deep-seated fracture zones might result in anomalously warm ground waters at a relatively shallow depth, and deep circulation of meteoric waters along faults is the prevailing model for the origin of the Hot Springs of Arkansas (Bedinger and others, 1974) and the Warm Springs of western Virginia (Geiser, 1979). Hence, the Ouachita belt may represent a buried analogue to the geothermal conditions at, for instance, Hot Springs, Arkansas.



## HOSSTON AND TRINITY SANDS UNDIFFERENTIATED

### General

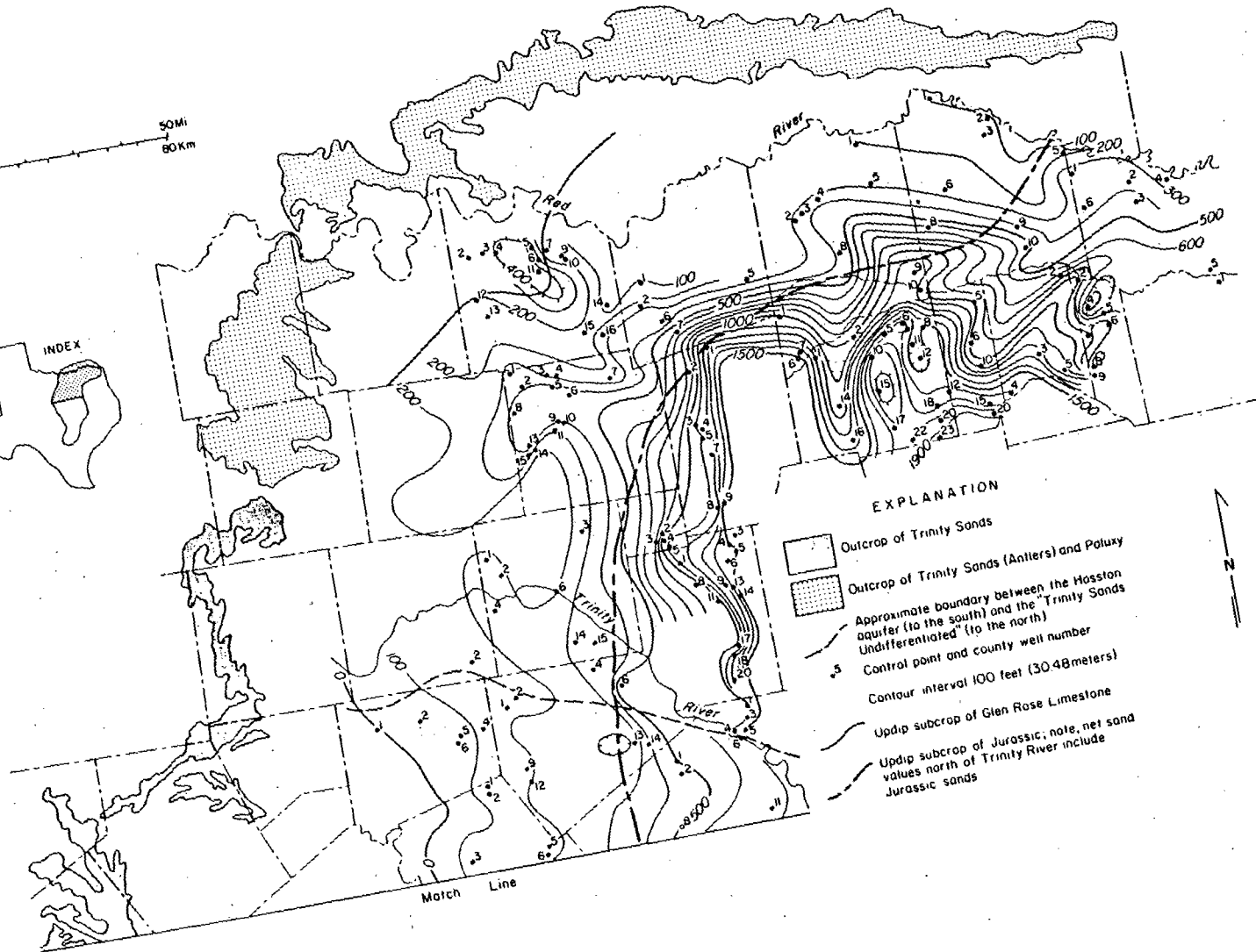
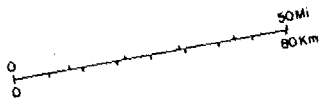
Strata deposited on the pre-Cretaceous surface consist of the various basal Cretaceous sandstone units. These sandstones are mainly riverine or deltaic deposits on the Texas Craton, but across the structural hinge strata, of terrigenous origin and much thicker lagoonal or offshore marine deposits mark the beginning of the Gulf coastal province.

As mentioned previously, the stratigraphy of the Lower Cretaceous units is complex, and this complexity has been exacerbated by diverse and sometimes overlapping or inconsistent names applied to the same or equivalent strata across the region. In hopes of simplifying this situation, while retaining enough of the stratigraphic nomenclature to communicate effectively, we refer to the basal Cretaceous units as being "Hosston and Trinity Sands Undifferentiated" (see fig. 12). We have drawn the boundary between the Hosston Sand and the Trinity Undifferentiated along a line parallel to, but southwest of, the Trinity River in Johnson, Tarrant, Ellis, and Navarro Counties. However, this boundary is somewhat arbitrary because the basal Cretaceous sands represent several depositional systems, and although the line separating the Hosston from the Trinity Sands is also a boundary between two of these systems, other system boundaries of equal or greater importance are not shown.

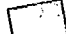




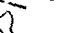

### Net-Sand Distribution of the Hosston/Trinity

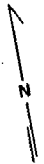
The major depositional systems composing the basal Cretaceous sands are delineated on the basis of aggregate thickness of sand strata as shown on the net-sand map (fig. 50). The values presented here are conservative, as sand thickness of 10 ft (3 m) or less was not included in the computations on which the net-sand map was based. Hence, sand thicknesses are somewhat less than those presented by Hall (1976), even though overall sand trends are the same.

The net-sand map shows clearly distinguishable dip-oriented thick sand trends that correspond to loci of fluvial deposition (fig. 51); the areas between these thick-sand trends are probably interfluvial areas within flood basins or along the delta plains of the Cretaceous river systems. Immediately downdip from the presumed fluvial channels, areas of variable areal extent commonly have either uniform sand thicknesses or have abrupt thickening of sand. These are thought to be deltaic deposits, which are of several types, as suggested by areal geometry and thickness of



**EXPLANATION**

-  Outcrop of Trinity Sands
-  Outcrop of Trinity Sands (Antlers) and Poluxy
-  Approximate boundary between the Hosston aquifer (to the south) and the "Trinity Sands Undifferentiated" (to the north)
-  Control point and county well number
-  Contour interval 100 feet (30.48 meters)
-  Updip subcrop of Glen Rose Limestone
-  Updip subcrop of Jurassic; note, net sand values north of Trinity River include Jurassic sands



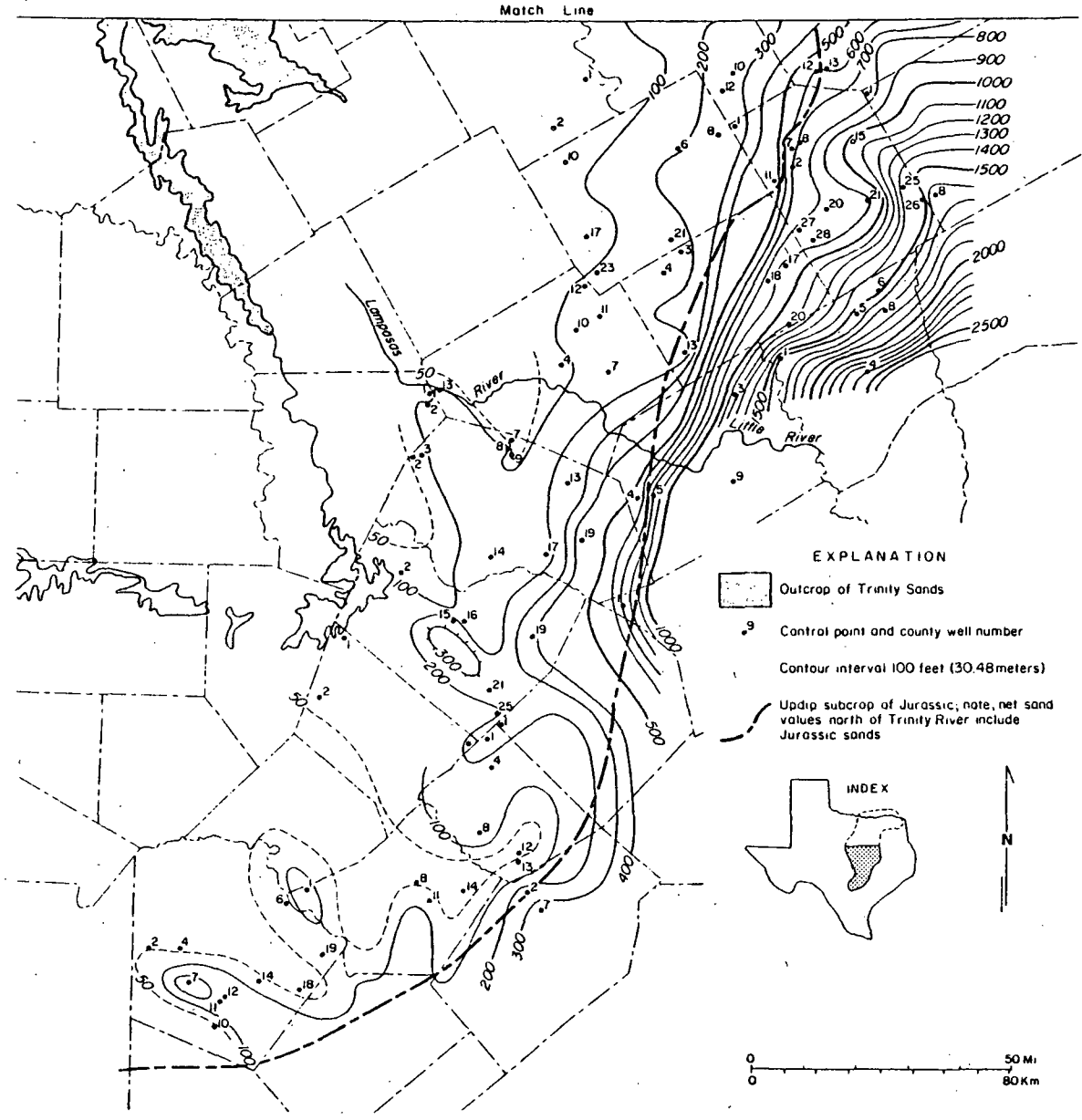


Figure 50. Net sand thicknesses of the Hosston/Trinity (on facing pages).

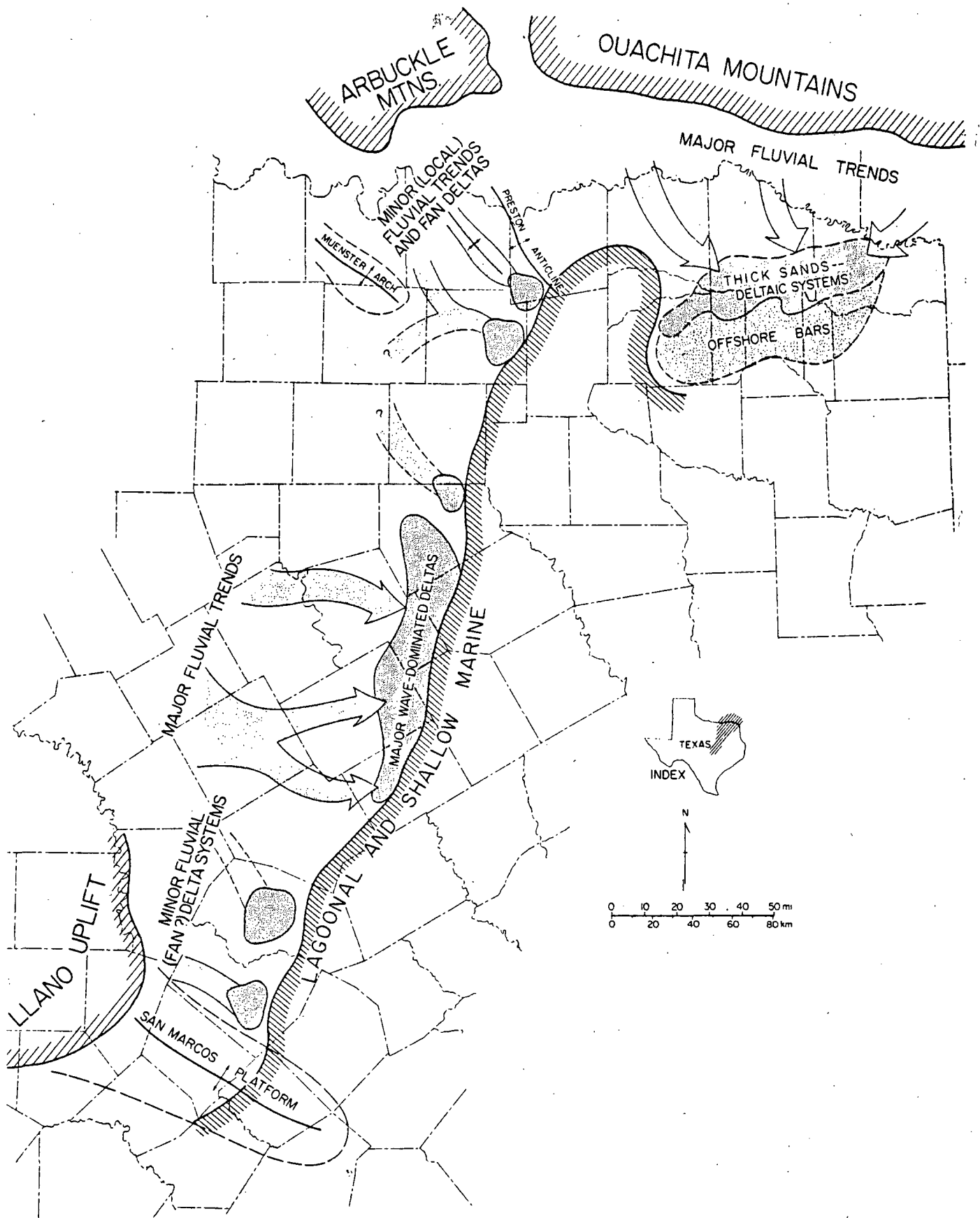


Figure 51. Schematic Hosston/Trinity paleogeographic map.

sand bodies. Some dip-oriented feeder systems terminate either without a broad expanse of sand of uniform thickness or without localized abrupt thickening of sands. We think these represent relatively small fluvial systems that derived sediment from a local source area and that terminated as small fan deltas. The largest of these occur in Grayson and Collin Counties, and lie within the Sherman Syncline. The headwaters of these fan systems probably drained the Arbuckle or Ouachita Mountains, which are only about 75 mi (121 km) to the north. A second type of delta occurs from Falls County north to Ellis County, in which the sand patterns occur as a broad expanse of sands of equal thickness. Hall (1976) has proposed that these represent high-destructive wave dominated deltas. The riverine part of this fluvial-deltaic system is the best documented of any of the Lower Cretaceous sand deposits, and the configuration of these ancient river systems coincides with the parts of the Hosston aquifer having highest yields and best water quality (Henningesen, 1962). The third type of delta occurs in northeast Texas. It has clearly delineated tributary feeder systems that course off the Ouachita uplands. These fluvial deposits terminate in a delta of a form similar to the high-destructive type in Central Texas, but there are also distal sand bodies of relatively great thickness, suggesting a delta-front sand deposit. This would seem to require protection from intense waves and currents (in contrast to the processes acting on the high-destructive delta system). Probably, in this area the Trinity sands were protected from wave action--perhaps by the Sabine Uplift farther south. The delta-front sands of this system offer some of the thickest terrigenous sand deposits in the region, yet these thick sands are not directly related to the outcrop of Trinity Sands only a few tens of miles to the north. Thus recharge probably does not readily occur between the fluvial systems and the sands of the offshore bar facies.

The lagoonal, prodelta, or other marine systems are denoted by abrupt increases in "sand" thicknesses beginning near the structural hinge zone where dips increase precipitously into the Gulf Coast Basin (fig. 34). Much of the apparent sand composing these deposits, however, is carbonate sand, such as dolomite or oolites (Bebout, 1977). Too, the abnormal thickening is partly caused by the probable inclusion of Jurassic strata as part of the aggregate sands measured as Hosston or Trinity Undifferentiated. These thick carbonate sand deposits are of a different genetic system from the dip-fed fluvial-deltaic sand bodies, and hence they are not in direct hydrologic communication with either the recharge areas or the major producing zones of the aquifers. Because of these genetic-geometrical relations, we have focused almost entirely on the geothermal aquifer properties of the fluvial and deltaic deposits that occur on the

Texas Craton. No water data exist for the lagoonal or marine shelf systems, but we project that water yields would probably be low and of limited duration, and adverse water quality conditions would pose problems with use.

### Structural Configuration of the Hosston/Trinity

The structural configuration of the Hosston/Trinity Sands (fig. 52) largely reflects the underlying pre-Cretaceous surface. The hinge zone marking the boundary between the Texas Craton and the Gulf coastal province persisted into Cretaceous time, although the updip limit of Sligo deposition in south-central Texas indicates a transgression of marine conditions during the late stages of Hosston/Trinity deposition. Other structural or topographic irregularities present on the late Paleozoic surface also apparently affected the Hosston/Trinity depositional configuration; for example, the salient that marks the change in strike orientation near the San Marcos Platform persists, as does the embayment in North Texas. The Preston Anticline and the Sherman Syncline appear on both structural maps, as does the (unnamed) high-relief area in Kerr County. However, structural features in southwest Texas, the Devil's River Uplift and the Chittim Anticline, affected the Hosston structural setting but is not noted on the structural map of the pre-Cretaceous surface. Also, some topographic structural irregularities on the pre-Cretaceous surface do not appear on the Hosston/Trinity structure map (the localized topographic high in Williamson County is one example).

Dip on the top of the Hosston/Trinity ranges from a low of approximately 10 ft/mi (2 m/km) on the Texas Craton in Bandera County to nearly 500 ft/mi (97 m/km) in the Gulf coastal province (Wilson County).

Although a few normal faults apparently have affected the pre-Cretaceous structural setting, normal faults become a major aspect of the regional structural setting of the Hosston/Trinity systems. Most of the faults displacing basal Cretaceous strata occur from Bexar County north into Travis and Williamson Counties. Likewise, maximum mapped displacement of approximately 350 ft (107 m) occurs along this trend. Most displacement is down-to-the-coast, but there is clearly defined up-to-the-coast faulting of the Luling System in Bexar, Guadalupe, and Caldwell Counties. Displacement there is as much as 400 ft (122 m). Both up-to-the-coast and down-to-the-coast faulting occurs in the Talco system, and a narrow graben is defined in Hopkins, Franklin, and Titus Counties. Detailed fault trends are not shown within the main part of the Mexia Fault Zone, and even though surface displacement indicates that the main aspect of faulting there is up-to-the-coast, local data indicate the



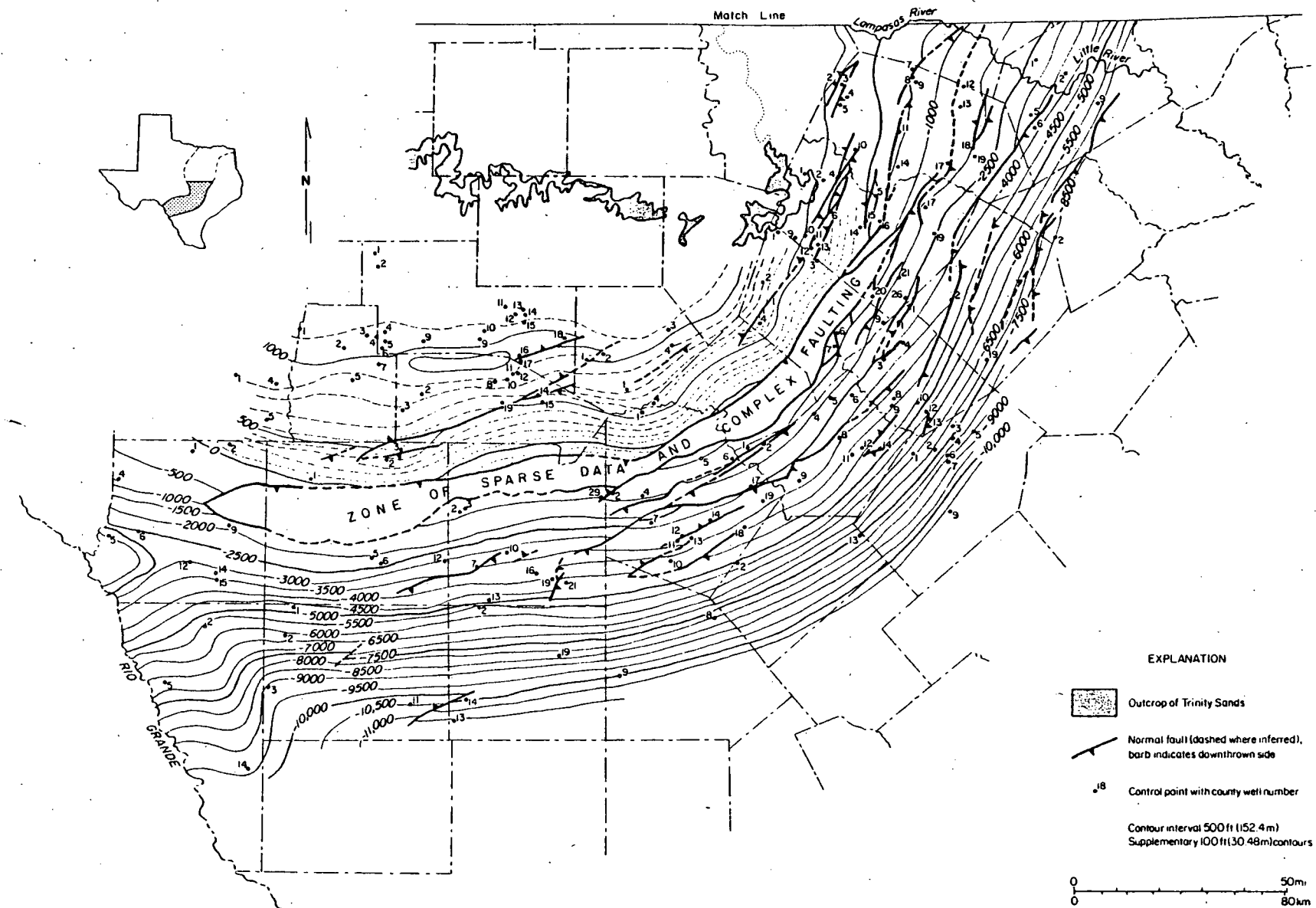


Figure 52. Structural configuration of the Hosston/Trinity (on facing pages).



major displacement to be down-to-the-coast (Hayward and others, 1979). Also, because of sparse data, the individual fault traces in part of the Balcones Fault Zone are not depicted; this area is denoted on the structure map as "zone of complex faulting."

The larger number of faults displacing Cretaceous strata as compared with the number that displace the underlying pre-Cretaceous rocks may be due to several factors. It may be a function of incomplete subsurface data for the pre-Cretaceous surface. Although in updip areas such as in Kerr and Bandera Counties, where control is of comparable quantity and quality for Cretaceous and pre-Cretaceous horizons, the Cretaceous strata nonetheless appear to be more intensely faulted. Still, more faults might displace the Paleozoic complex than are depicted on the structural map of the pre-Cretaceous surface; pre-Cretaceous faults might not appear on the map because of small scale or low density of control. Another explanation for the disparity in the number of faults affecting the pre-Cretaceous surface and the Lower Cretaceous strata might be the differences in competency of rocks affected. The stresses that result in intense faulting of the Cretaceous sands simply might not have deformed the underlying pre-Cretaceous complex in a way that is discernible on the maps presented here. A third possibility, and one suggested by certain interpretations of the central part of the study region (Hayward, 1978) is that growth faulting may have occurred during deposition of the Hosston. However, a comparison of fault trends to isopach or net sand data does not support this on a region-wide basis at our working scale. More detailed investigations, however, might prove this hypothesis to be correct.

#### General Aquifer Properties of the Hosston/Trinity

Data on water level, water quality, and water temperature are presented for an area from Travis County, north to Cooke and Grayson Counties at the Oklahoma border. The scarcity of water data in relation to the broad scope of the maps of the Hosston/Trinity lithic framework is due to the limited areal extent in which the Hosston-Trinity is used as an aquifer. In northeast Texas, no known localities exist east of Dallas, Collin, and Grayson Counties where the Trinity sands are tapped for ground-water supplies. In south-central Texas, there are a few localities within the Balcones Fault Zone in Bexar and Uvalde Counties where the Hosston supplies water needs, but these data points are too scattered to allow confident extension of our maps into that area. The San Marcos Platform appears to have acted as a barrier, south of which lithic properties are not conducive to ground-water production within the Balcones Fault Zone. Updip of the Balcones Fault Zone, in Kendall, Kerr, and Bandera Counties, water from the Hosston is commonly used for domestic and livestock

purposes. But in these areas, the aquifer lies at relatively shallow depths and is close to its outcrop (recharge) area; hence, it does not exhibit elevated water temperatures. Also, no continuous water data link this part of the Hosston with the main part of the study region farther east; therefore, we omitted that part of the Hosston from our consideration of aquifer properties.

#### Water Level of the Hosston/Trinity

The water level map for the Hosston/Trinity is based on data collected by the Texas Department of Water Resources during November 1976 (fig. 53). Because the data points used to construct this map were collected at nearly the same time, the contour lines approximate the potentiometric surface at that time. Assuming that these contours delineate the potentiometric surface, flow paths can be constructed (Hall, 1976), and possible ground-water divides are discernible. Also, cones of depression are easily seen on this map, and they correlate with areas of major withdrawal from the aquifer. Zones of intensive ground-water production also affect the locations of ground-water divides and the convergence of flow lines; thus water level (potentiometric surface) is a result of the natural aquifer conditions and the intensity of human use of the ground-water supply.

The most notable area where water level has declined in apparent response to human use is along the "Interstate-35 growth corridor" (Allen, 1975; Baldwin, 1974) from Waco north to Ellis and Johnson Counties. As noted by Hayward and others (1979), the effect of this "trough of depression" is to reverse the potentiometric gradient for the Hosston aquifer east of the trough, and this probably eliminates recharge east of the I-35 corridor. The trough might also adversely affect water quality because of movement of lower-quality waters from down-dip areas farther east in response to the reversal of the "normal" potentiometric surface. Other local areas of depressed water level occur in western Travis County in response to intensive residential development along the lakes there, and in Tarrant and Dallas Counties, owing to local municipal, residential, and industrial uses in those urban areas.

The apparent "natural" effects on the water level of the Hosston aquifer include the various structural features of the region and the configuration of sand bodies. In general, the water level surface is oriented in the same direction as structural dip, except where intensive use results in depression cones or troughs. But because of artesian conditions, the dip of the water level is subdued compared with the inclination of the aquifer host formation; commonly the water level surface dips basinward at

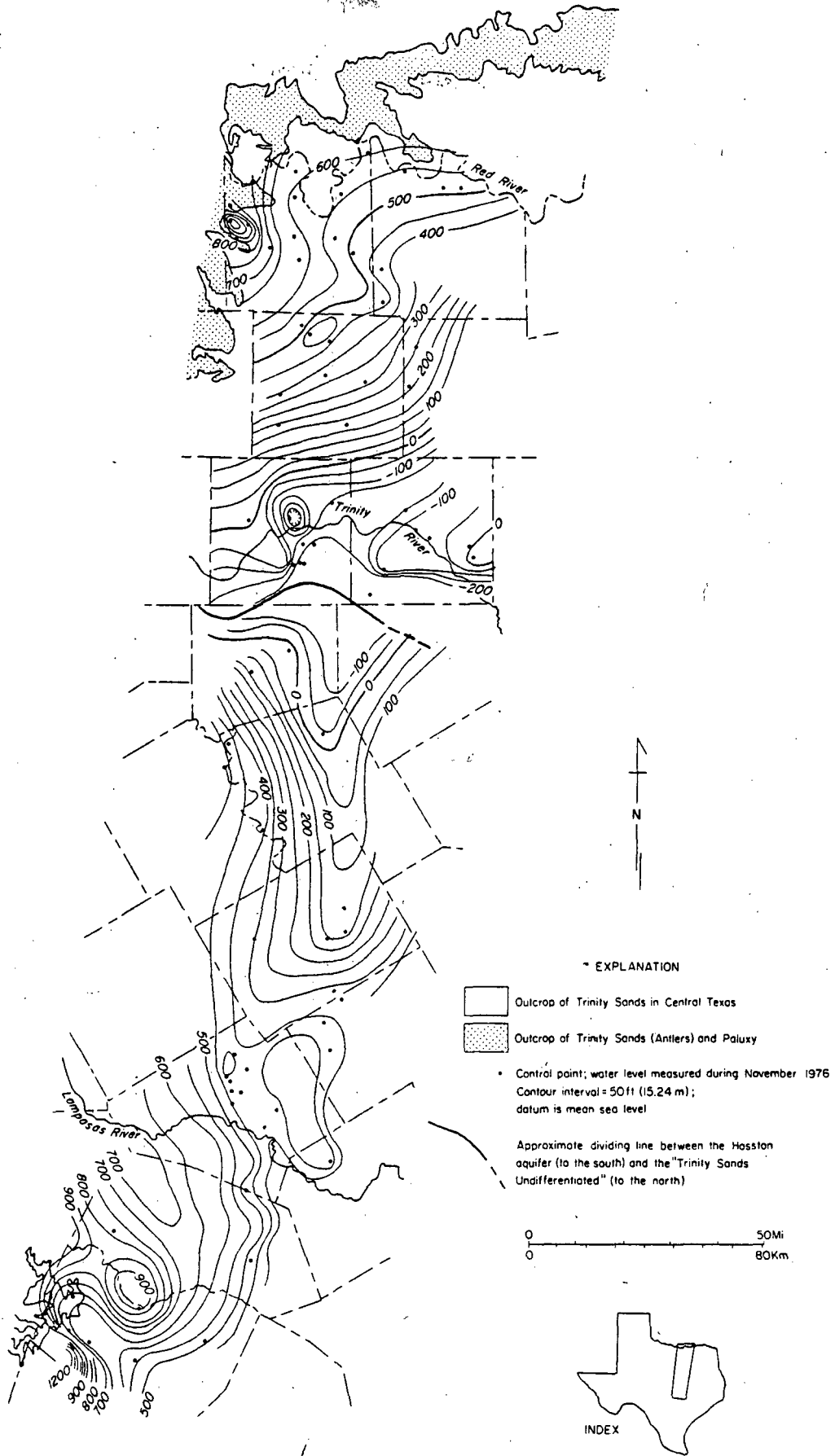


Figure 53. Water level contours for the Hosston/Trinity aquifer.

approximately 4 ft/mi (0.8 m/km). Hence, in the eastern part of the aquifer, the water commonly rises more than 2,000 ft (610 m) under artesian pressure.

Various local effects on water level occur throughout the region. Areas of relatively high water level correspond to high net-sand thicknesses, and the San Marcos Platform, which is an area of thin net sands, delineates an apparent groundwater divide. Other examples include the water level divides trending from northwest to southeast in Williamson County, and from west to east in northern Bell County. The apparent divide near the Tarrant and Johnson county line is probably due to discontinuities of data because of nomenclatural changes between the Hosston aquifer and the various other Trinity sands.

#### Water Quality of the Hosston/Trinity

As expected, total dissolved solids (TDS) content of Hosston/Trinity ground water increases with increased aquifer depth (fig. 54). Values range from less than 500 mg/l in updip areas to more than 10,000 mg/l downdip. Another general control on water quality in the updip reaches of the aquifer is thickness of sand bodies. Thicker sands generally possess better water quality (lower TDS), as noted in southwestern Travis County and in eastern McLennan County where low TDS values roughly conform to configuration of relatively high sand thicknesses. There are, however, deviations from these general conditions, and these deviations may result from (1) pollution of the aquifer from human activities at the ground surface, (2) improper casing of wells and, thus, mixing of waters from various levels, (3) faults that provide conduits among different strata, and (4) major changes in facies or depositional systems.

Human-derived contamination commonly occurs in the updip reaches of the aquifer, where pollutants may enter in the recharge zone and are evidenced by localized increases in TDS content. Such a condition might have caused the anomalously high TDS values contoured in northwestern Travis County. However, the increase there might also be explained by circulation along faults of waters from various strata. The area in northwestern Travis County is bounded by faults; also, it lies immediately off a major sand trend so that a facies change might have contributed to the local anomaly. Clearly, the source of localized waters having high TDS values is not easily ascertained. Often a combination of processes might produce the observed anomalies.

Certain water-quality effects are not local anomalies, but occur region-wide instead. A striking example is the precipitous increase in TDS content at the boundary between the fluvial-deltaic systems and the prodelta, lagoon, and shelf (?) systems.

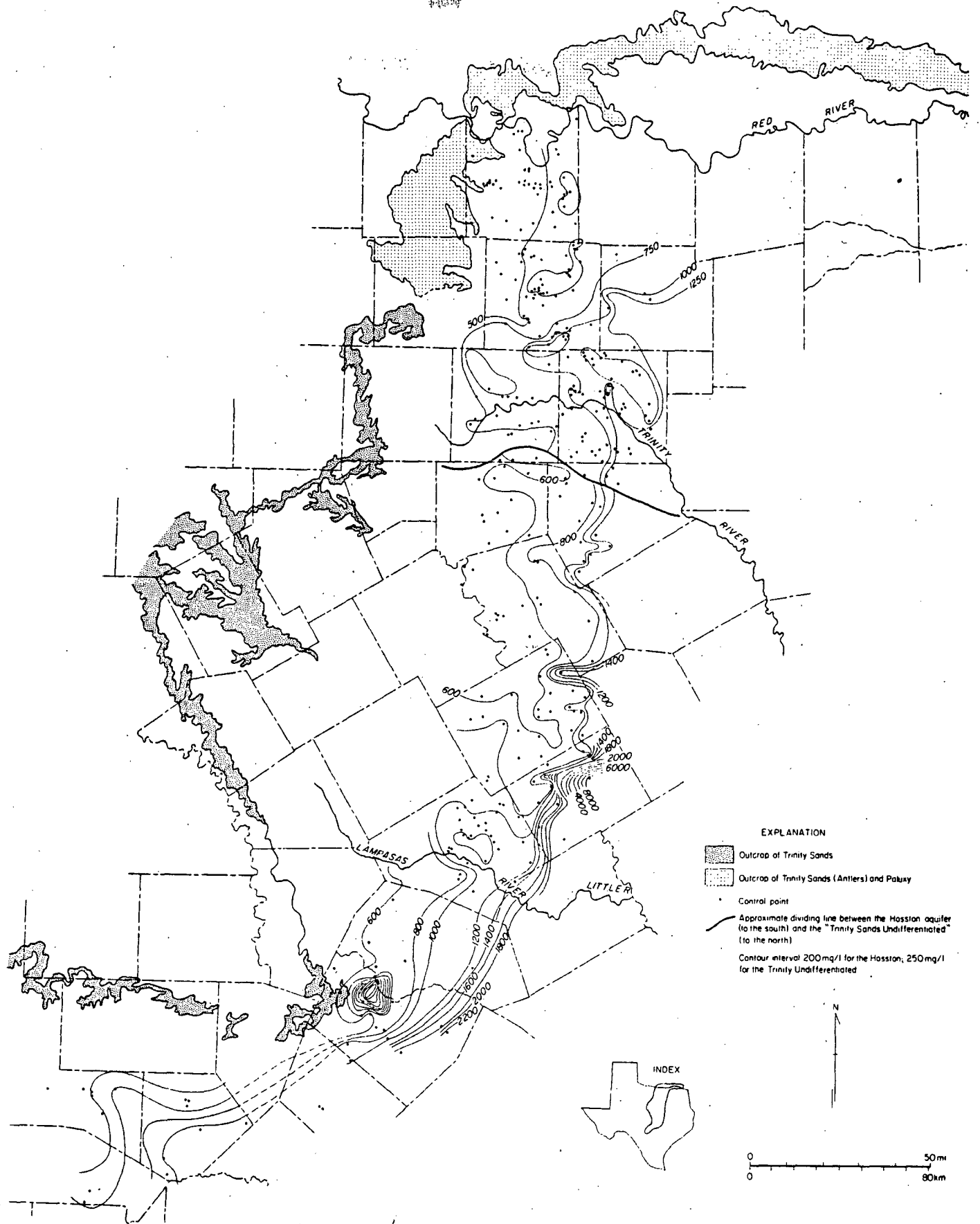


Figure 54. Total dissolved solids contours for Hosston/Trinity ground water.

This condition is most clearly seen along the downdip terminus of the high-destructive wave-dominated delta system in Falls, McLennan, and Hill Counties. There, dissolved solids are generally less than 800 mg/l within the fluvial and deltaic deposits, but values on the downdip side of this depositional boundary are commonly more than 1,000 mg/l. Hall (1976) also noted a change in chemical character of waters from the calcium and magnesium bicarbonate ion suite in waters from fluvial sands to sodium bicarbonate in waters from deltaic deposits. Hall attributed progressively higher sulfate waters in downdip reaches of the aquifer to mixing with waters from the Glen Rose Limestone. Higher sulfate content, however, is expected in waters of marine origin (Hem, 1970).

Piper diagrams showing major anion and cations of Hosston waters in McLennan (fig. 55) and Travis Counties (fig. 56) demonstrate changes in water chemistry from updip to downdip parts of the aquifer. Both counties lie along the Balcones Fault Zone, hence in both areas the Hosston occurs across a range of depth and represents a variety of depositional modes. However, in Travis County the change from updip to downdip is more compressed in that the fluvial deposits occur in the western part of the county, whereas prodelta and lagoonal (?) facies occur farther east. Thus, the water chemistry in Travis County shows some attributes of the fluvial systems as well as attributes of deltaic and lagoonal strata; whereas in McLennan County the water characteristics are typical of deltaic systems, and only to a lesser extent do they reflect the typical ionic content of fluvial facies.

#### Water Temperature of the Hosston/Trinity

Water temperatures range from less than 70° F (21° C) near the outcrop in Cooke County to more than 140° F (60° C) in Falls County (fig. 57). Water temperature values, like water quality, generally reflect structural configuration and net-sand thicknesses of the aquifer (figs. 50 and 52). Simply stated, the deeper the aquifer, the hotter the waters; whereas dip-oriented sand trends mediate water temperatures. Anomalously low water temperatures occur in structurally deep parts of the aquifer in eastern Travis County and in south-central McLennan County. These trends correlate approximately with fluvial and deltaic sands in those counties. However, these generalizations are ambiguous in places; in Hill County, for example, relatively higher water temperature values occur along a fluvial trend, just as the relation between water temperature and TDS is not altogether straightforward at every locality.

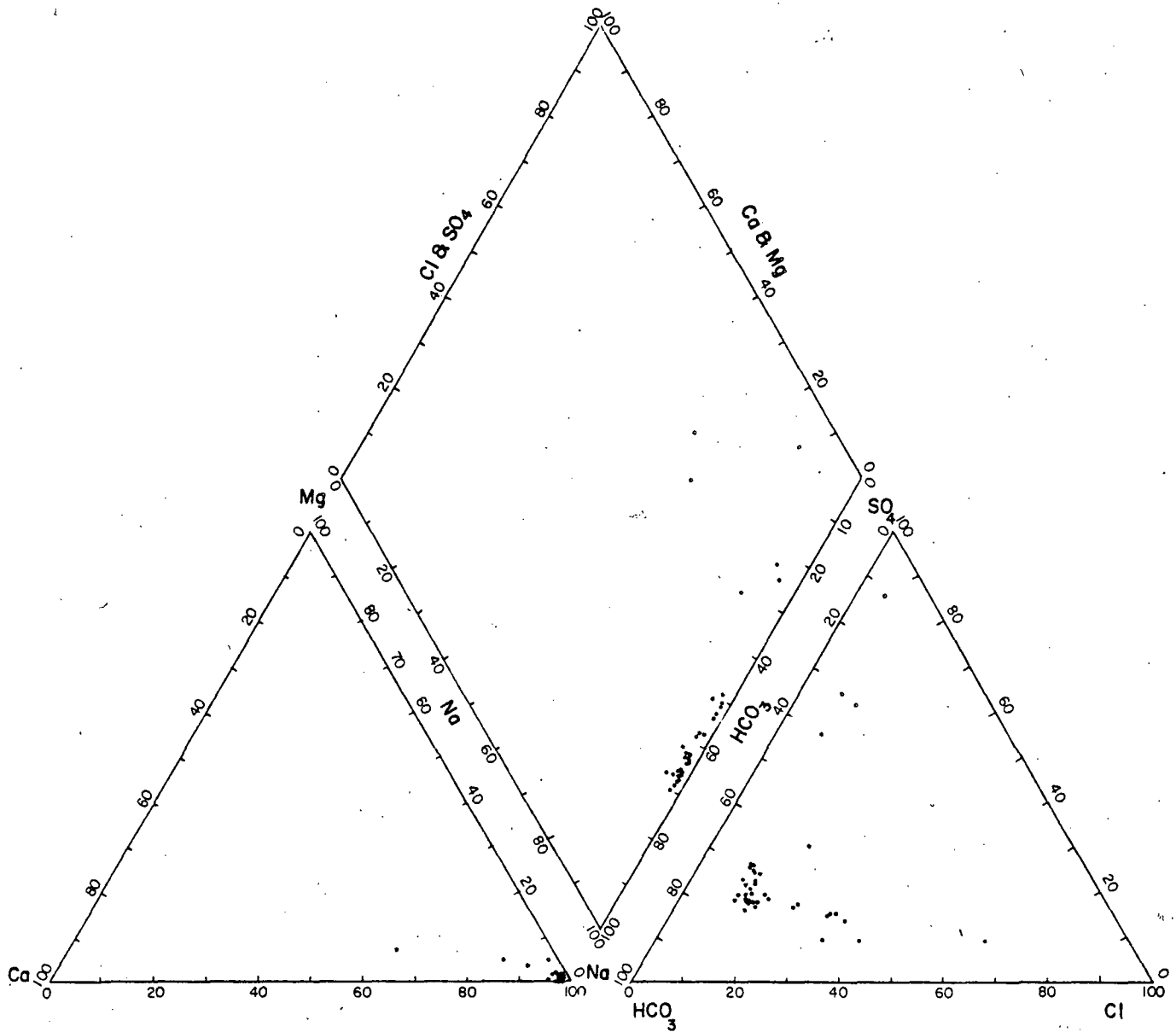


Figure 55. Piper diagram for Hosston ground water--McLennan County.

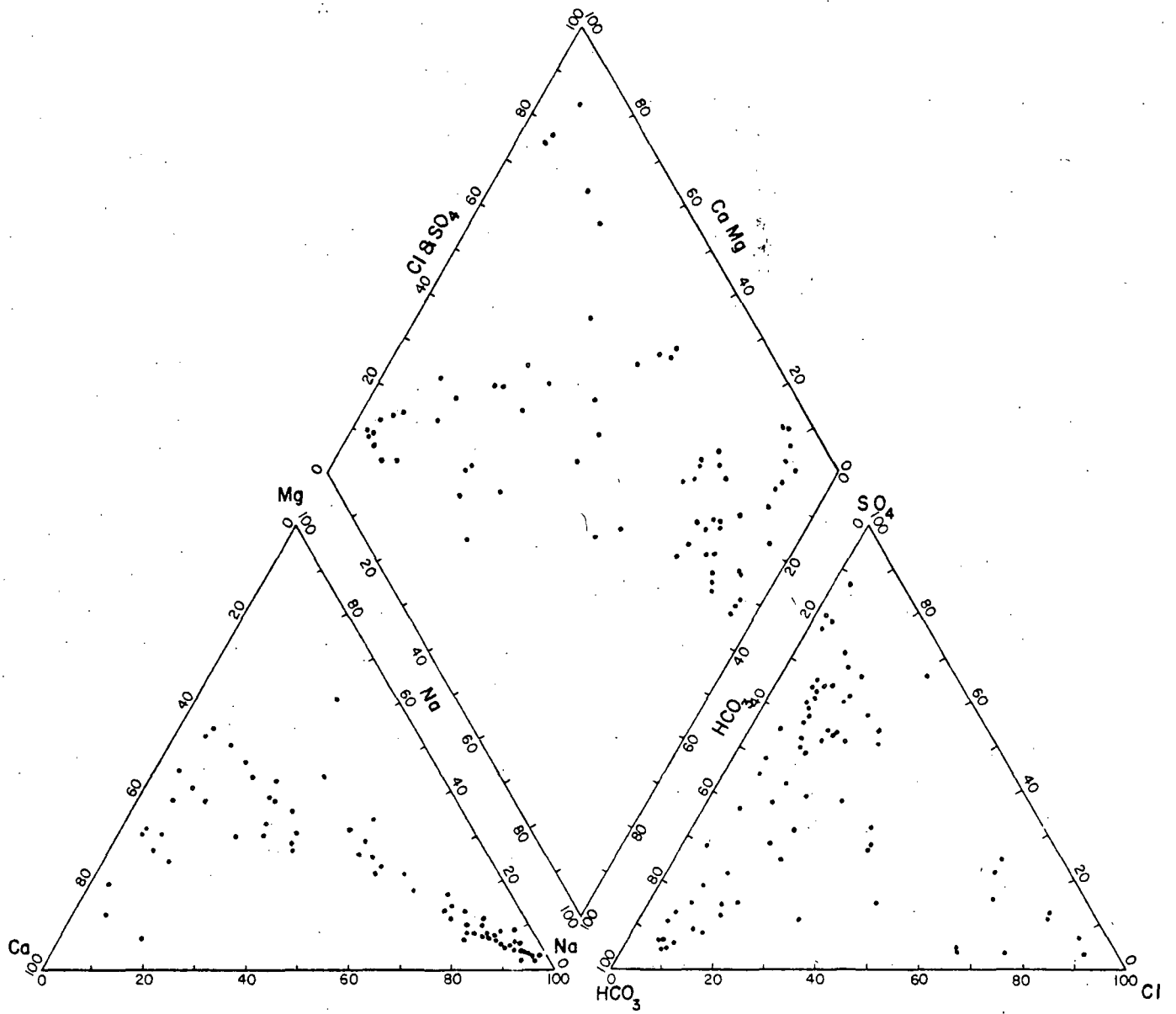


Figure 56. Piper diagram for Hosston ground water--Travis County.



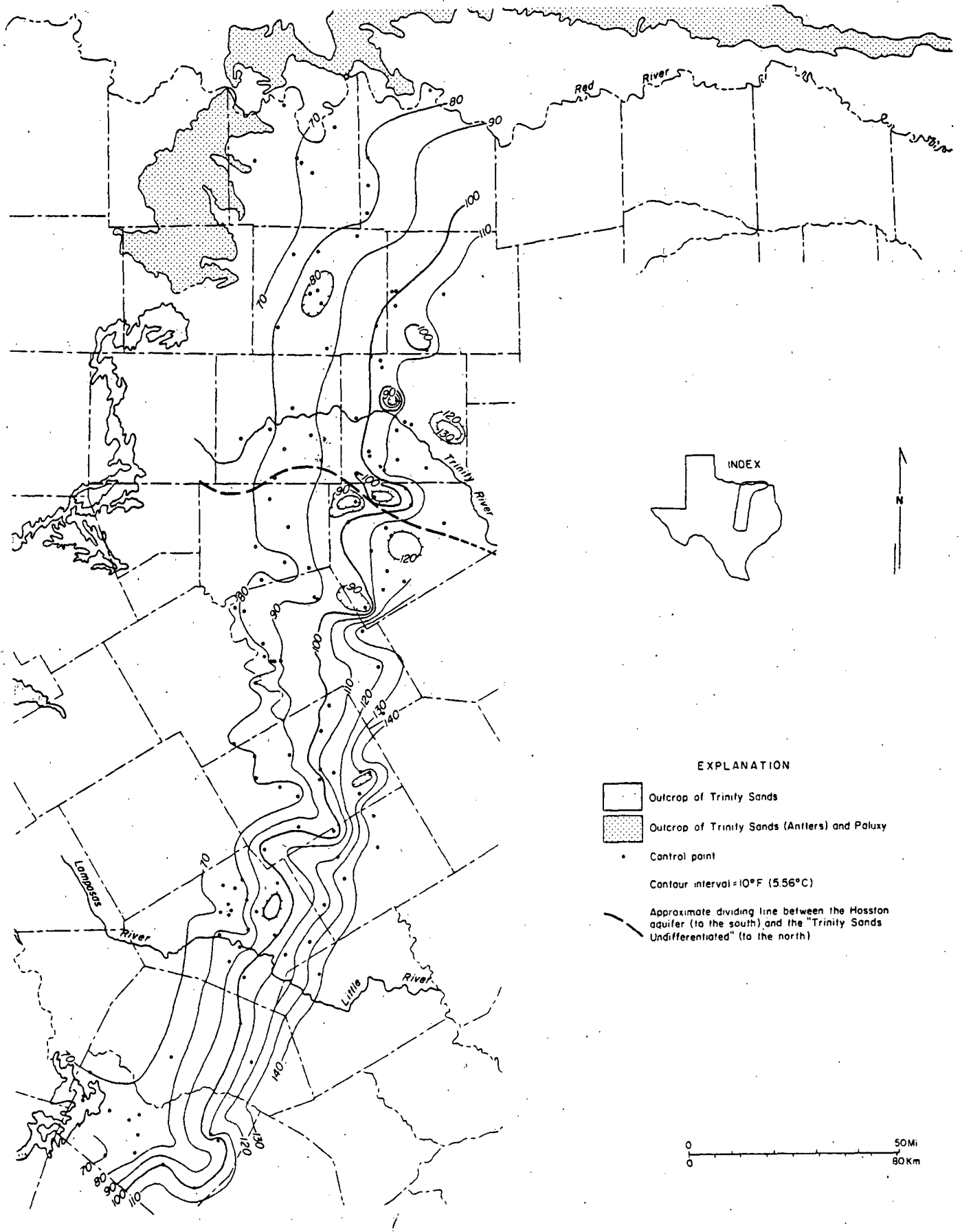


Figure 57. Water temperature contours for Hosston/Trinity aquifer.

Three scatterplots that display temperature versus depth, TDS versus depth, and temperature versus TDS, show some expected and some unexpected relationships when the water data are considered in the aggregate (i.e. in a non-site-specific context). The temperature-depth plot (fig. 58) displays a trend that is expected: it is a positive linear plot that shows the direct relationship between these parameters. The TDS-depth plot (fig. 59) shows that, contrary to expectations, dissolved solids are relatively insensitive to depth; TDS values predominantly trend along the 791 mg/l line, regardless of depth. Many of the anomalies that deviate from this trend are for wells in Travis County, where, as noted previously, contamination may be the cause of the high TDS values. The temperature versus TDS plot (fig. 60) shows the corollary to the other scattergrams; this TDS is relatively insensitive to changes in temperature. In other words, wells that are hotter than usual have satisfactory ranges of dissolved solids. Again, several deviations from this predominant trend occur in Travis County, where contamination may have resulted in low-temperature waters possessing abnormally high dissolved solids.

#### Geothermal Potential of the Hosston/Trinity

The demonstrated trend whereby water temperatures are shown to increase without a concomitant increase in dissolved solids bodes well for multiple use of the Hosston/Trinity waters for both drinking supply and for geothermal heat production. The geographic extent of this potential is dramatically shown by plotting all localities where Hosston/Trinity waters are tapped for public use, and these localities are compared to the 90° F (32° C) water temperature line and the 1,000 mg/l isopleth (fig. 61). Yet, even in towns that use the waters of higher TDS, the resource potential is still present. The drilling costs and the pumping costs are already borne. The heat is presently wasted.

To illustrate the caloric value of these waters, we obtained municipal water-use records from the Texas Department of Water Resources, and we tabulated mean January ground-water consumption over a five-year period (table 1). A few of these municipal wells have water level and water temperature data on file, and for these we computed energy budgets: debits incurred in lifting the water versus credits obtained from the heat, assuming that the heat would be used for space heating. The City of Taylor, for example, pumps an average of 31,469,800 gal (119,120,000 l) of water every January. Water level is approximately 88 ft (21 m); water temperature is 116° F (47° C); and mean minimum January temperature is 37° F (3° C). Using these figures, we calculate the net energy debit for that month to be  $2.96 \times 10^7$  Btu ( $7.46 \times 10^6$  kg-cal)



TDS(mg/l)

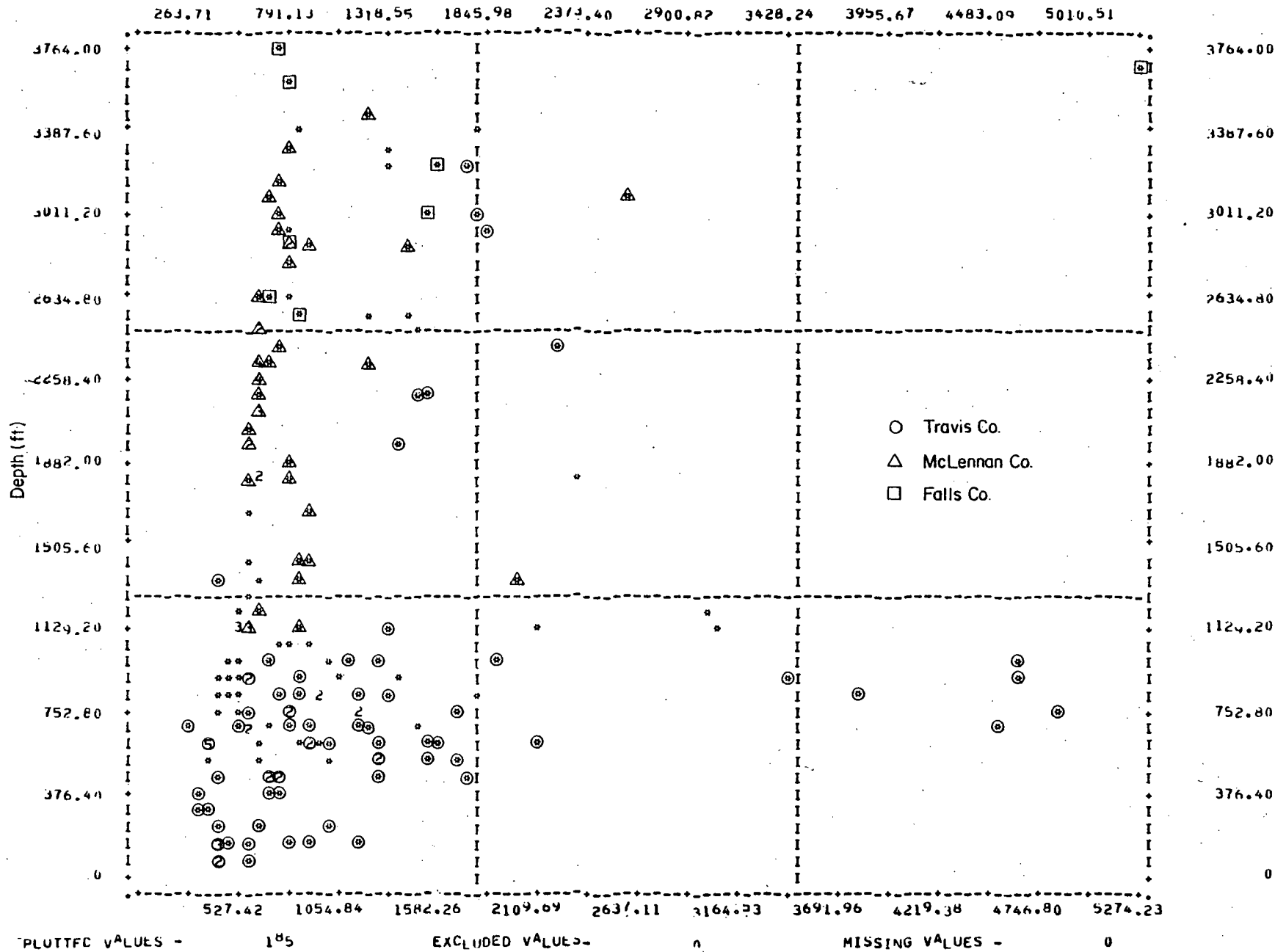


Figure 59. Total dissolved solids/depth scattergram for Hosston ground water.

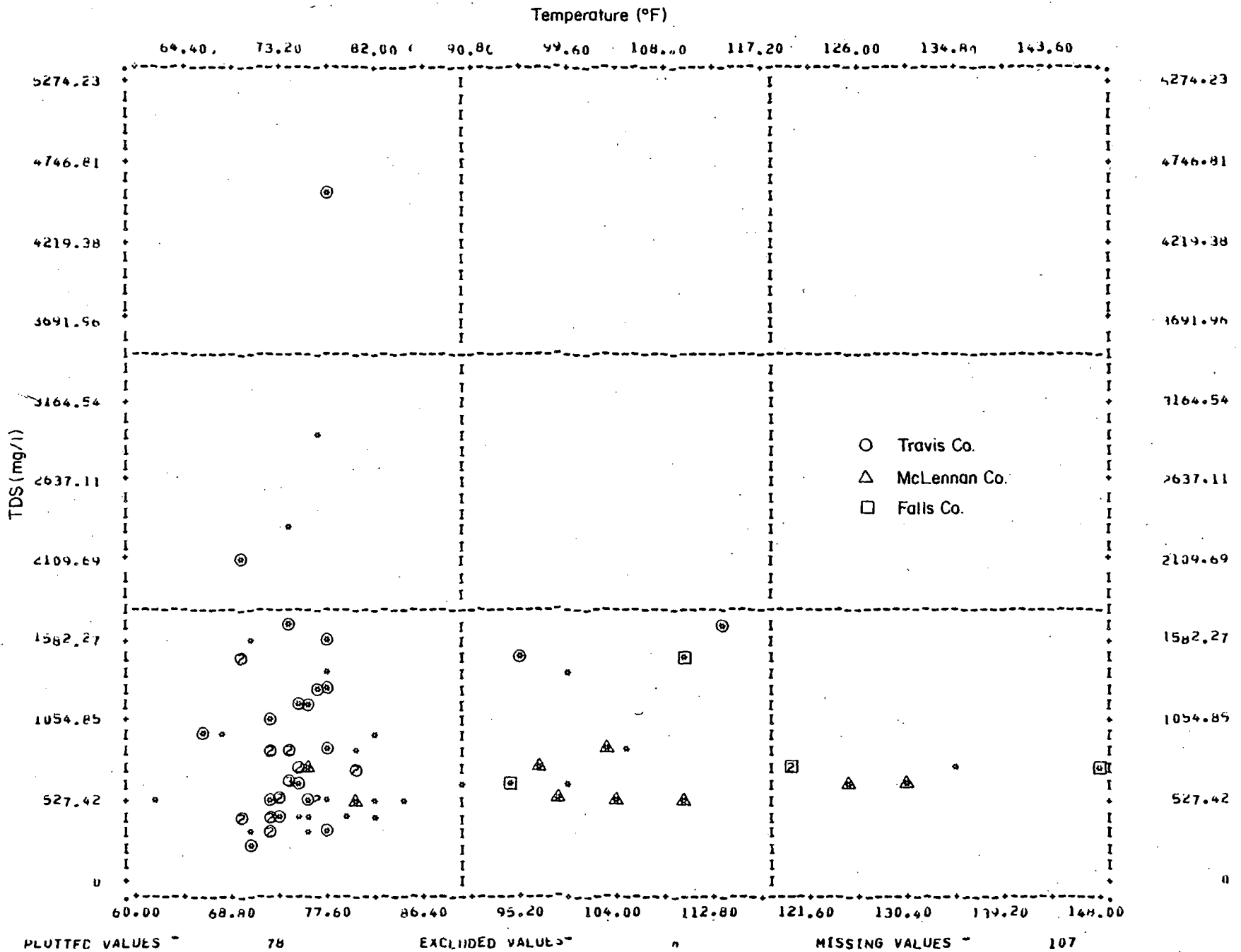


Figure 60. Temperature/total dissolved solids scattergram for Hosston ground water.

Table 1. Selected municipal ground-water withdrawals--Hosston/Trinity undifferentiated (data from Texas Department of Water Resources).

County	Municipality	Mean January Pumpage (1972-1976)	Mean Yearly Pumpage (1972-1976)
Bell	Heidenheimer	289,640	4,301,394
Bell	Holland	1,409,698	19,716,396
Bell	Little River	2,917,400	44,639,775
Bell	Pendleton	1,642,827.5*	19,713,930
Bell	Rogers	2,601,500*	26,545,600
Bell	Temple	195,233*	2,998,466*
Bell	Troy	2,434,370	36,890,730
Collin	Celina <sup>⊙</sup>	3,445,420	44,923,840
Collin	Frisco <sup>⊙</sup>	7,540,000	102,232,000
Dallas	Addison	5,221,700*	12,395,600*
Dallas	Carrollton	55,200,000*	240,413,000
Dallas	Cedar Hill	13,882,022	197,491,099
Dallas	Coppell <sup>⊙</sup>	3,847,733*	35,005,267*
Dallas	DeSoto	35,185,400	496,757,256
Dallas	Duncanville	8,403,600	227,792,000
Dallas	Kleburg	12,576,600	162,383,640
Dallas	Irving	118,542,000*	1,312,432,800
Dallas	Lancaster	26,850,000	367,214,600
Dallas	Wilmer#	5,149,100*	62,371,615
Ellis	Midlothian	9,875,920	131,823,840
Ellis	Waxahachie	1,766,544	25,821,393
Falls	Chilton	741,119*	8,893,430
Falls	Golinda	266,400	5,820,160
Falls	Lott	1,419,890*	18,272,884
Falls	Perry	370,294	5,320,039
Falls	Satin	184,401*	2,212,813*
Hill	Abbott	1,200,000	14,841,960
Hill	Aquilla	245,270	3,638,030
Hill	Blum	737,020	11,687,690
Hill	Covington	2,030,503	19,563,929
Hill	Hillsboro	32,007,000	426,805,800
Hill	Hubbard	5,163,627*	58,816,390*
Hill	Itasca <sup>⊙</sup>	6,124,600	90,406,484
Hill	Malone	719,707	8,719,397
Hill	Mt. Calm	811,460	10,316,460
Hill	Penelope	213,360*	3,686,132
Hill	Whitney	4,283,060	61,898,420
Limestone	Prairie Hill	2,019,730	22,483,275

\* indicates less than 5 years of measurements

# draws from both Hosston/Trinity and Paluxy aquifers

⊙ draws from both Hosston/Trinity and Woodbine aquifers

Table 1. (cont'd)

County	Municipality	Mean January Pumpage (1972-1976)	Mean Yearly Pumpage (1972-1976)
McLennan	Axtell	887,208	10,646,496
McLennan	Bellmead	16,168,600	211,718,200
McLennan	Bruceville	405,448	6,041,252
McLennan	China Spring	298,400	4,774,600
McLennan	Crawford	989,468*	15,484,669
McLennan	Eddy	862,944	14,684,186
McLennan	Elm Mott	2,958,160	36,284,875
McLennan	Hewitt	3,482,100	55,763,620
McLennan	Lacy-Lakeview	11,006,660	145,753,420
McLennan	Leroy	831,200	12,187,200
McLennan	Lorena	1,505,060	21,402,424
McLennan	Mart	11,111,280	136,609,944
McLennan	McGregor	15,609,480	200,292,352
McLennan	Moody	2,355,920	27,840,520
McLennan	Riesel	2,320,412	24,617,852
McLennan	Robinson	9,078,400	133,075,000
McLennan	Ross	1,750,000*	26,256,344
McLennan	Waco	7,410,550*	53,314,650*
McLennan	West	7,420,800	102,980,800
McLennan	Woodway	10,999,667*	225,275,180
Milam	Buckholts	565,400*	7,908,625*
Travis	Austin	912,500*	10,950,000*
Travis	Jonestown	957,103*	11,485,239
Travis	Manor	2,161,560*	23,053,508
Williamson	Andice	83,719*	1,004,623
Williamson	Bartlett	3,310,340	44,420,656
Williamson	Florence	2,065,340	29,618,860
Williamson	Granger	6,220,600	97,266,200
Williamson	Jarrell	1,419,460	22,533,860
Williamson	Liberty Hill	1,295,413	18,310,301
Williamson	Taylor	31,469,800	421,969,000

- \* indicates less than 5 years of measurements  
# draws from both Hosston/Trinity and Paluxy aquifers  
⊙ draws from both Hosston/Trinity and Woodbine aquifers

and the energy credit to be  $2.07 \times 10^{10}$  Btu ( $5.22 \times 10^9$  kg-cal). Given the prevailing (conservative) price of  $\$2.5 \times 10^{-6}$  per Btu ( $\$9.9 \times 10^{-6}$  per kg-cal), we see an asset worth up to \$51,750 during a single "average" winter month.

These dollar values are probably overstated because we did not attempt to account for efficiencies of heat-exchange systems. In other words, the values presented here reflect the total heat available during one specific month; the actual usable heat content obtainable may be less by approximately 50 percent owing to efficiencies of heat exchange systems (Marshall Conover, personal communication, 1979). Also, the temperature differential is probably somewhat high, as we computed our values using the long-term January mean minimum temperature. However, for that part of the water used for water heating, the ambient air temperature is irrelevant and the caloric value as computed could be applied to domestic or industrial hot water demands. This is of no mean consequence, since water heating accounts for approximately 40 percent of domestic energy use (Ray Tessmer, personal communication, 1979). For domestic wells, a few simple plumbing modifications can make this resource a viable option for many homes throughout the region.

The resource potential as computed and as shown in figure 61 is for areas that presently produce Hosston or Trinity ground water. There are, however, other areas having geothermal potential on the basis of our regional geologic assessment. The most evident unexplored area is the deep, high net-sand trends associated with the deep fluvial and deltaic systems of the Hosston/Trinity in Bowie, Red River, Morris, Titus, Franklin, Lamar, and Hopkins Counties. Water quality from similar depositional systems in the shallower Paluxy Sand indicates that these deep Trinity waters would probably present water quality problems; but there is a clear potential for use of the Trinity waters, and it warrants further study.



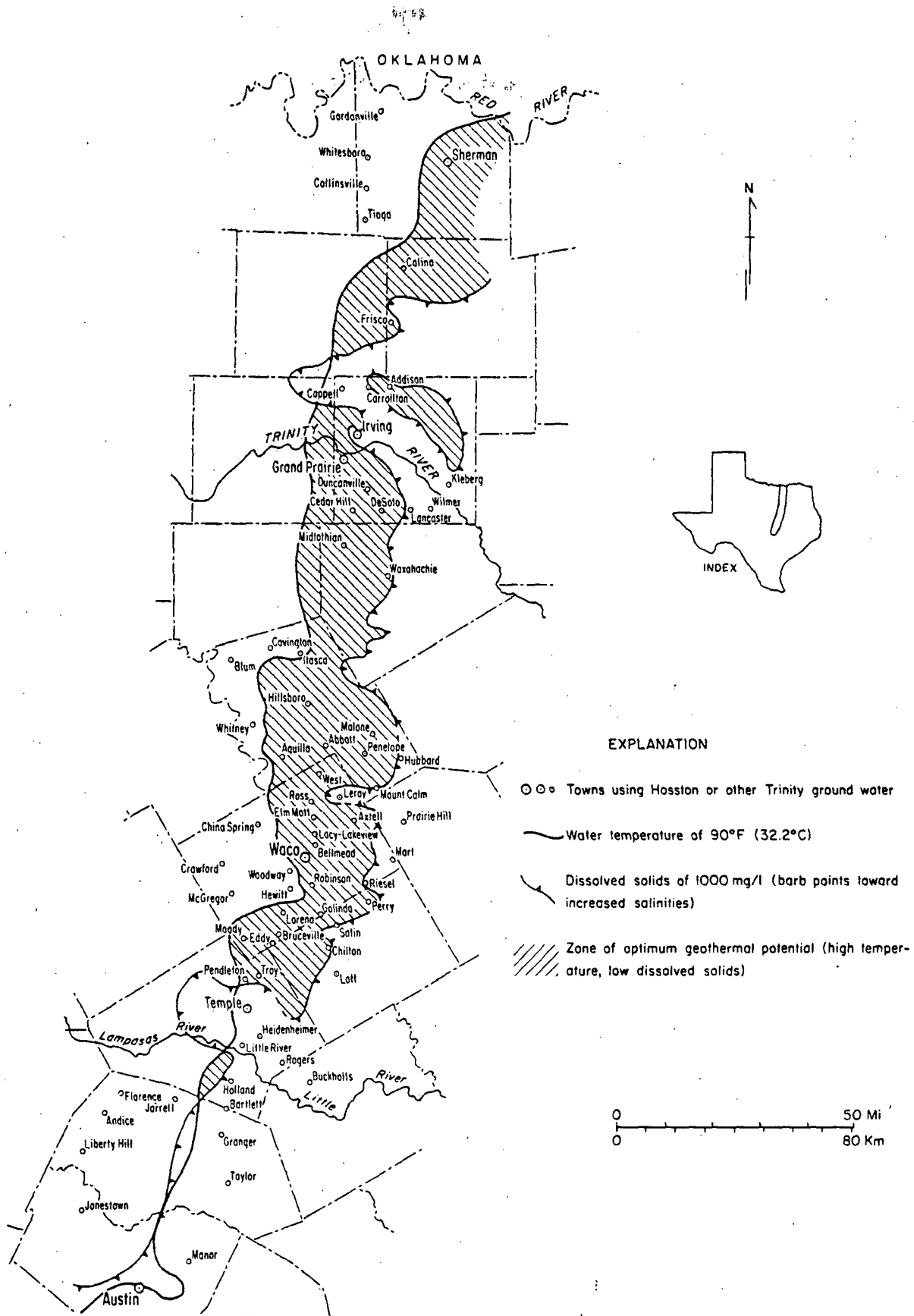


Figure 61. Municipalities using Hosston/Trinity ground water compared to areas of optimum geothermal potential.

## HENSEL SAND

### General

The Hensel Sand is the uppermost of the Trinity sands in the area south of the Trinity River. It represents a depositional environment similar to that of the Hosston, but it is neither as areally extensive nor as thick as the Hosston. The downdip limits of the Hensel are marked by facies changes to mud and limestone deposits of the Pearsall Formation in south-central Texas (Loucks, 1976), and to the Rodessa Limestone farther north in Central Texas. The northern limit is the arbitrary (nomenclatural) boundary with the Trinity Sands Undifferentiated that occurs near the Trinity River. North of that line, the Hensel is equivalent to one of the many stacked, undifferentiated Trinity Sands (fig. 13).

### Thickness of the Hensel

The isopach map (fig. 62) of the Hensel Sand is drawn from Hays County north into Ellis and Johnson Counties; only sparse data were available in Hays, Blanco, and Comal Counties, hence a coherent isopach or net-sand picture could not be drawn across the entire areal extent of the Hensel aquifer. The areas included on this map, however, encompass the entire reaches of (modest) geothermal potential in the Hensel.

The Hensel "signatures" on electric logs indicate that the unit is dominantly terrigenous sand (figs. 14 and 17). Hence, the isopach map is essentially a net-sand map. This assumption is corroborated by the close parallel of geometry and thickness of isopachous lines to net-sand thicknesses of Hensel sand bodies as mapped by Hall (1976). The main deviation occurs where the sands appear to be thickening basinward in the central part of the study region. This probably indicates the interfingering of part of the Rodessa lime facies (fig. 36), and thus the inclusion of both limestone and sandstone beds in these isopach values.

The Hensel, like the Hosston, represents a series of Cretaceous fluvial and deltaic systems trending from west to east off the Texas Craton in the area delineated on the isopach map. Farther to the southwest, in Gillespie, Kerr, and Bandera Counties, the Hensel probably consisted of a series of small fluvial systems coursing off the Llano area a few miles to the north.

Because the Hensel terrigenous deposits were derived from smaller or shorter-lived fluvial systems, they did not prograde as far east as did the Hosston fluvial and

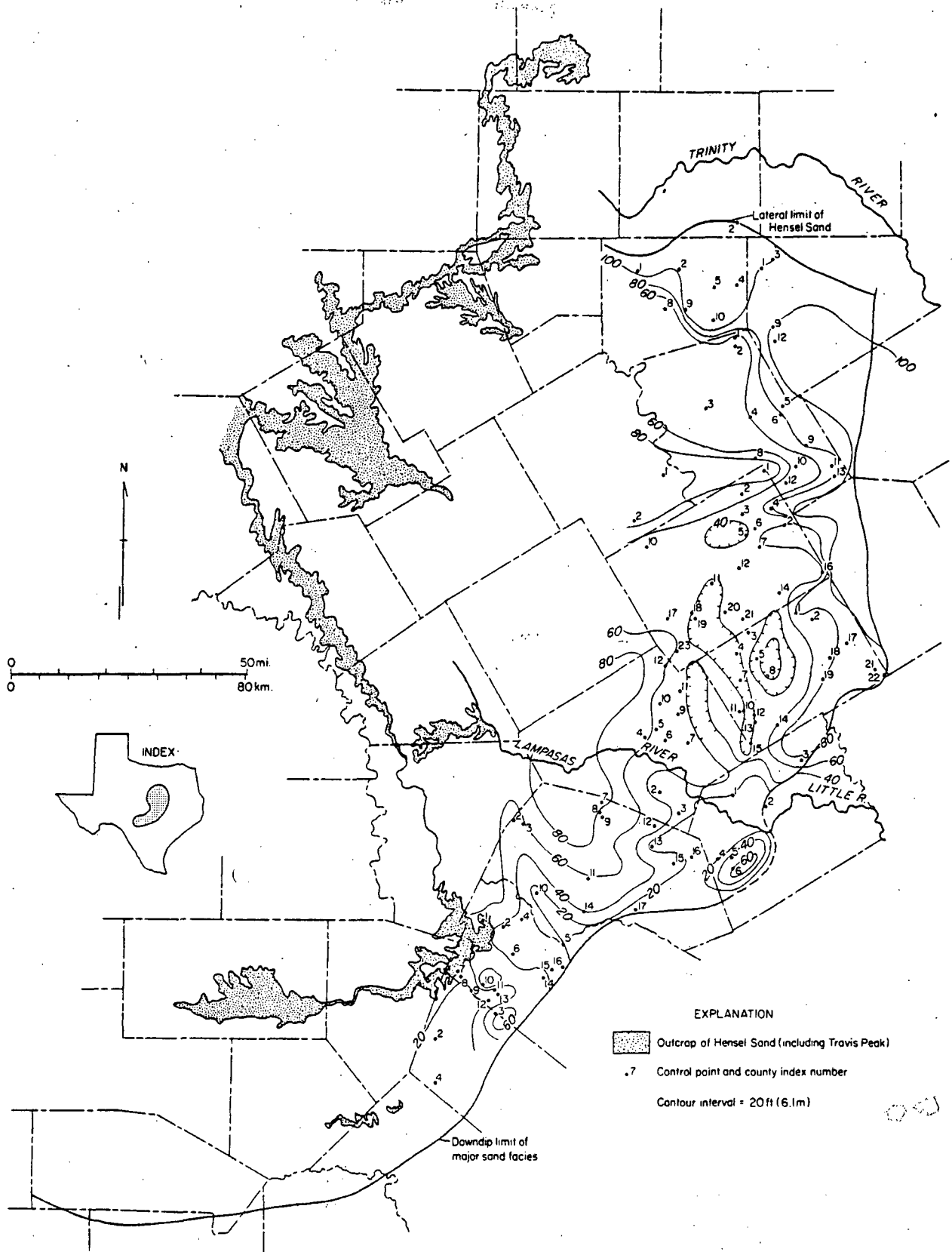


Figure 62. Isopach map of Hensel Sand.

deltaic systems. Like the Hosston, though, the fluvial deposits terminated in a series of small wave-dominated deltas (Hall, 1976). Also there are apparent offshore bar deposits as seen in Milam County; however, these relatively thick deposits may be carbonate sands, and might be similar to the subtidal and intertidal marine, and lagoonal systems of the Hosston, such as those described by Bebout (1977).

### Structural Configuration of the Hensel

We mapped the structural features of the Hensel Sand (fig. 63) only for those areas where net sands are sufficiently thick for the unit to be a potentially viable geothermal aquifer. There, the structural configuration of the top of the Hensel is similar to that of the Hosston (fig. 52). Dips of Hensel beds range from approximately 10 ft/mi (2 m/km) in Kerr and Kendall Counties to more than 120 ft/mi (23 m/km) in Falls County. As with the Hosston, the structural hinge zone is clearly seen at the locus of increased dip.

Normal faults that displace the Hensel are fewer than those displacing the Hosston; in almost every instance, however, faults seen on the Hensel map also affect the Hosston. This reduction of fault traces upward in the section may be due to (a) growth faulting during deposition of the Hosston or (b) upward propagation of some faults that displace subjacent Paleozoic rocks. Fault displacement is of generally the same magnitude for both the Hosston and the Hensel; the stratigraphic offset ranges from approximately 100 to 300 ft (30 to 90 m), and displacement is most commonly mapped at about 100 ft (30 m).

### General Aquifer Properties of the Hensel

The Hensel Sand is an aquifer that serves mainly for domestic purposes and livestock watering (Klemm and others, 1975). Most of this water use is in the updip reaches of the aquifer, in the areas closest to recharge zones and where the sands occur in well-defined fluvial trends. Hence, most of the areas where the Hensel aquifer is used extensively are areas of moderate water temperature values, approximating mean annual air temperatures of the recharge zones. Many of the areas where the Hensel is heavily drawn upon lie outside the region studied here (notably west of Bell, McLennan, and Hill Counties in the central part of our study region); another area where the Hensel is used extensively is in Kendall, Kerr, and Bandera Counties, but in both areas the aquifer temperatures approximate mean annual air temperature values. In neither area does the Hensel show promise as a geothermal resource.

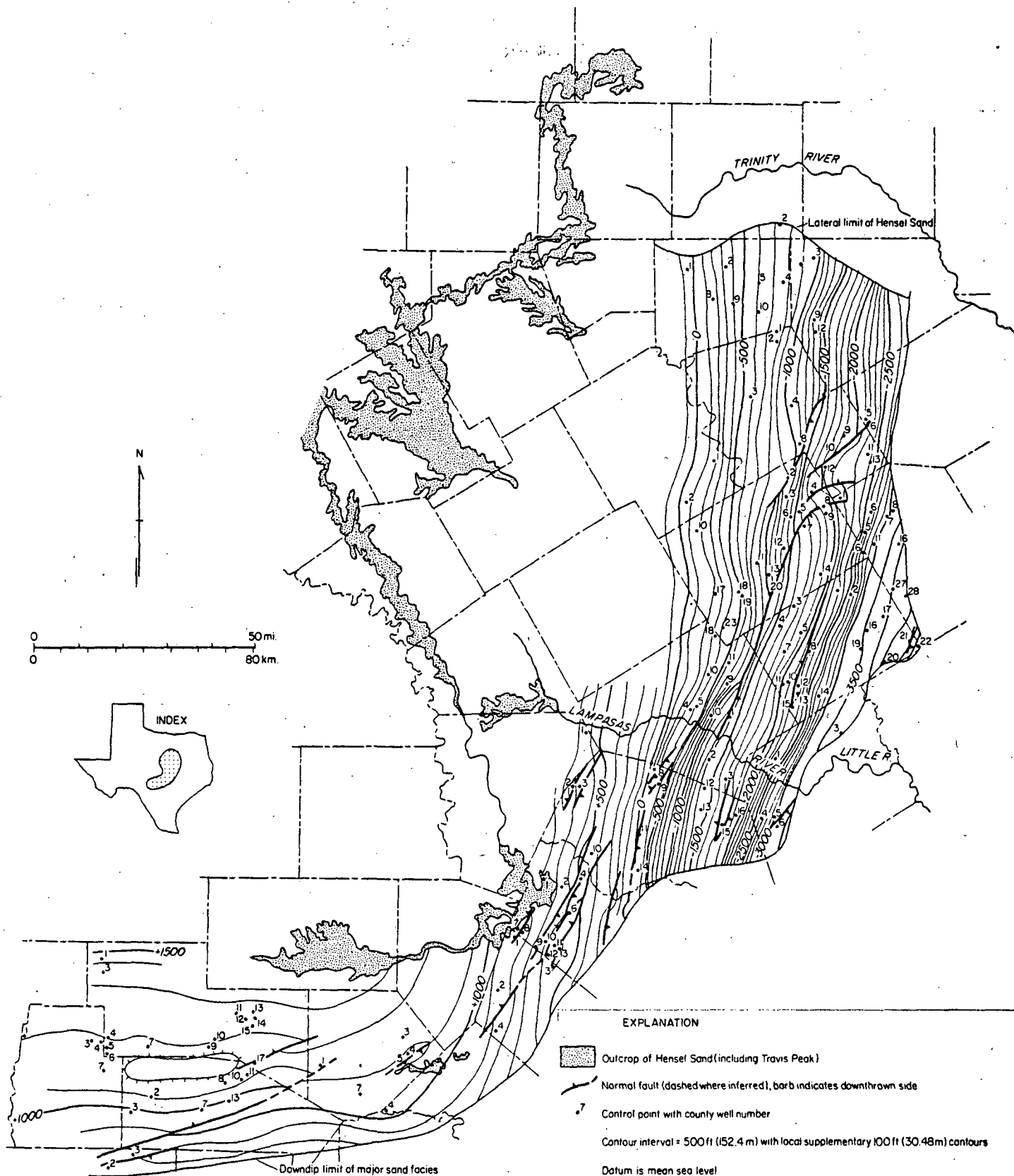


Figure 63. Structural configuration of Hensel Sand.

In the downdip parts of the Hensel aquifer--in the locality where geothermal waters would be expected--facies changes abruptly modify the lithic character of the host rock. There are, however, a few data points in Travis, Bell, and McLennan Counties (fig. 64) indicating that waters from the Hensel exhibit temperatures greater than 90° F (32° C). These values, however, occur near the downdip terminus of the Hensel Sand, in areas of expected low aquifer productivity and high dissolved solids.

In summary, the Hensel aquifer is attenuated in its downdip reaches, and thus, its aquifer potential is severely limited in those areas where elevated temperatures might occur. For this reason, the Hensel does not appear to be a viable source of low-temperature geothermal waters, except perhaps at a few scattered localities.

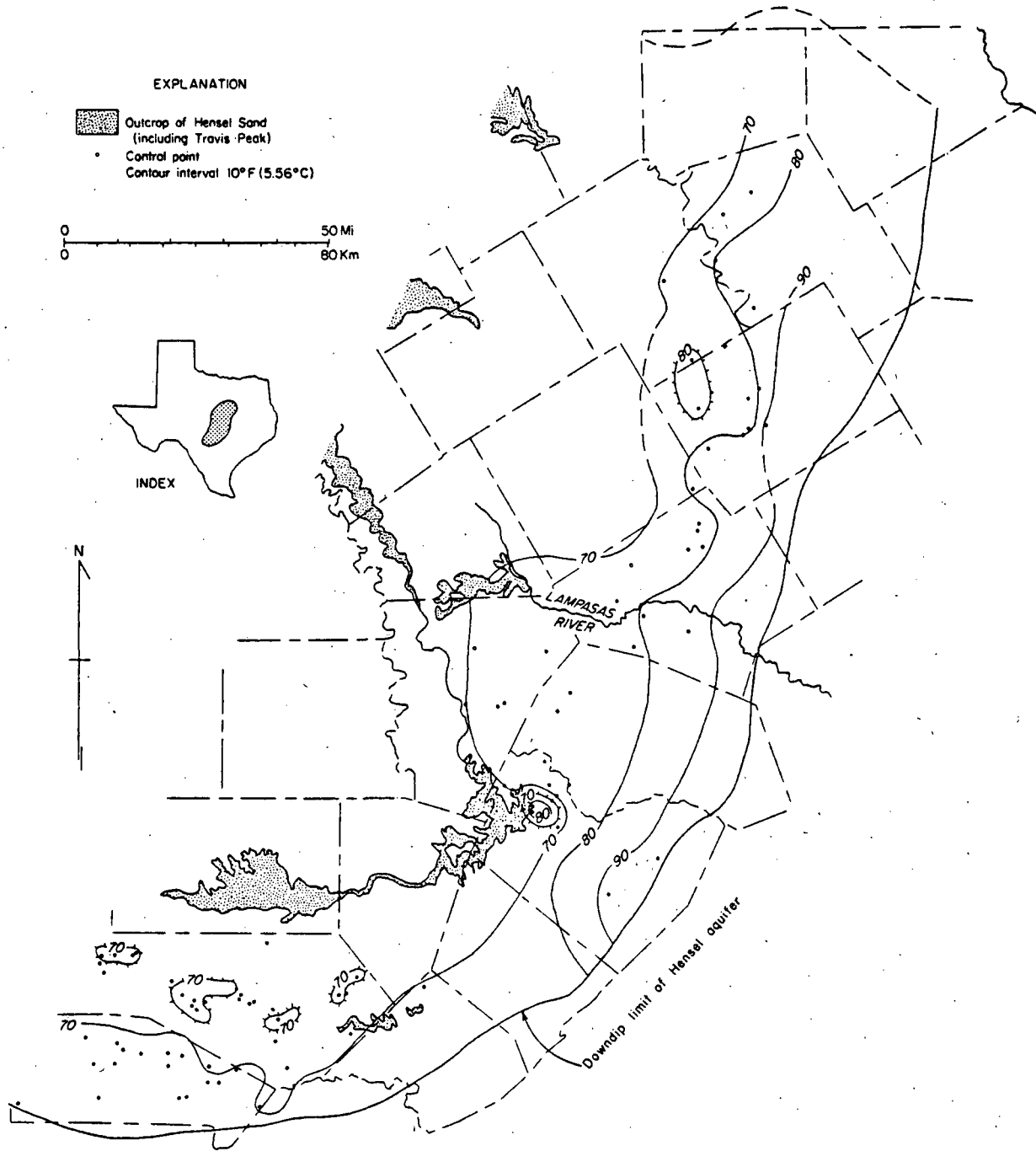


Figure 64. Water temperature contours for Hensel Sand.

## PALUXY SAND

### General

The Paluxy Sand is a terrigenous sandstone unit that was deposited in the northern part of the Gulf coastal province (the East Texas Basin) mainly from fluvial and deltaic systems coursing off the Ouachita and Arbuckle highlands. The Paluxy Sand thins toward the south, where its marine strandplain and offshore bar sand facies thin to a feather edge. There mud deposits and marl become progressively thicker, and these deposits in Central Texas make up the limestones and marls of the Walnut Formation. In the northwesternmost part of the study region (in Grayson County) the Glen Rose Limestone, which normally separates the Paluxy from the basal Trinity Sands, terminates. North of the limit of Glen Rose deposition, the Paluxy Sand is indistinguishable from the Trinity Sands Undifferentiated unit; in that area, the Paluxy is considered part of the Trinity (see figs. 12 and 41).

### Net-Sand Distribution of the Paluxy

On the northeastern margin of the East Texas Basin, the Paluxy net-sand trends suggest a major delta system that prograded into the basin from the north and northeast. There, aggregate sand thicknesses of more than 400 ft (122 m) form the delta lobes; there are, however, no clear indications of thick strike-oriented sand bodies, such as those composing the offshore bars or delta-front sands distal to the subjacent Trinity delta system. All the Paluxy delta systems are probably wave-dominated, and Caughey (1977) corroborates this major delta trend. He also reported, however, on a coastal barrier facies near the mouth of the main Paluxy deltas in northeast Texas. These barriers are not indicated on our net-sand map, though local thick sand deposits (such as in Kaufman County) suggest possible offshore bars within the larger prodelta-marine shelf system.

Thick, narrow, dip-oriented sand trends with thicknesses as much as 300 ft (91 m) on the net-sand map (fig. 65) indicate that the Paluxy was deposited as a series of locally derived fluvial systems that terminated in fan deltas (fig. 66) on the northwestern margin of the East Texas Basin. Caughey (1977) attributed the Paluxy in this area as being part of a strandplain system; however, the dip-oriented geometry, the proximity to a sediment source, and the similarity to (indeed, coalescence with) basal Trinity fluvial-deltaic systems led us to the conclusion that these deposits are



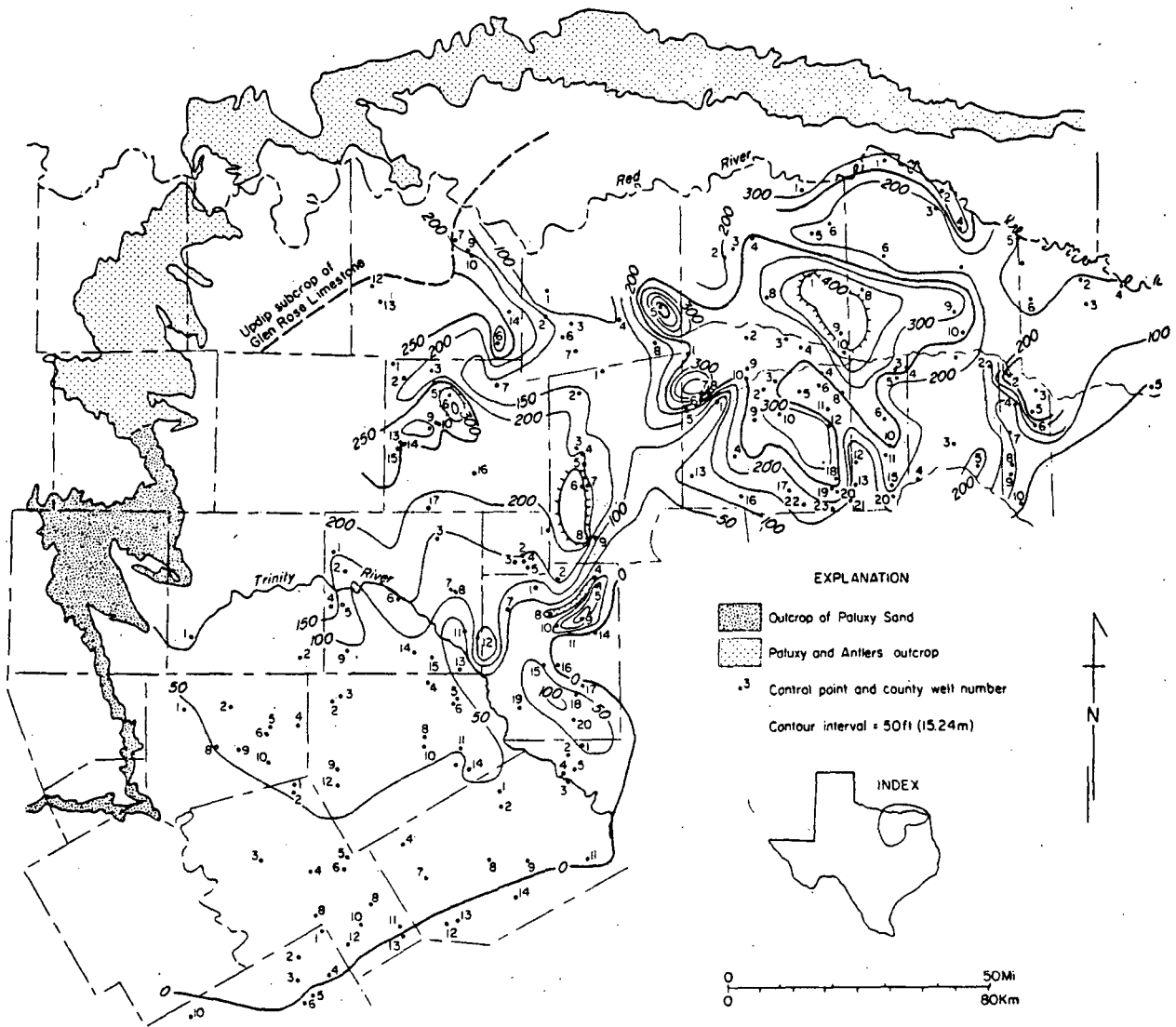
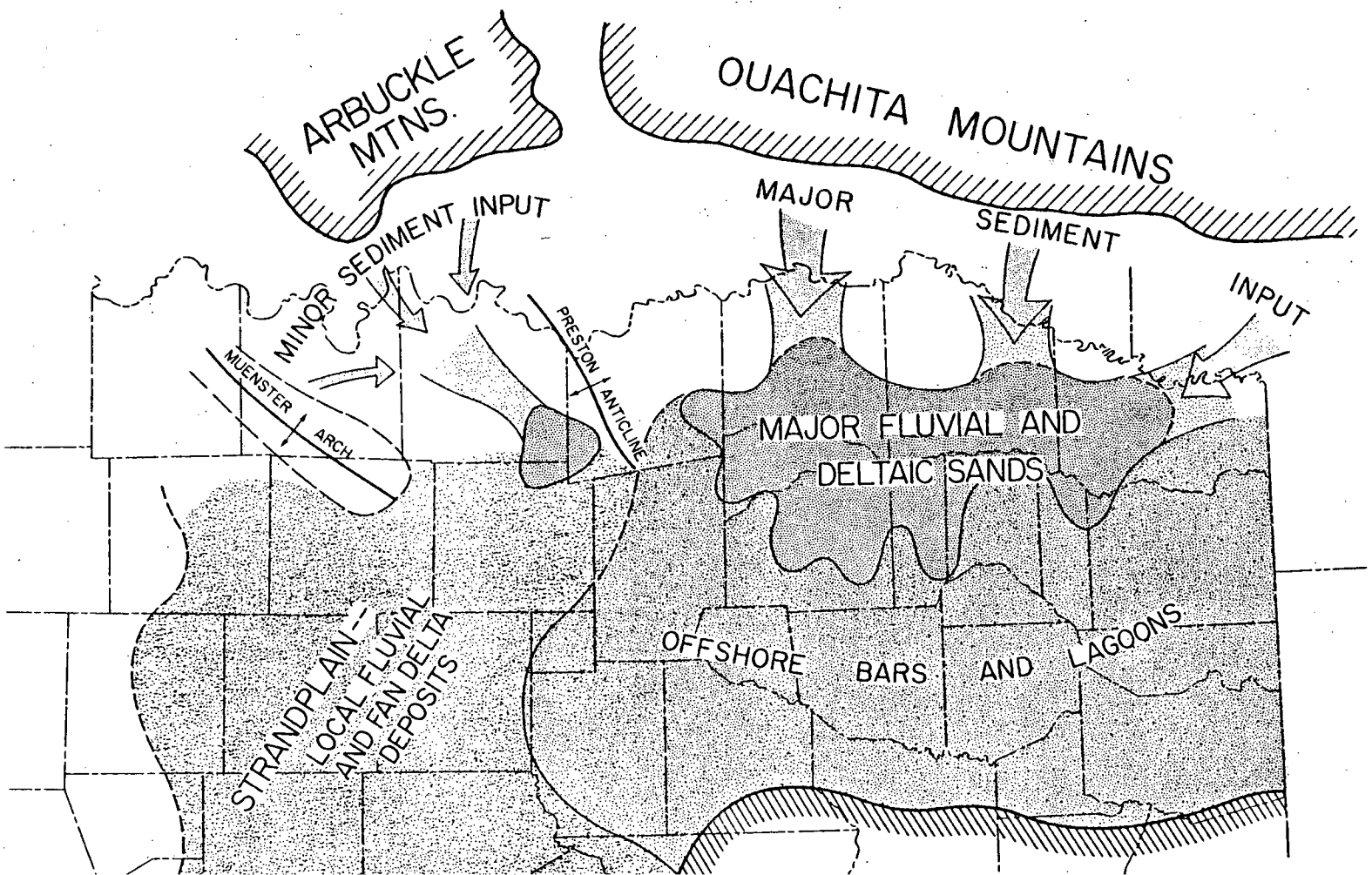


Figure 65. Net-sand thicknesses of the Paluxy.



part of a fluvial-fan delta system. Furthermore, work in the outcrop area of the Paluxy in Texas and Oklahoma indicates that the Paluxy Sand there is of fluvial origin (D. Hobday, personal communication, 1979). Clearly, there are probably both dip-fed and strike-fed sand bodies within this part of the Paluxy.

### Structural Configuration of the Paluxy

The Paluxy Sand (as with the Trinity Sands below) exhibits marked changes in dip across the structural hinge that separates the Texas Craton from the Gulf coastal province (fig. 67). In its updip reaches in Johnson County, the Paluxy dips range from 30 to 50 ft/mi (up to 10 m/km). Typical dips measured farther into the East Texas Basin are 125 ft/mi (24 m/km); maximum dip values presented here are 160 ft/mi (30 m/km) in Kaufman County.

The change in strike from a northeast-southwest trend to an east-west orientation marks the major embayment noted on both the pre-Cretaceous and the Hosston/Trinity structural maps. This flexure zone is denoted by a normal fault that strikes northwest-southeast and that is displaced down-to-the-west into the Sherman Syncline. But the major faults that displace the Paluxy occur along the Talco Fault Zone, and the northern parts of the Mexia and the Balcones Fault Zones also affect the Paluxy structural setting.

The Talco Fault System defines a narrow graben that trends roughly east-west near the Sulphur River along the Delta and Hopkins county line, and between Red River County and Franklin, Titus, and Morris Counties. Overall net displacement across the fault zone is down-to-the-coast; stratigraphic displacement along the northern part of the graben is commonly more than 1,000 ft (300 m), whereas up-to-the-coast displacement at the southern extremity of the graben is generally no more than 700 ft (213 m). However, in Hopkins County, at the western limit of the Talco system, up-to-the-coast displacement is as much as 1,300 ft (395 m), which is approximately equal to maximum down-to-the-coast displacement. The geometry of faulting in the Talco Fault Zone is similar for both the Paluxy and the Hosston. However, down-to-the-coast displacement is somewhat more for the Hosston. Up-to-the-coast displacement is roughly equivalent for both horizons.

The north-south-trending Mexia Fault Zone extends into Kaufman and Hunt Counties. There, up-to-the-coast displacement of the Paluxy is approximately 250 ft (75 m). Farther south, in Henderson and Navarro Counties, the strike of individual faults changes to more of a northeast-southwest direction, and there the down-to-the-

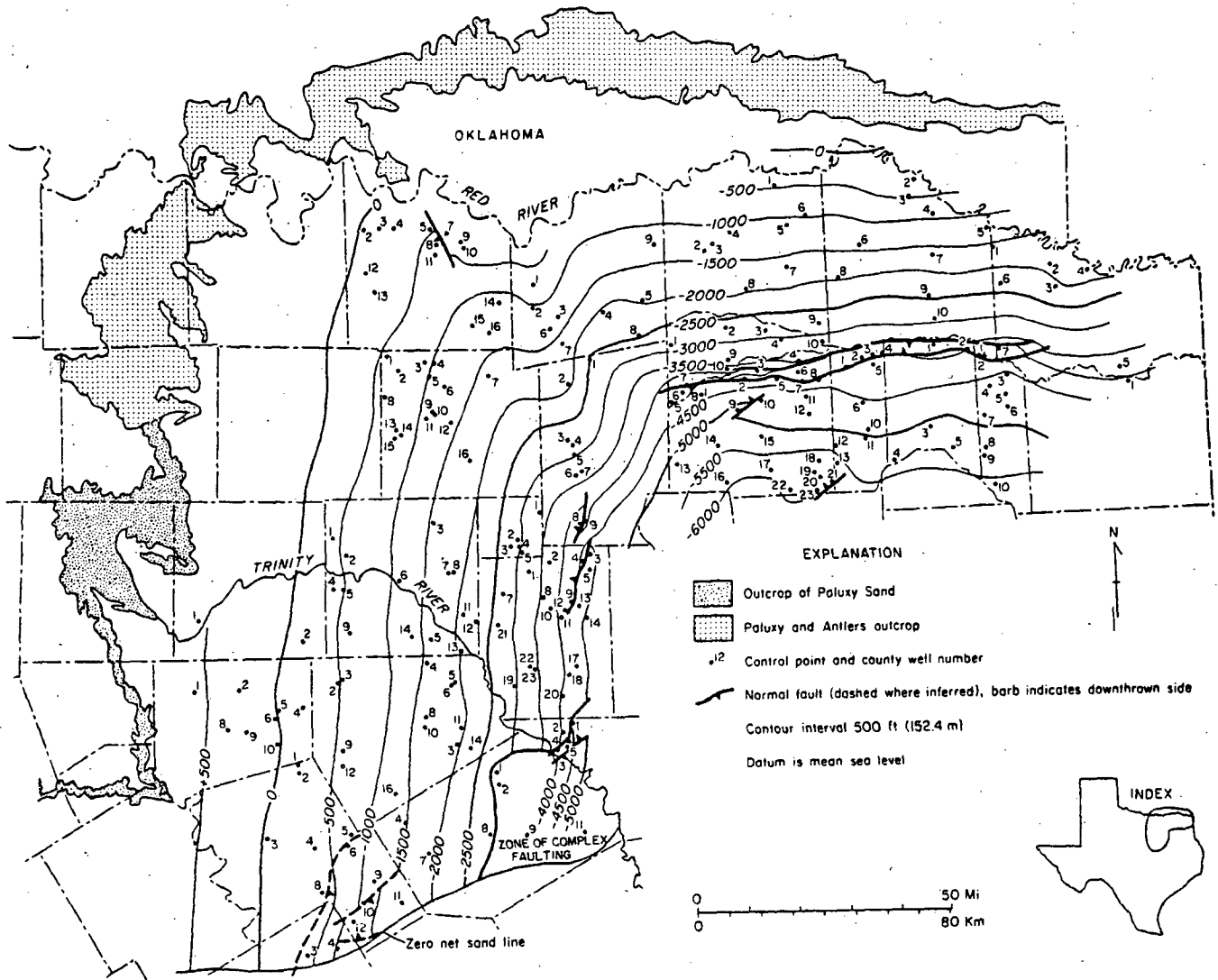


Figure 67. Structural configuration of the Paluxy.

coast displacement is approximately 250 ft (75 m), whereas up-to-the-coast displacement is no more than 200 ft (60 m).

The northernmost extension of the Balcones Fault system displaces the Paluxy in Hill County; there stratigraphic offset is approximately 275 ft (84 m) in a down-to-the-coast direction.

### General Aquifer Properties of the Paluxy

Examination of data on water level, water quality, and water temperature demonstrates a pronounced discontinuity in the Paluxy aquifer in that there is a western set of wells clustered in Denton, Collin, Tarrant, Dallas, and Johnson Counties, and an eastern cluster of wells in Hunt, Delta, Lamar, and Red River Counties. The dissimilarity of data between these two areas indicates that two Paluxy aquifers exist in two distinct geologic settings. The western Paluxy aquifer occurs in an area of sparse lithic control, but its geologic setting appears to be the sands distal and marginal to the locally derived fan-delta systems, and the marine strandplain-shelf sands of Caughey (1977). A net-sand low of less than 100 ft (30 m) separates the western Paluxy aquifer from the eastern Paluxy aquifer. There are few water wells in our data base that penetrate the Paluxy across this sand "divide" separating the two distinct aquifers. The eastern aquifer taps sands that compose the distributary-channel sands of the delta system that trends into the basin from the north and northeast.

### Water Level of the Paluxy

The water level map for the Paluxy (fig. 68) is based on data collected by the Texas Department of Water Resources during November 1977. These contours approximate the potentiometric surface of the aquifer, and thus, they can be used to predict flow paths. In western Tarrant County, one well occurs in the outcrop area of the Paluxy, where the aquifer is under water table conditions. East of the outcrop area, the structural contours dip basinward at a rate twice as high as that of the dip of water level contours. Hence, in most of the area contoured, the Paluxy aquifers are under artesian conditions in which water levels rise as much as 2,000 ft (610 m) above the top of the aquifer host rock in Rockwall County.

Strike of the water level contours are approximately parallel to structural strike near the Paluxy outcrop, but this situation changes in Dallas and Collin Counties. There, water level contours encircle the Dallas metropolitan area, probably in response to extensive pumping in eastern Tarrant and western Dallas Counties.

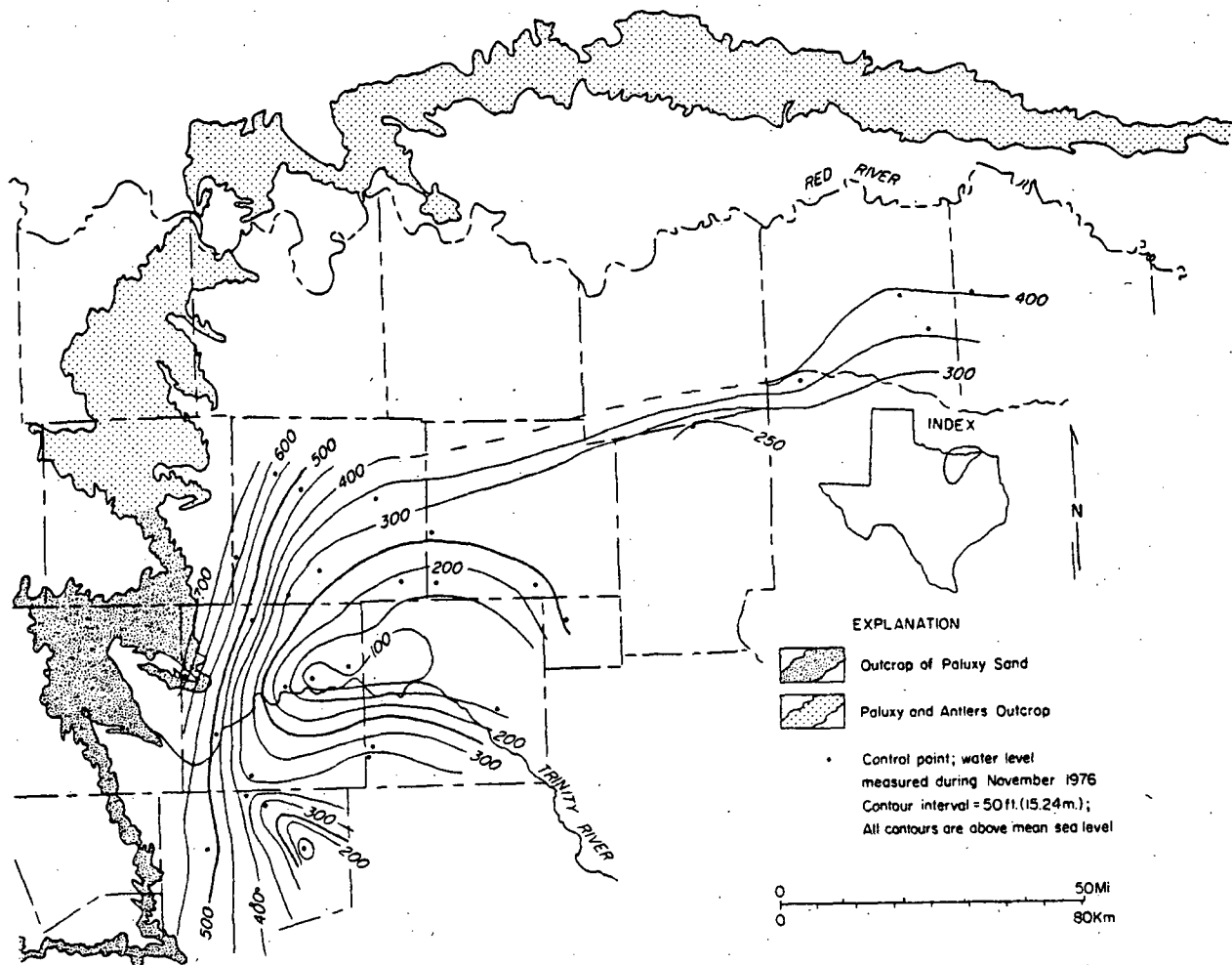


Figure 68. Water level contours for the Paluxy.

Another factor affecting the change in strike of the water level contours in Collin County is the presumed presence of the ground-water divide separating the two Paluxy aquifer systems along the zone of thin net sands. Another localized closure of water level contours is seen in eastern Johnson County, and this probably results from extensive pumpage in the vicinity of Alvarado, a community lying in the center of this cone of depression.

In the eastern Paluxy aquifer, the water level contours trend in the same general strike directions as the Paluxy structural contours, but data points are not sufficiently close to denote possible cones of depression there. The structural dip in Lamar County is approximately ten times the inclination of the water level surface, and this difference results in ground water rising more than 2,200 ft (670 m) under pressure. Depths to the "static" water level in Lamar and Red River Counties is no more than 165 ft (50 m), yet the aquifer in that area lies at a depth of commonly more than 2,000 ft (610 m).

#### Water Quality and Water Temperature of the Paluxy

The map depicting TDS content of Paluxy ground water clearly shows the discontinuity between the eastern and western Paluxy aquifer systems (fig. 69). Along the ground-water divide in Grayson, Hunt, eastern Collin, and western Fannin Counties, there are no water quality data—probably because of a paucity of water wells there. In the western Paluxy aquifer, data points are more numerous than in the eastern system, and ground water in the updip reaches is of a higher quality compared with water from wells across the ground-water divide.

Most wells in Tarrant and Denton Counties have dissolved solids values of less than 750 mg/l, whereas all wells in Lamar, Delta, and Red River Counties have values of more than 1,000 mg/l. This can be partly explained by the fact that the Paluxy lies beneath Tarrant and Collin Counties at a shallow depth—only a few hundred feet beneath the ground surface—whereas the wells in Lamar County penetrate the aquifer at depths of more than 1,500 ft (455 m). More important for water quality, however, is the presence of dip-oriented fluvial sand channels that provide direct hydrologic communication with a recharge area in the western part of the aquifer. In the eastern part of the Paluxy, the Red River probably acts as a hydrologic base level. Further, even though the Paluxy is not exhumed, the Red River nonetheless probably diverts meteoric waters flowing downdip from the recharge area in Oklahoma. In short, the eastern Paluxy aquifer is recharged along its depositional trend—both from the east

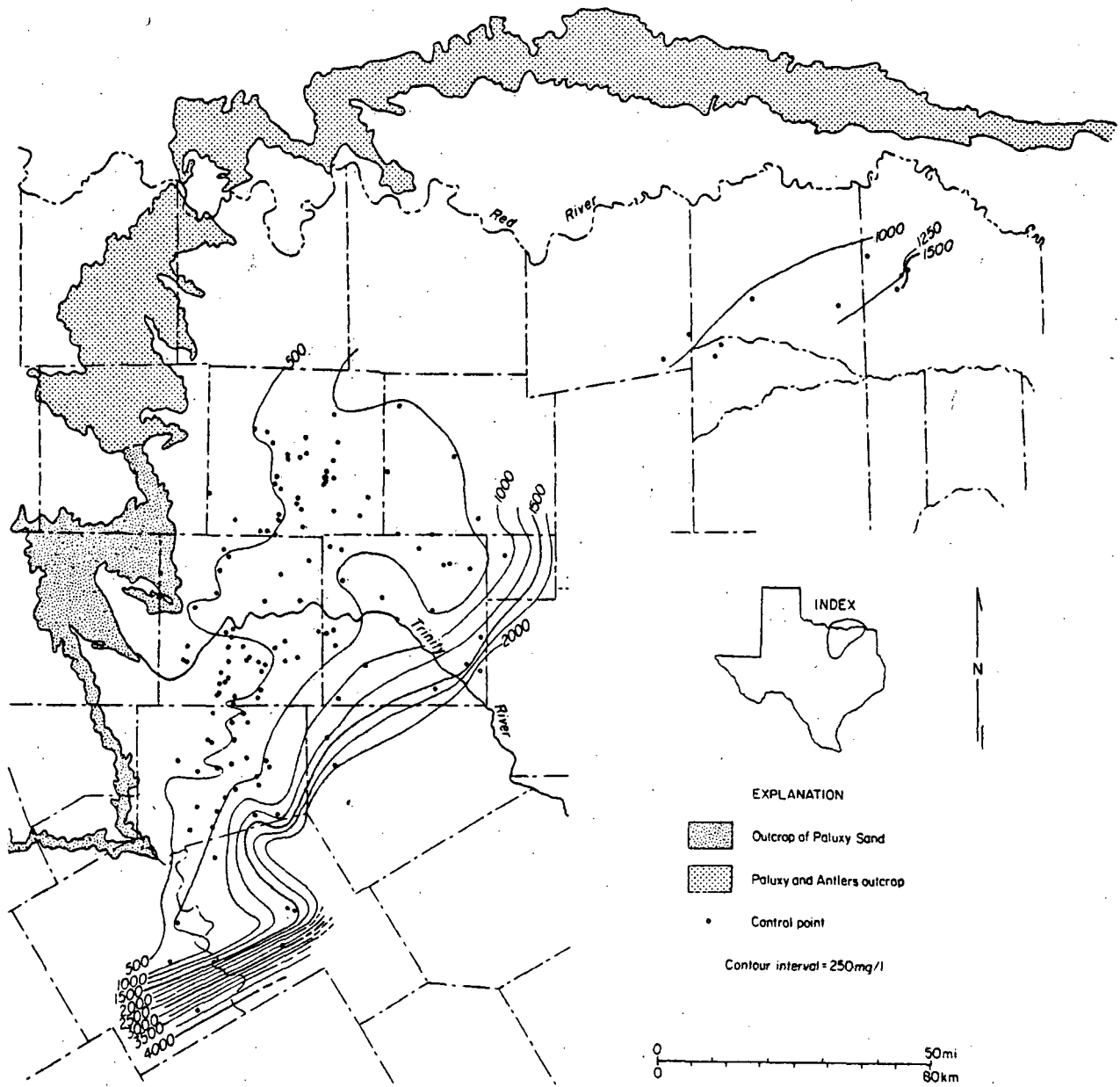


Figure 69. Total dissolved solids contours for Paluxy ground water.



and from the north. But since flow lines probably converge toward the Red River, the result is less recharge and a lower quality of ground water in this part of the Paluxy.

In all instances, water quality correlates directly with thick sand bodies; zones of thick sand generally display relatively low TDS values. This is true for the deep delta lobes in the eastern part of the Paluxy; water quality is better there (lower TDS) than for areas of equivalent depth (but of lower thickness of net sands) in the western part of the aquifer. Similarly, as the net sands of the aquifer thin to the south, water quality becomes progressively worse, and this is most dramatically seen near the zero net-sand line in Bosque and Hill Counties, where dissolved solids content of the water increases precipitously.

Ground-water temperature, like the other aquifer attributes, clearly delineates the two distinct hydrologic areas within the Paluxy Sand (fig. 70). In the western part, temperatures are mostly less than 90° F (32° C); whereas in the eastern area the three wells, for which temperature data exist, are all above 110° F (43° C).

Temperature isopleths, as expected, trend parallel to structural strike, and water temperature increases with increasing depth. The temperature/depth relation is further substantiated by a scattergram of all Paluxy water data (fig. 71). The Paluxy TDS values increase only moderately with increasing depth (fig. 72), although the increase in TDS is somewhat greater than that charted for the Hosston/Trinity. Nonetheless, a comparison of temperature to TDS (fig. 73) indicates that geothermal potential exists for many localities within the Paluxy because there are several wells producing water at greater than 100° F (38° C), but which have dissolved solids concentrations low enough for the water to be potable.

### Geothermal Potential of the Paluxy

There are only a few localities where the Paluxy is used for public water supply (table 2); it is, like the Hensel Sand, commonly used to supply domestic and livestock needs. However, there are two localities—one in the Dallas metropolitan area in the western part of the Paluxy aquifer system and one in Fannin and Lamar Counties in the eastern part—where the geothermal potential is indicated by water temperature values greater than 90° F (32° C) and dissolved solids content less than 1,000 mg/l (fig. 74). A computation of the energy value of Paluxy water was done for the town of Ben Franklin in Delta County; this locality is the only public water supply that draws from the Paluxy and that has the requisite data for this computation. During an average January, Ben Franklin, Texas, pumps 783,000 gal (2,963,890 l) of water at a temperature of 112° F (44° C) from a depth of 145 ft (44 m). The mean minimum

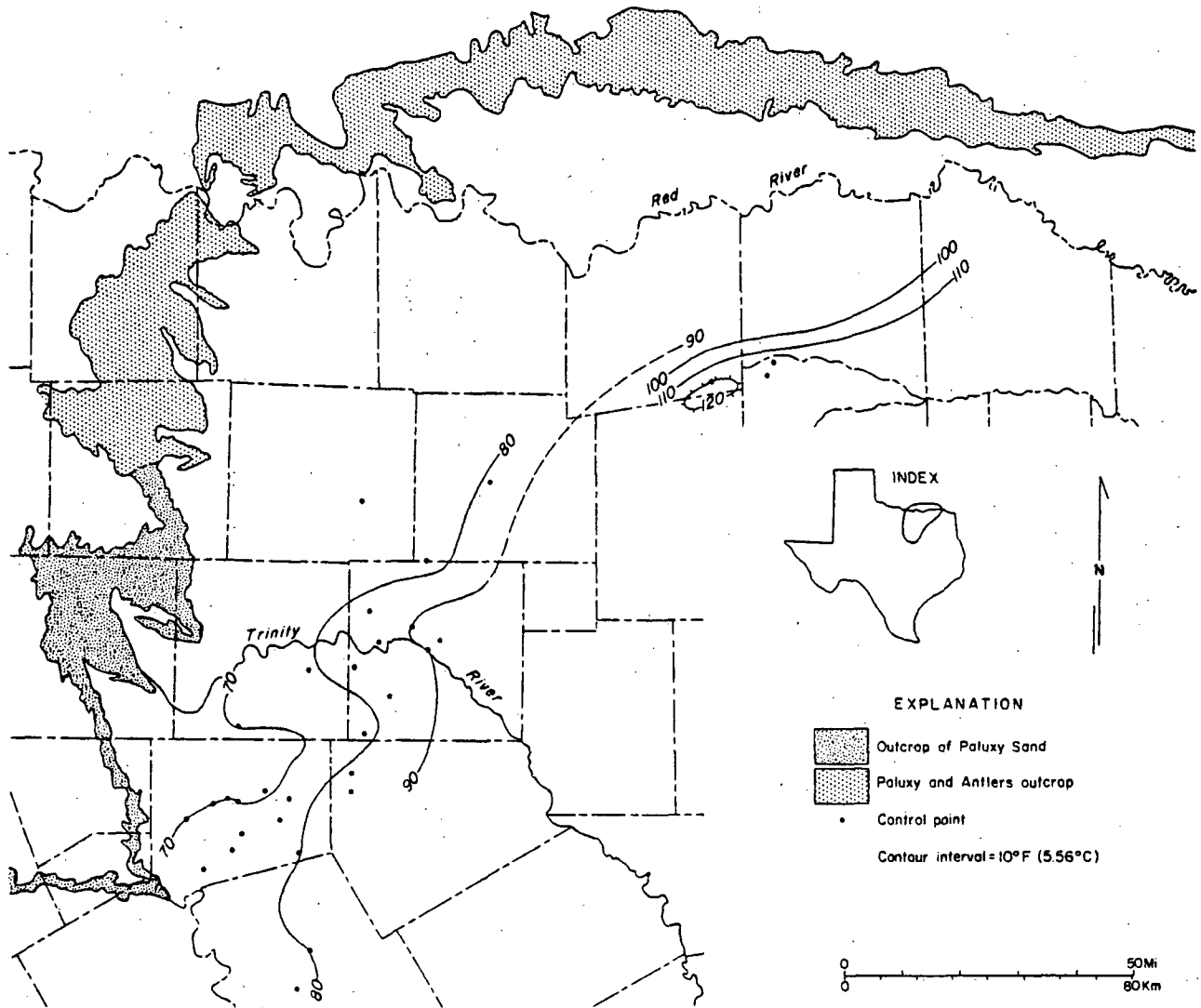


Figure 70. Water temperature contours for the Paluxy.

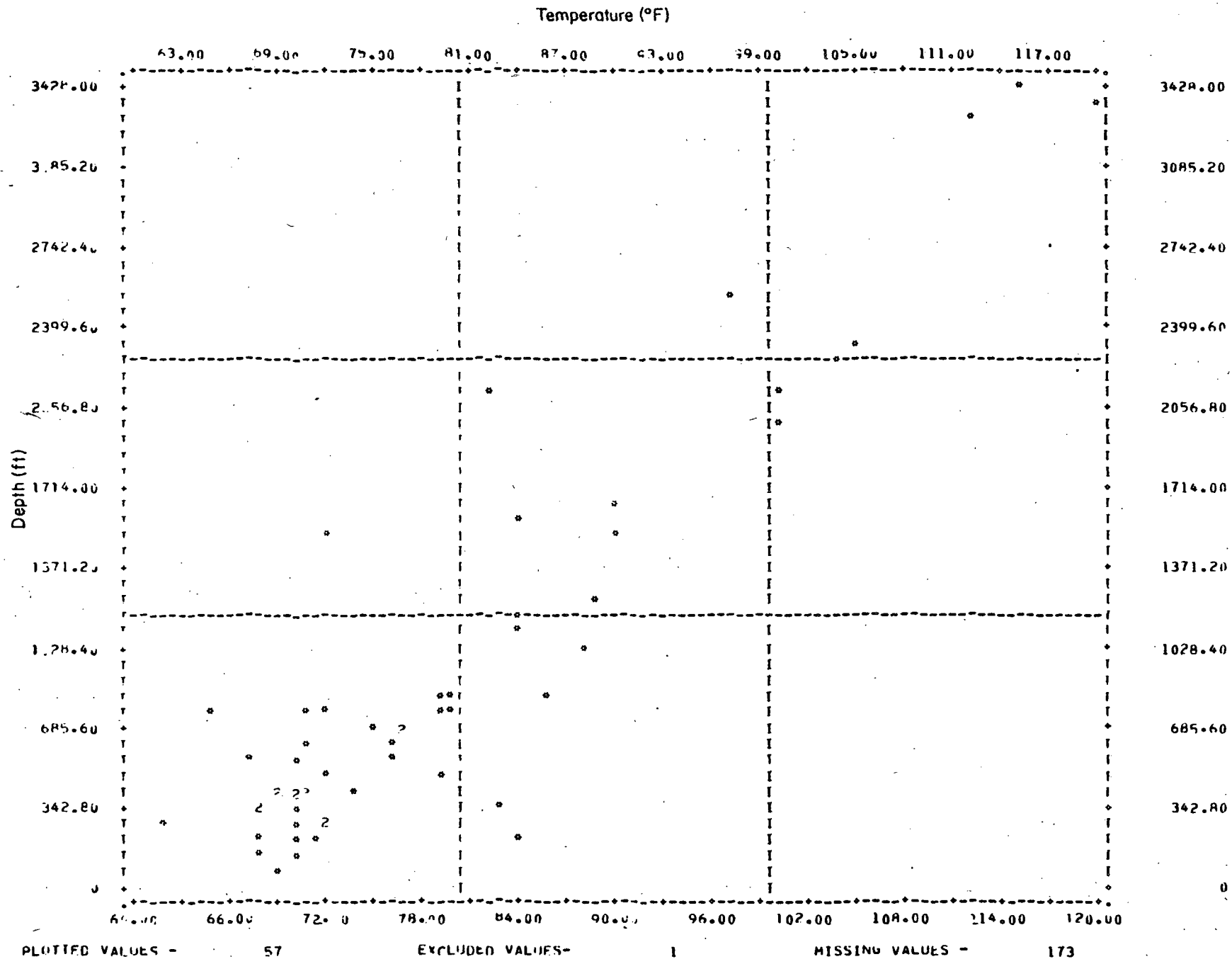


Figure 71. Temperature/depth scattergram for the Paluxy.



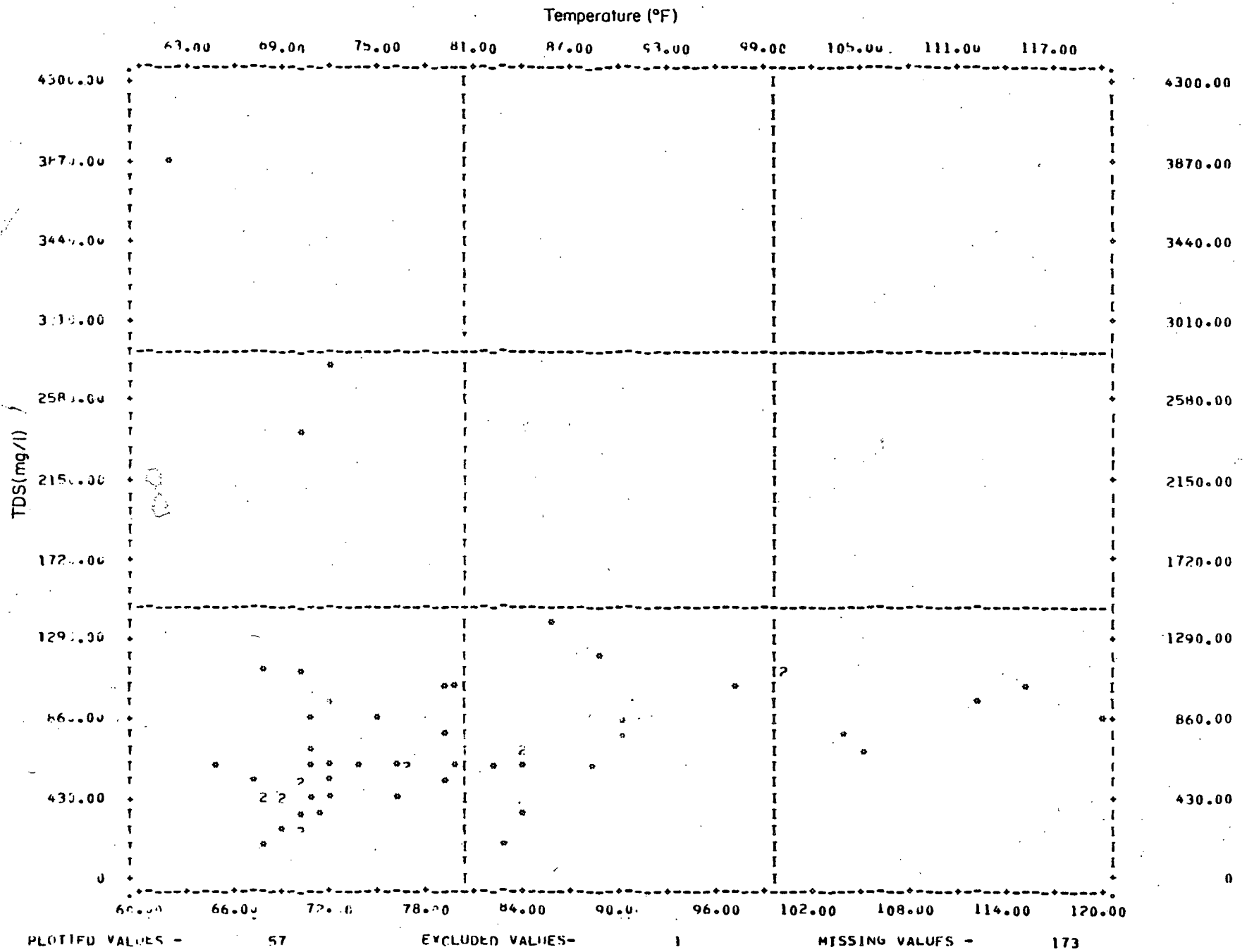


Figure 73. Temperature/total dissolved solids scattergram for the Paluxy.

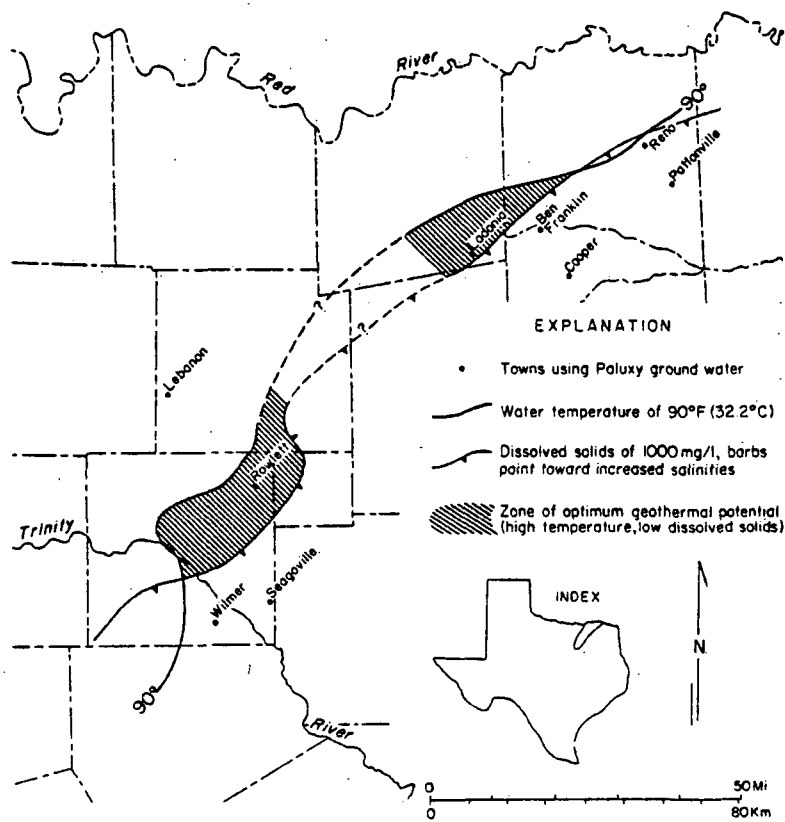


Figure 74. Municipalities using Paluxy ground water compared to areas of optimum geothermal potential.

Table 2. Selected municipal ground-water withdrawals--Paluxy aquifer  
(data from Texas Department of Water Resources).

County	Municipality	Mean January Pumpage (1972-1976)	Mean Yearly Pumpage (1972-1976)
Collin	Lebanon	1,964,015.5*	23,568,186
Dallas	Seagoville <sup>+</sup>	2,548,250*	48,507,671
Dallas	Rowlett	1,991,040	27,092,824
Dallas	Wilmer <sup>#</sup>	5,149,100*	62,371,615
Delta	Ben Franklin	783,500*	10,974,400
Delta	Cooper	1,201,322	13,935,822
Fannin	Ladonia <sup>+</sup>	1,496,000*	28,226,750*
Lamar	Pattonville	729,396	9,017,715
Lamar	Reno	1,018,500*	16,083,200

- \* indicates less than 5 years of measurements
- # draws from both Hosston/Trinity and Paluxy aquifers
- draws from both Hosston/Trinity and Woodbine aquifers
- + draws from both Paluxy and Woodbine aquifers

January temperature there is approximately  $32.5^{\circ}$  F ( $0.3^{\circ}$  C). Hence, the energy debit owing to pumping is  $1.22 \times 10^6$  Btu ( $3.07 \times 10^5$  kg-cal) during January; the energy assets during the same time period are  $5.19 \times 10^8$  Btu ( $1.31 \times 10^8$  kg-cal). The total (maximum) energy credits for water pumped for municipal consumption is  $5.18 \times 10^8$  Btu ( $1.31 \times 10^8$  kg-cal). This modest energy balance does not reflect heat exchange efficiencies, but the main point is that the water is already produced, regardless of the heat. Any heat that can be extracted is essentially free, once the installation costs of using the heat are paid. As mentioned with respect to the Hosston/Trinity where a single-family dwelling consumes this hot-water, these costs are mainly for plumbing modifications to feed the water directly into the hot water distribution system of the home.

The probable area of greatest geothermal production within the Paluxy is within the deep sand trends of the fluvial-deltaic systems that compose the eastern part of the Paluxy aquifer. The hottest water temperatures presently produced from the Paluxy are yielded from wells that tap the marginal parts of this delta system. Other wells farther up the depositional trend (toward the Red River and Bowie County) might yield elevated temperatures but without the generally poor water quality observed farther west in Delta and Lamar Counties.



## EDWARDS LIMESTONE

### General



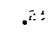
The Edwards Limestone is the only nonterrigenous unit investigated in this survey of low-temperature geothermal resources; it is an important aquifer in south-central Texas, supplying water along the Balcones Fault Zone from Kinney County north to Bell County. In its main aquifer reaches, however, water quality is consistently high and water temperature reflects average ambient air temperatures over the recharge areas. Farther downdip, notably in Atacosa, Caldwell, and Gonzales Counties, the Edwards is a reservoir rock for petroleum. Between the artesian aquifer zone and the local hydrocarbon accumulations downdip, there is a zone within the Edwards where variable amounts of water are produced having dissolved solids concentrations greater than 1,000 mg/l and commonly having elevated temperatures. This "bad-water zone" has historically yielded waters for local health resorts, such as at Terrell Wells in Bexar County. Hence, because it is known to yield warm water locally and because it provides an easily recognized structural datum in south-central Texas, we chose the Edwards as one of our targets for assessing lithic framework and water attributes.

The Edwards Limestone, however, does not persist as a significant unit throughout the study region. It becomes progressively thinner to the north, and as the Edwards thins, limestone strata equivalent to the underlying Comanche Peak become thicker; in North-Central and northeast Texas there is a nomenclatural change from Comanche Peak to Goodland Limestone (fig. 12). We did not continue our investigation far beyond the Lampasas and Little Rivers because that is where the Edwards thins markedly, and it is no longer an important aquifer beyond Bell County.

### Structural Map of the Edwards Limestone

The structural map of the Edwards Limestone provides a detailed view of faults in south-central Texas (fig. 75). In general, the geometry of faults displacing the Edwards is similar to that seen on the Hosston structure map. However, there are areas, such as in Bexar County, where more detailed control for the Edwards has resulted in a more complex local pattern of faulting compared with that of the Hosston structure map. Also, there are areas, such as in Maverick County, where

EXPLANATION

-  Outcrop of Edwards Limestone in Balcones Fault Zone
-  Normal fault (assumed where inferred), barb indicates downthrown side
-  Control point with county well number
- Contour interval = 500 ft (152.4 m) with local supplementary 100 ft (30.48 m) contours
- Datum is mean sea level

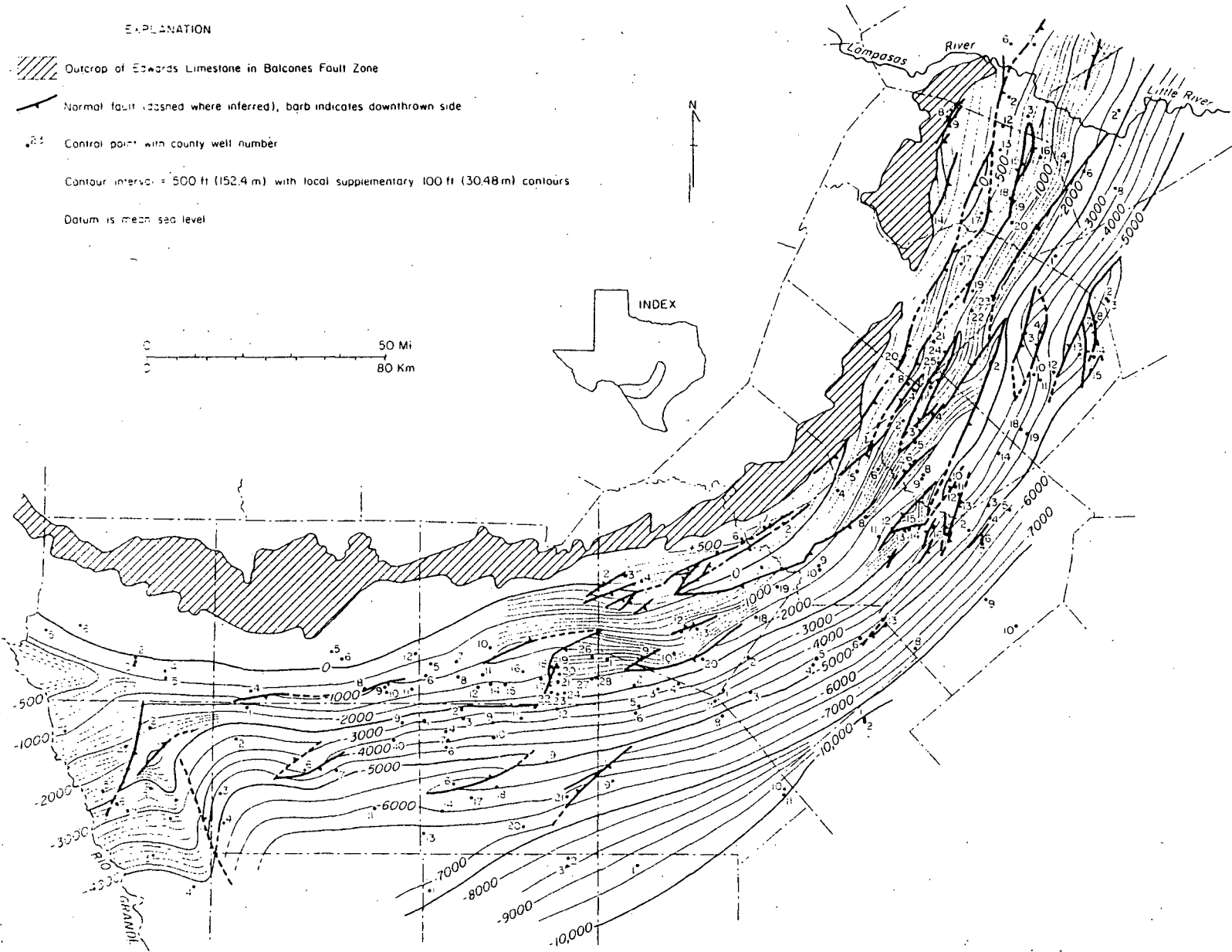


Figure 75. Structural configuration of Edwards Limestone.

faults displacing the Edwards are mapped where no faulting of older strata is discerned.

Magnitude of fault displacement is generally somewhat greater for the Edwards compared with the Hosston. Down-to-the-coast faulting in the Balcones system is commonly as much as 300 ft (90 m) compared with a usual range of from 100 to 300 ft (30 to 90 m) for the Hosston. Maximum down-to-the-coast displacement mapped for the Edwards is 1,500 ft (457 m) in Bastrop County. Up-to-the-coast displacement of the Edwards occurs from Bastrop County into Caldwell County, and discontinuously from Guadalupe County into Bexar, Medina, and Zavala Counties. There is not a clearly defined up-to-the-coast Luling Fault System except perhaps within Caldwell and Bastrop Counties. Usual displacement there is somewhat greater than 100 ft (30 m), whereas maximum offset is approximately 600 ft (182 m) in Bastrop County.

The structural hinge is not as clearly evident on the Edwards structure map, probably because we lack extensive subsurface control updip from the hinge zone. There are nonetheless, increasing rates of dip in a basinward direction. Lowest dips measured are approximately 40 ft/mi (8 m/km) in Williamson County, and dips increase markedly into the Gulf Coast Basin where inclinations greater than 160 ft/mi (30 m/km) are common. The maximum dip measured for the Edwards Limestone is approximately 300 ft/mi (58 m/km) in northern Zavala County.

Several regional structural features are evident on the Edwards structure map. The Chittim Anticline and related faults appear in Maverick County. An east-trending anticline (possibly part of the Devil's River Uplift) occurs in southwestern Kinney County. The San Marcos Platform does not appear as a structural high at the scale presented here, but it is evidently the locus of the most intensive faulting in the region.

#### Thickness of the Edwards

The Edwards has been studied regionally by Rose (1972), who proposed the reclassification of the Edwards to group status with several component formations both in outcrop and in the subsurface. In this study, we are more concerned with thickness and structural attributes in the shallow subsurface, especially in the area within or immediately downdip of the Balcones Fault Zone. It is there that we presumed the geothermal potential of the Edwards to be greatest; the rock unit lies at a relatively shallow depth, yet its hydrologic and geochemical attributes still might allow production of low-temperature geothermal waters. Hence our isopach map (fig.

76) represents the aggregate thickness of the Edwards without regard to the various "formations" delineated by Rose.

This isopach map shows the thinning of the Edwards from west to east along strike, from thicknesses greater than 1,300 ft (400 m) in the Maverick Basin to less than 150 ft (46 m) in Bell County. Our mapping did not extend basinward far enough to show the pronounced thickening associated with the Stuart City Reef Trend (Bebout and Loucks, 1974), but the map does show a general basinward thickening trend, as expected. Local thick and thin areas might represent either small reef deposits, or they might be a result of attenuation owing to the well having penetrated a fault that displaced the Edwards (and thus shortened the section). A broad, thin area in Gonzales County probably is a result of the San Marcos Platform.

The major area of potential geothermal waters from the Edwards is within Medina, Bexar, and Guadalupe Counties. In that area, the Edwards in the subsurface is generally about 500 ft (150 m) thick. Farther west, in Uvalde County, thickness of the Edwards is more than 800 ft (240 m). However, we have generally concluded that structural attributes, and not stratigraphic setting, are most important in determining the various hydrologic attributes of the Edwards.

#### General Aquifer Properties of the Edwards

Within the study region, the Edwards aquifer consists of two parts--the fresh-water artesian system, and the "bad-water zone." Within the fresh-water part of the aquifer, water quality is uniformly high; concentration of dissolved solids generally ranges from 250 to 500 mg/l. Water temperature in the fresh-water zone is commonly less than 75° F (24° C). Within the bad-water zone TDS values range from 1,000 mg/l to 9,000 mg/l in a few wells. Water temperature within the bad-water zone is commonly greater than 100° F (38° C), although several data points in Guadalupe County indicate bad-water wells having temperatures comparable to those of the fresh-water part of the aquifer. Conversely, in southern Uvalde County, several wells have moderate TDS values (mostly less than 700 mg/l), water temperatures greater than 80° F (27° C), and a maximum value of 93° F (31° C).

The bad-water line that separates the two parts of the Edwards aquifer within the Balcones Fault Zone is delineated on the basis of the 1,000 mg/l isopleth. This line has been attributed to fault control and to facies changes, but it probably is a hydrologic barrier, representing the downdip limit of long-term phreatic transfer of meteoric waters from high structural and topographic levels in the western part of the region to the low-lying discharge points in the east (Abbott, 1975). The main lithic

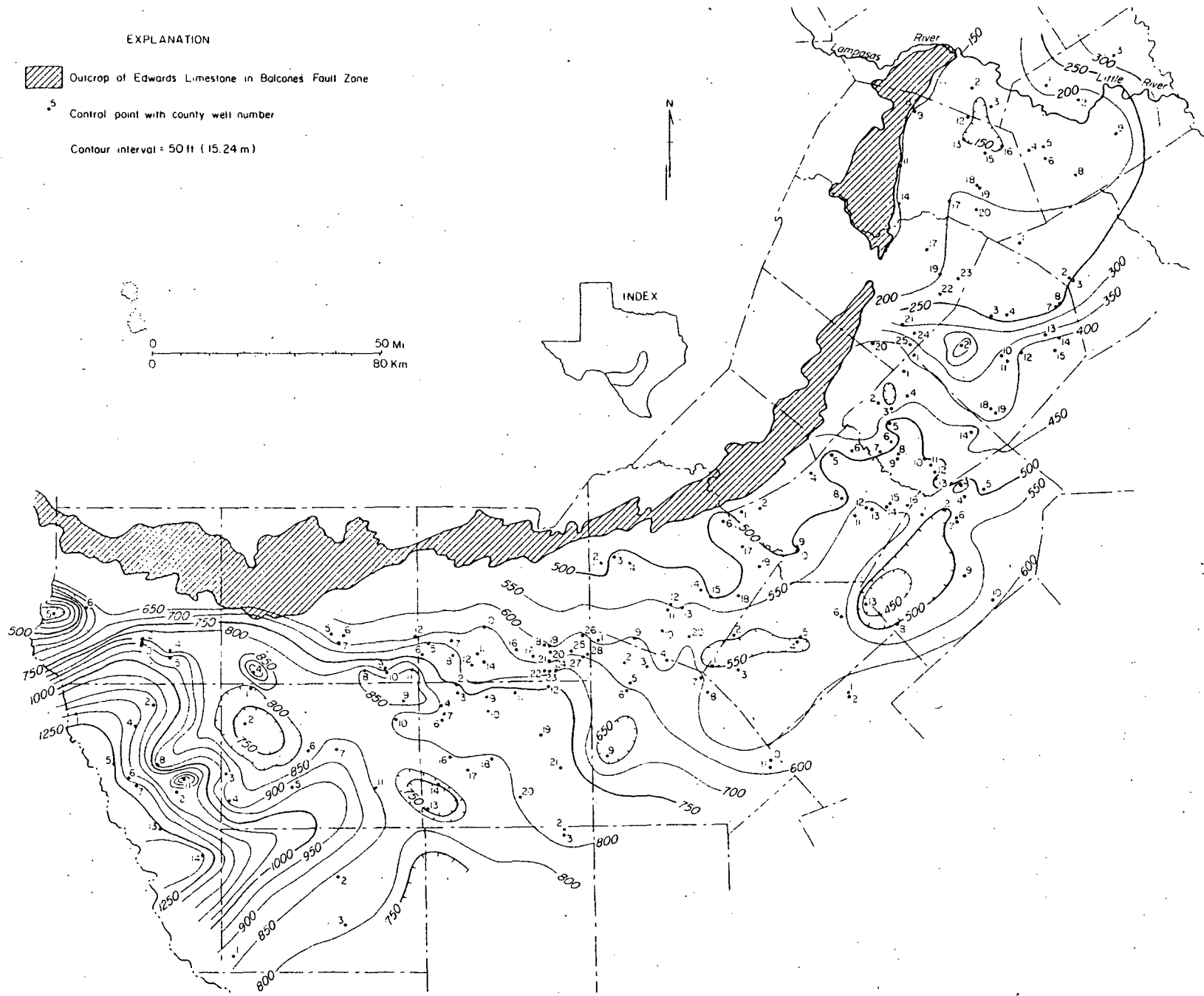


Figure 76. Isopach map of Edwards Limestone.

difference across the bad-water line is the absence of alteration owing to solutional activities of fresh water (Abbott, 1974). Water-level data are sparse across the bad-water line, but the closely spaced contours in eastern Travis and Williamson Counties suggest lower effective permeability values there (fig. 77).

Obviously, in a geothermal context, the "bad-water zone" of the Edwards Limestone is the major area of interest. However, just as obviously, water quality attributes across the bad-water line impose severe constraints on multiple use.

Southern Bexar County has a number of hot water wells producing from the Edwards (fig. 78), but TDS content is generally above 4,000 mg/l (fig. 79). Moreover, a geochemical study of the bad-water zone of the Edwards shows anomalous contents of base metals, particularly lead; too, there are wells tapping the Edwards in which fluorite is precipitating in the well bore (Dennis Prezbindowski, personal communication, 1978). These facts, in context of the regional structural setting, show that the chief significance of these Edwards waters is in relation to hydrothermal ore deposition. It appears that we are witnessing a Mississippi Valley-type ore deposit in a formative stage.

In short, the geothermal resource potential of the Edwards Limestone is not great, mainly because water chemistry prevents the use of the water as a potable supply. Even though Bexar County wells have water temperatures above 100° F (38°), waters from these localities are too saline to use for drinking. Only in southeastern Uvalde County does the Edwards yield water that might be used for drinking and heating needs. Yet, there the heat value is low.

In its artesian, fresh-water system, the Edwards suggests yet other possibilities. There the high yield, constant temperature, and low TDS values present a potential for using ground-water heat pumps to extract the caloric difference between summer and winter air-temperature extremes. That potential, however, involves different avenues of research than are employed here; nonetheless such an assessment warrants further study.

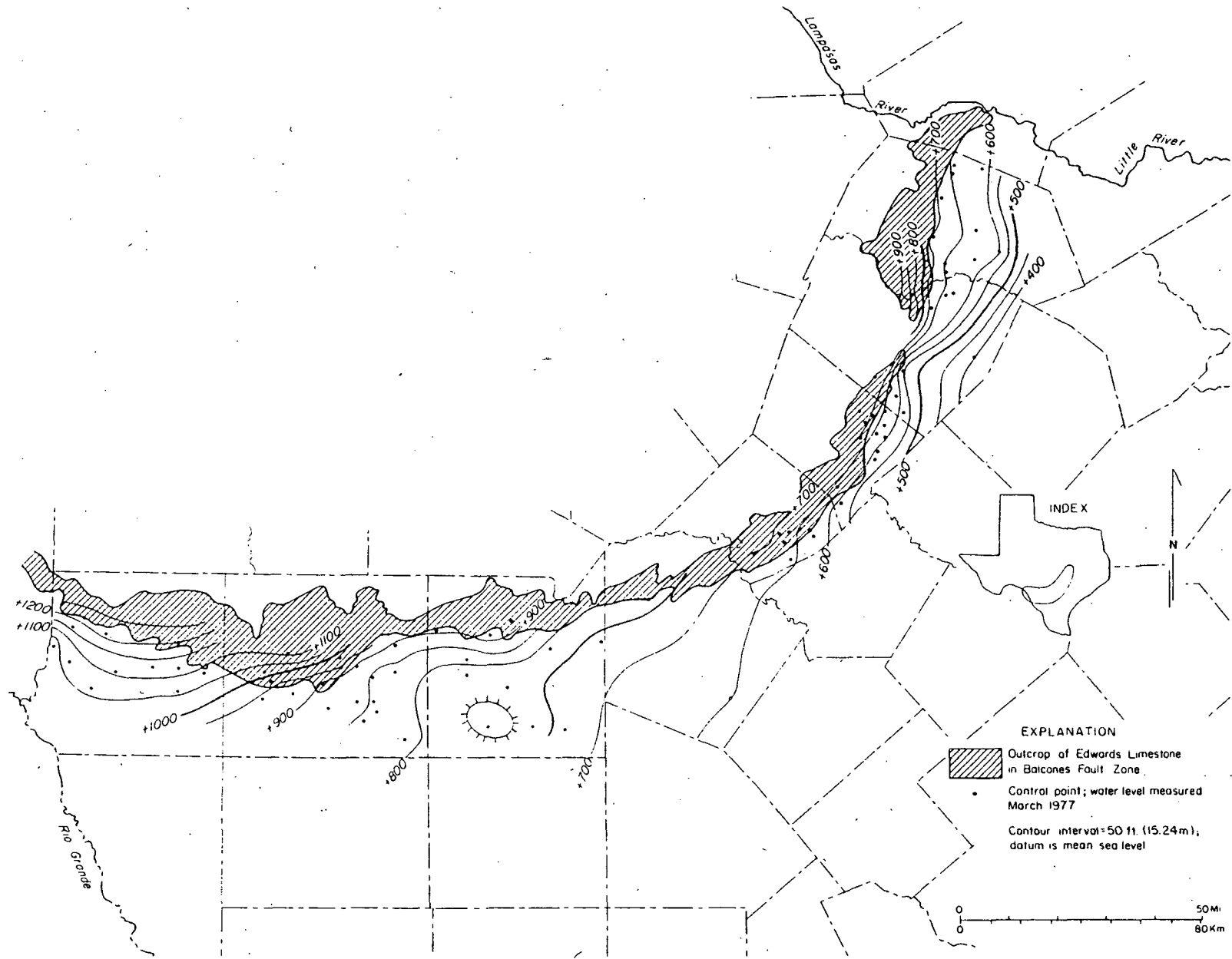


Figure 77. Water level contours for the Edwards.

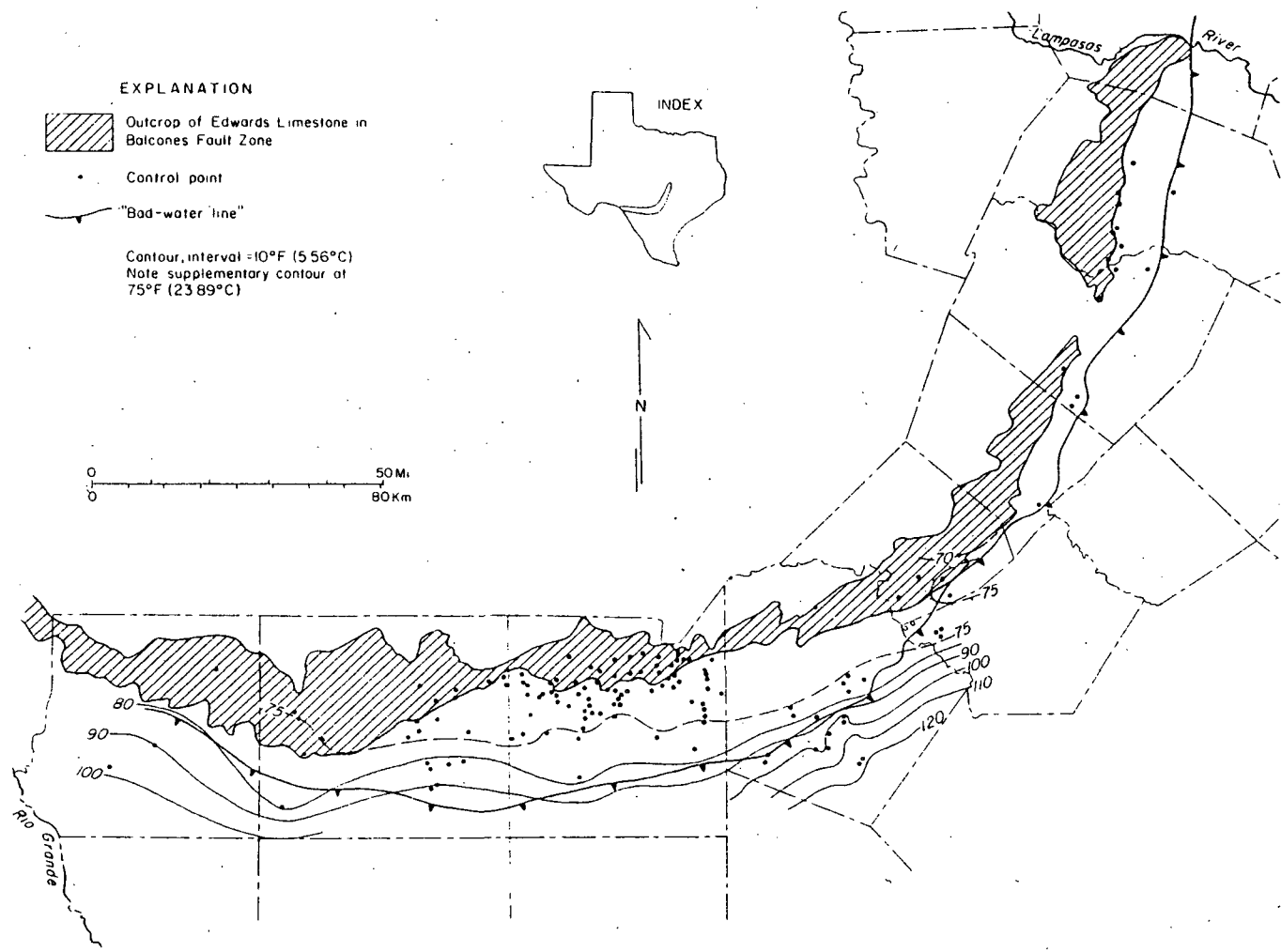


Figure 78. Water temperature contours for the Edwards.



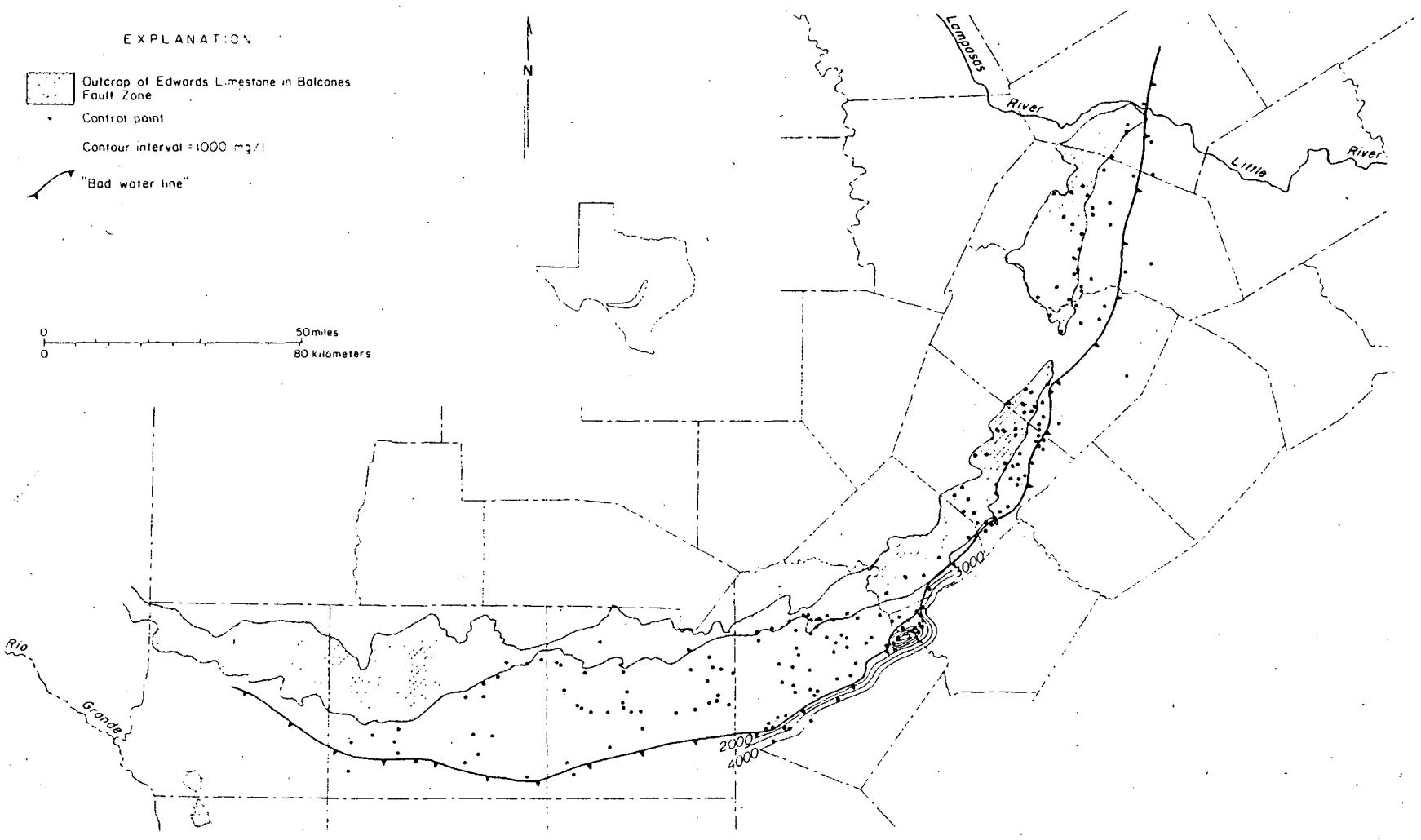


Figure 79. Total dissolved solids contours for the Edwards ("bad-water zone").

## WOODBINE SAND

### General

The Woodbine Sand is the youngest formation that we studied in our survey of low-temperature geothermal aquifers. It is of Upper Cretaceous (Cenomanian) age, whereas the other aquifers surveyed are all part of the Lower Cretaceous. Being stratigraphically higher, the potable water zone of the Woodbine aquifer extends farther into the East Texas Basin. In its downdip reaches, the Woodbine is an important petroleum reservoir, and in this context a survey of the geothermal attributes of the Woodbine has previously been conducted (Plummer and Sargent, 1931). However, this study focused on the downdip parts of the formation, where hydrocarbons occur, and not on the areas updip, where potable waters occur.

The Woodbine Sand was deposited into the northeastern part of the East Texas Basin by fluvial and deltaic systems that coursed off the Ouachita highlands. The Woodbine has been subdivided into two units--the lower Dexter Member and the upper Lewisville Member (Oliver, 1971). The Dexter Member consists of fluvial and deltaic sands deposited as the Woodbine systems prograded southward. The Lewisville Member consists of sands and muds deposited in shelf-strandplain systems during the marine-transgressive phase of Woodbine deposition. The Woodbine thins to the south, and marine (prodelta) muds represented by the Pepper Shale occur south of the zero net-sand line in the vicinity of McLennan and Falls Counties.

### Net-Sand Distribution of the Woodbine

The net-sand map of the Woodbine shows both dip-oriented trends of the Dexter fluvial systems, and the strike-oriented sands composing parts of the high-destructive delta system and the coastal barrier-strandplain (Lewisville) systems (fig. 80). Our study did not extend far enough into the basin to depict fully the depositional geometry of the Woodbine, but comparison of sand geometry and the orientation of these sands with the Woodbine outcrop allows a more complete understanding of various hydrologic properties. Of great importance is the fact that the outcropping sands of the Woodbine Formation are generally distal or marginal to the major depositional trends (fig. 81). Unlike the Hosston/Trinity and the Paluxy, the Woodbine does not have major dip-oriented, high permeability sand bodies that provide conduits for recharge from the outcrop areas in North-Central Texas into the deep subsurface. Instead, the marginal (strike-oriented) sands have a relatively limited areal extent.

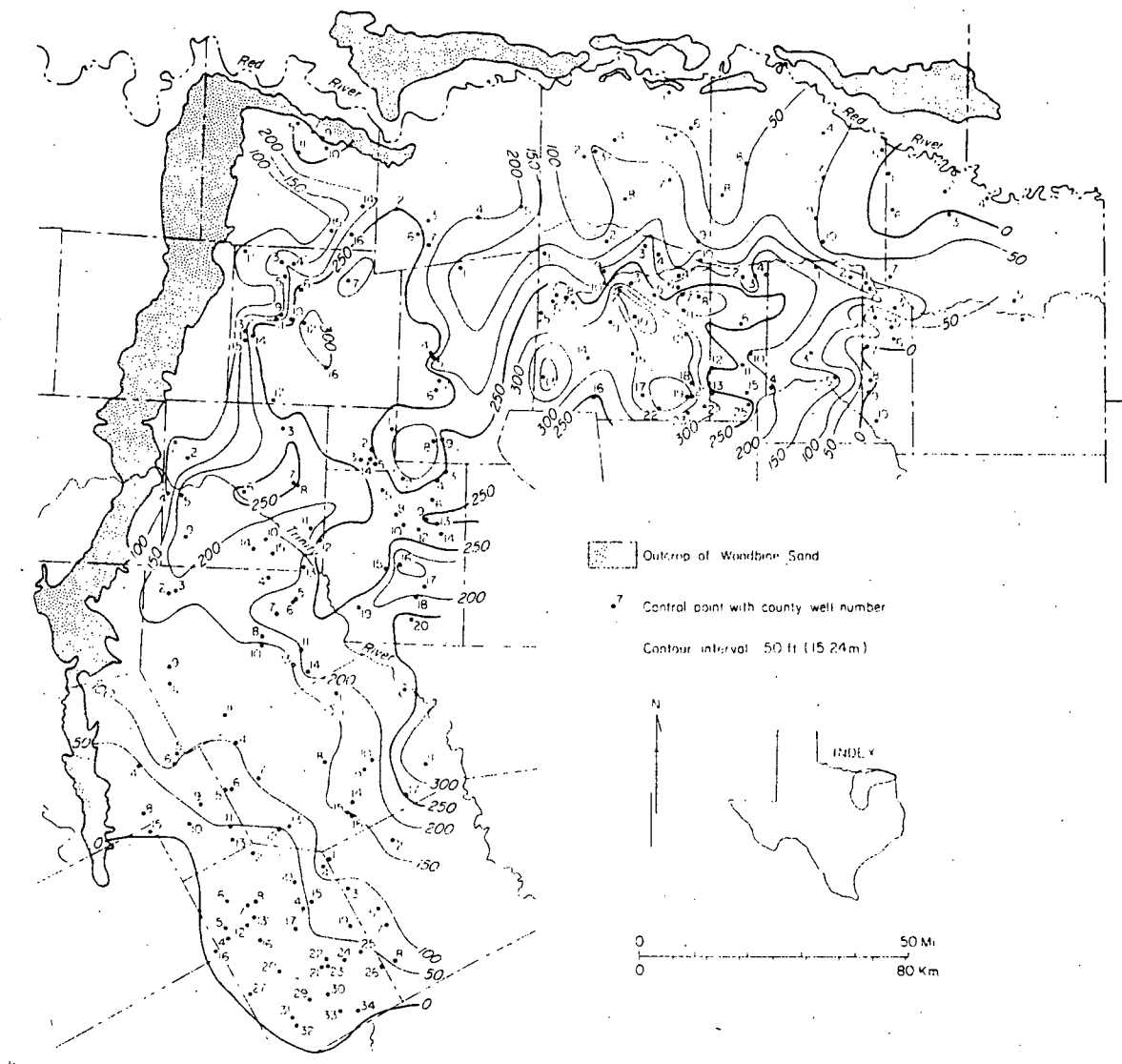


Figure 80. Net-sand thicknesses of the Woodbine.

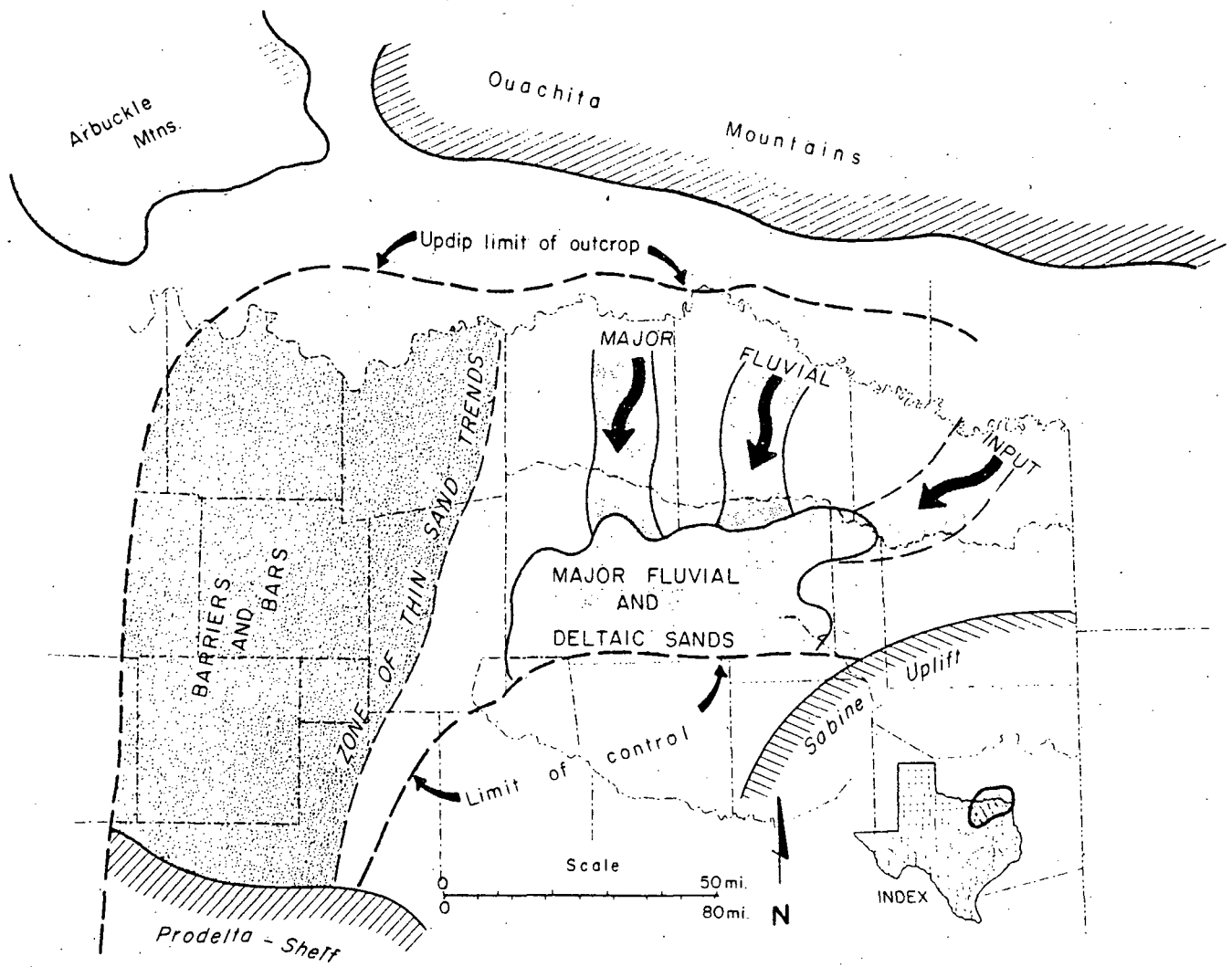


Figure 81. Schematic Woodbine paleogeographic map.

For this reason, aquifer properties there have (as expected) a high degree of lateral variability. Some dip-oriented sand trends provide conduits from the Woodbine outcrop in Oklahoma north of Lamar and Red River Counties, Texas; also there are major sediment feeder systems trending from the east, so that the major depositional trend appears to reflect the overall geometry of the subjacent fluvial deltaic systems of the Hosston/Trinity and the Paluxy. In all instances, the deltas debouched into an embayment with sediment derived mainly from the Ouachita Mountains to the north and from other sources to the east.

### Structural Configuration of the Woodbine

The structural configuration of the Woodbine is similar to those of the Hosston/Trinity and the Paluxy. The structure contours drawn on the top of the Woodbine Sand parallel the Woodbine outcrop, with dips generally increasing from the Texas Craton into the East Texas Basin (fig. 82). The strike of the Woodbine trends roughly north-south throughout most of Texas, but the same flexure zone as noted for other strata occurs in Grayson County, where the Woodbine outcrop and structure contours bend abruptly and parallel the Red River in an east-west trend. The Sherman Syncline and the Preston Anticline are both visible on the Woodbine map. The same general fault system noted on other horizons in North-Central and northeast Texas displace the Woodbine as well. Our structural map extends only over the areas having measurable sand strata within the Woodbine. And, although this structure map extends beyond the area in which potable water is produced from the Woodbine, it does not extend into the most distal parts of the deltaic systems in the north-central part of the East Texas Basin.

Regional dip on the Woodbine Sand south of the flexure zone ranges from approximately 35 ft/mi (7 m/km) in Johnson and Ellis Counties to a maximum of more than 175 ft/mi (33 m/km) in Hunt County. East of the flexure, dips range from approximately 40 ft/mi (8 m/km) in Lamar County to about 200 ft/mi (38 m/km) in Delta County. Rates of dip are generally somewhat less south of the Talco Fault Zone, being locally as little as 40 ft/mi (8 m/km) in Morris County. This decrease in dip is due to the effect of the Sabine Uplift, an important structural element during Woodbine deposition.

Geometry of faults that displace the Woodbine is almost identical to those affecting the Paluxy. Displacement of the Woodbine, however, is commonly somewhat less than the offset mapped for the Paluxy. The displacement mapped across the graben composing the Talco Fault Zone shows the Woodbine to have maximum up-to-

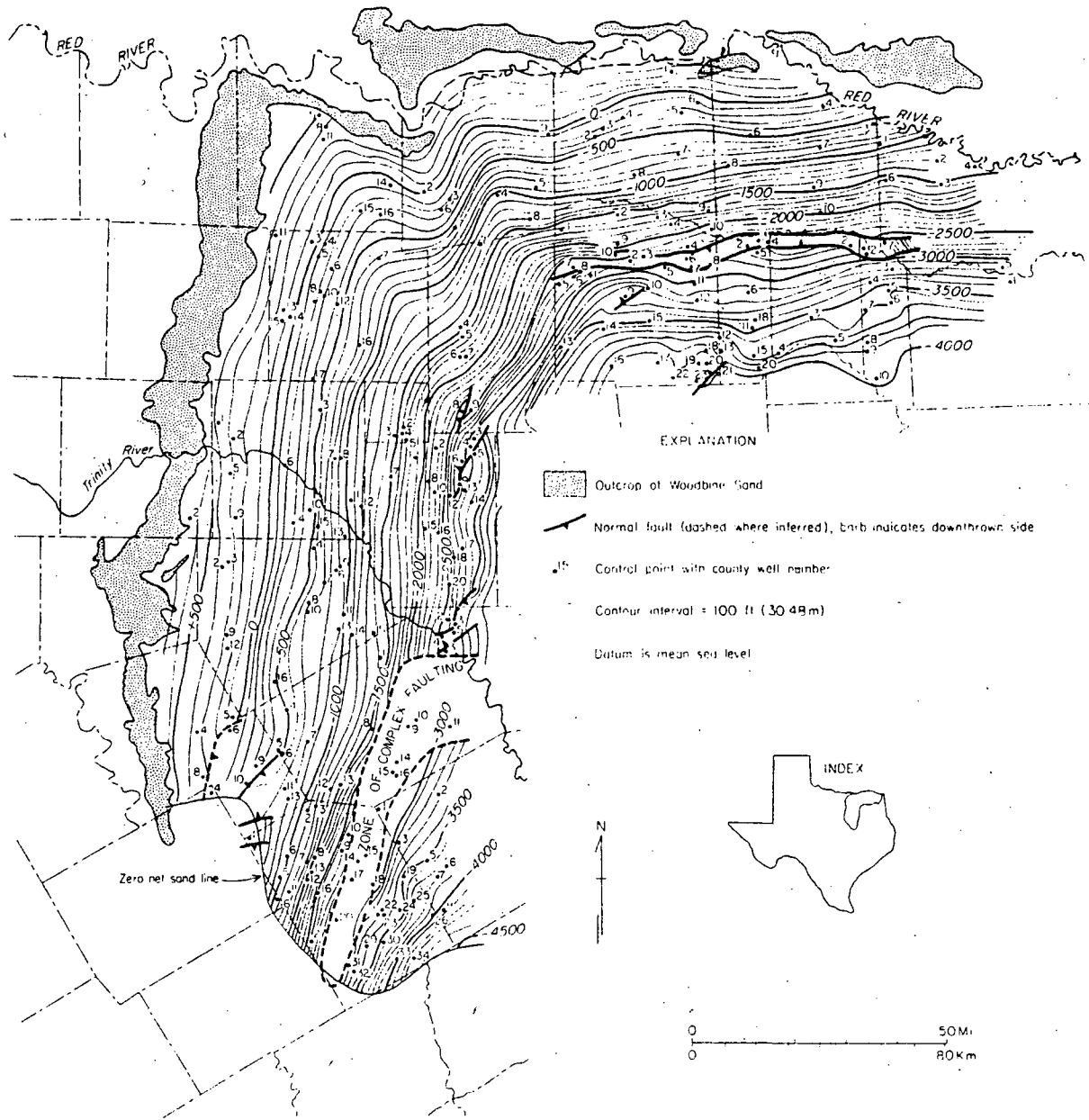


Figure 82. Structural configuration of the Woodbine.

the-coast displacement of 500 ft (150 m) in Titus and Morris Counties. Maximum down-to-the-coast displacement is approximately 700 ft (213 m) in Red River County. Usual net stratigraphic offset across this fault zone is 400 to 500 (120 to 150 m) in a down-to-the-coast direction compared to 600 to 800 ft (180 to 240 m) for the Paluxy. In the northern part of the Mexia Fault Zone, up-to-the-coast displacement of as much as 300 ft (90 m) is seen in Kaufman County. As with the other structural maps, fault displacement is not shown in the part of the Mexia Fault Zone lying within the central part of the study region; instead it is denoted as a "zone of complex faulting." Down-to-the-coast displacement of approximately 200 ft (60 m) occurs in Hill County in the northernmost extension of the Balcones Fault System.

#### General Aquifer Properties of the Woodbine

The Woodbine Sand yields potable water--and thus is an aquifer--from Hill and Navarro Counties, north to Cooke and Grayson Counties, and from there, east to Lamar County. As expected, most ground-water production occurs in the updip parts of the aquifer in areas closest to the outcrop (recharge zone). But as already mentioned in the context of net-sand distribution, the Woodbine outcrop represents environments marginal to the major depositional systems. That is, most of the Woodbine Sand in the updip areas near the outcrop is made up of marginal parts of strike-fed facies (probably strandplain and offshore bar deposits). Hence, unlike the Hosston/Trinity and the Paluxy Sands along the western margin of the East Texas Basin, there are no evident dip-oriented fluvial systems that trend normal to the outcrop strike. The major dip-oriented Woodbine Sands occur in Lamar County and farther east in Red River and Bowie Counties. Our data do not indicate that these fluvial and deltaic sands produce ground water; the easternmost ground-water production occurs near the zone of thin sands that trends northeast-southwest in Fannin, Lamar, and Hunt Counties and that delineates the boundary between fluvial-deltaic systems and the strandplain-barrier systems farther west.

#### Water Level of the Woodbine

The water level contours of the Woodbine Sand lie generally parallel to the structural contours of the formation (fig. 83), and the flexure zone where the structural trends change from a north-south to an east-west orientation is clearly evident on the water level map. South of the flexure, the water level surface generally dips basinward at about 12 ft/mi (2.3 m/km) compared with a minimum regional dip of approximately 35 ft/mi (7 m/km) there. East of the flexure the water

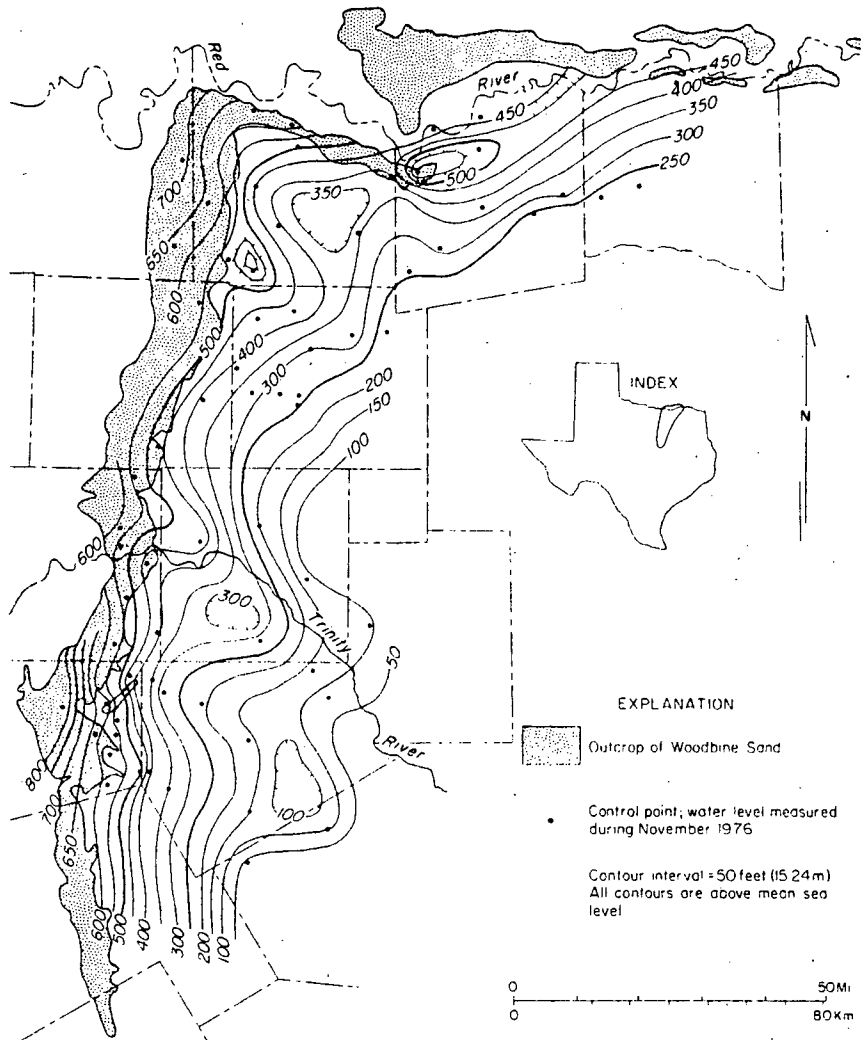


Figure 83. Water level contours for the Woodbine.



level is inclined southward at about 14 ft/mi (2.7 m/km) compared with structural dip there of approximately 80 ft/mi (15 m/km) in Lamar County. The Woodbine aquifer is clearly under artesian conditions throughout most of its extent, but there are numerous wells in the outcrop area and in the shallow subsurface that are apparently under water table conditions.

There is no consistent, region-wide relation between water level contours and sand trends, except in Ellis County where the sands thin abruptly in a southward direction. In that area there is a marked convergence of water level contours, indicating lower rate of ground-water flow; dip of the water level surface is almost 27 ft/mi (5 m/km) in Ellis County.

Unlike the relation between surface drainage network and water levels of the deeper aquifers studied (the Hosston/Trinity and the Paluxy), surface water drainage patterns clearly affect the ground-water level contours of the Woodbine. An elongate trend having a relatively high potentiometric surface occurs beneath the Trinity River in Dallas and Tarrant Counties. A similar high occurs beneath the East Fork Trinity River in Grayson and Collin Counties, and a local closure of water level contours occurs in Fannin County immediately south of the Red River. These relations suggest that, even though the aquifer is under artesian conditions, there is some recharge through confining beds from the major perennial streams overlying this aquifer.

Local areas of relatively low water-level surfaces are probably the result of well pumpage. Examples occur in southeastern Ellis County, in southern Dallas County, and in central Grayson County. In all instances, these "cones of depression" occur in an area of probable municipal or industrial withdrawal from the Woodbine.

#### Water Quality of the Woodbine

Water quality attributes of the Woodbine aquifer are indicated on the map that shows contoured isopleths of TDS values of selected water wells (fig. 84). This map shows two major trends with respect to water quality: (1) TDS values increase with increasing aquifer depth, and (2) TDS values decrease with increasing sand thickness. The relation between water quality and sand thickness is easily seen in eastern Dallas County and northeastern Collin County, where relatively low TDS content correlates geographically with thick sand bodies in those areas (see fig. 80). Conversely, a striking correlation between poor water quality and thin sand trends is evident in southern Grayson County and northern Collin County. The precipitous water-quality decline in southeastern Fannin County parallels contours denoting the zone of thin sands that separates the major Woodbine depositional systems. There is also an abrupt

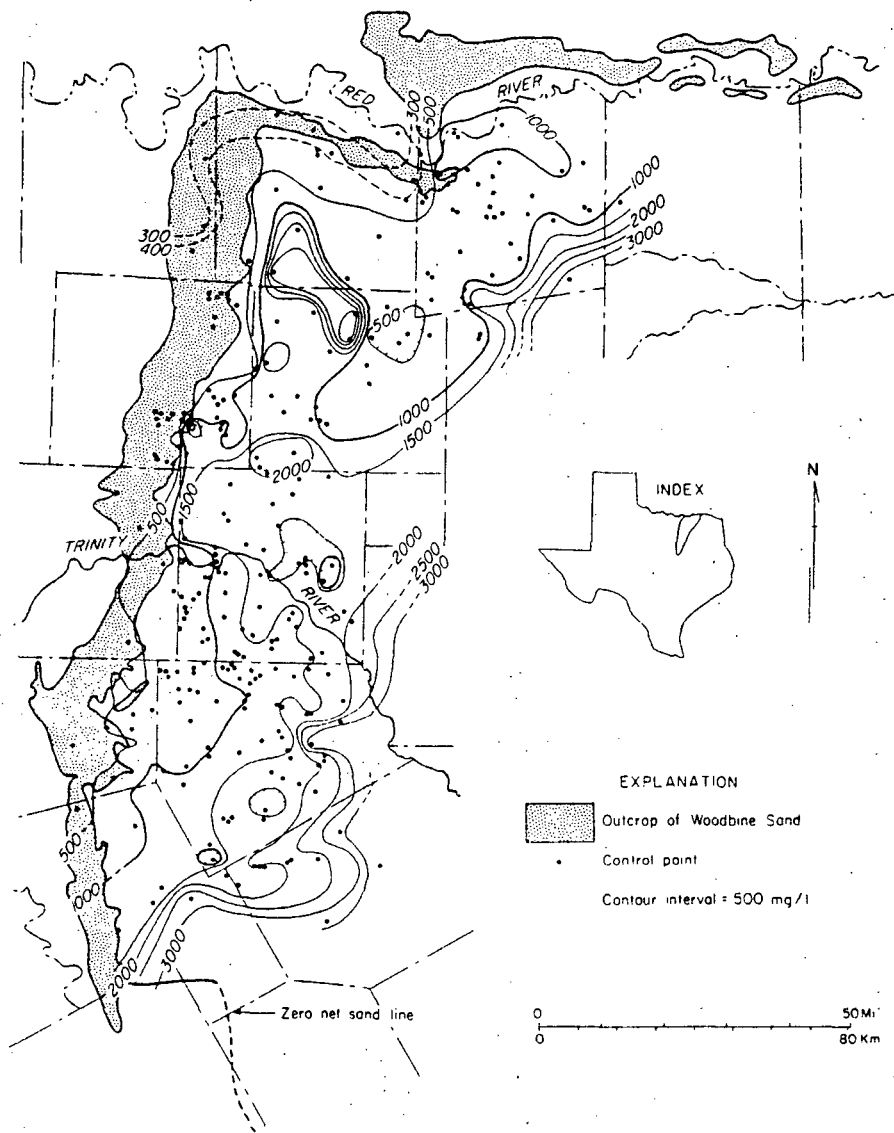


Figure 84. Total dissolved solids contours for Woodbine ground water.

total dissolved solids increase in Hill and Navarro Counties, near the southern limit of measurable sands in the Woodbine.

The relation between TDS and depth is graphically presented as a scattergram of all Woodbine water quality values available from the Texas Department of Water Resources computer files (fig. 85). This plot shows a considerable range in TDS values with respect to depth, and the general trend shows a somewhat higher rate of increase in TDS with depth compared with similar plots for the other aquifers investigated. The plot that compares water temperature with TDS (fig. 86) also shows a considerable amount of scatter, but, as with the Hosston/Trinity and Paluxy scattergrams, the TDS values are not extremely sensitive to changes in temperature. Still, for a given temperature increment, the increase (or amount of scatter) for TDS data is somewhat greater than for other aquifers.

#### Water Temperature of the Woodbine

Water temperature data for the Woodbine aquifer are sparse; moreover, the density of these data points is unevenly distributed. Thus, there are areas (indicated as dashed isopleths on figure 87) where water temperature values are inferred.

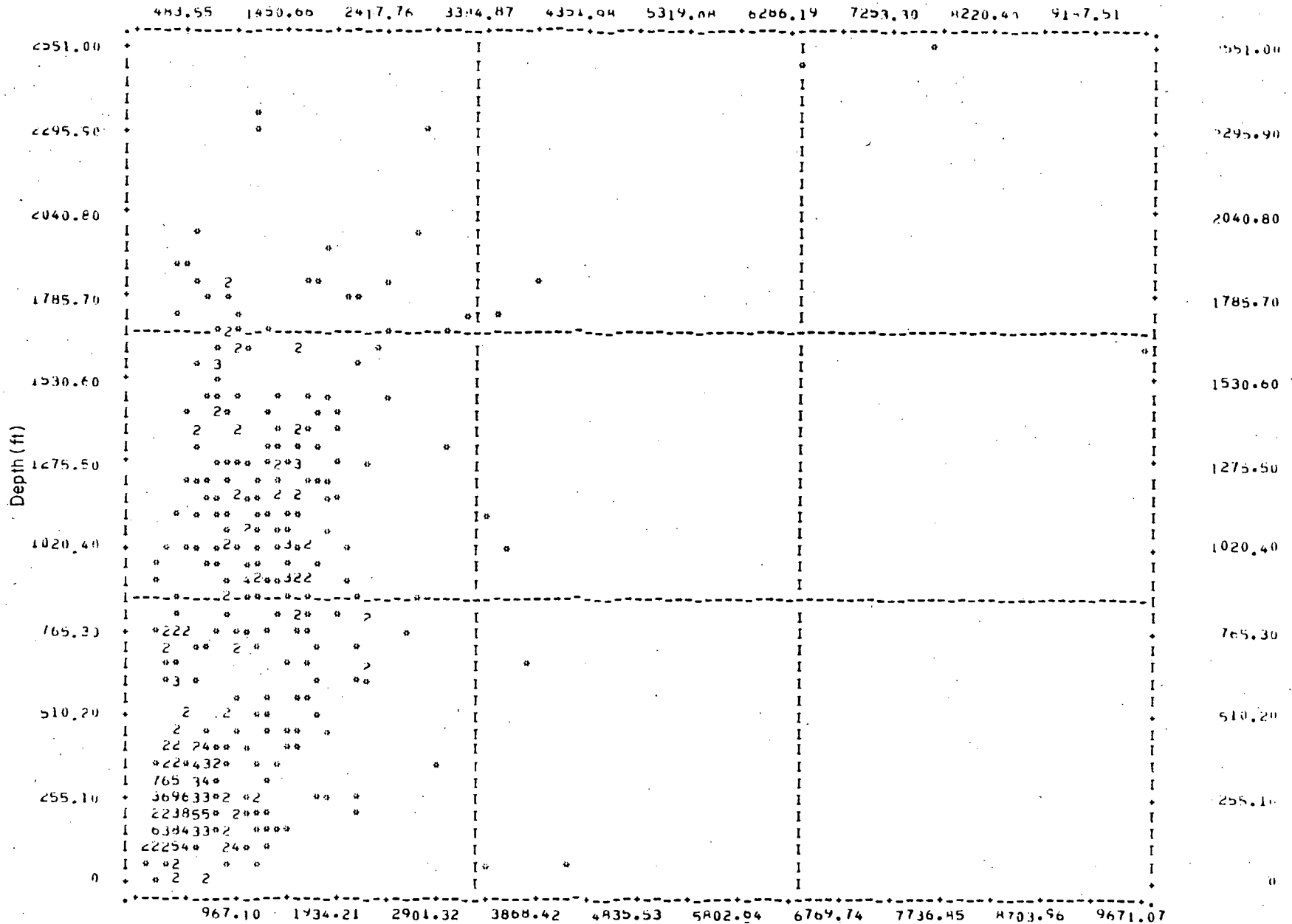
Temperatures of Woodbine ground water ranges from less than 70°F (21°C) near the outcrop, to a maximum of approximately 100°F (38°C) in Fannin County. As with water quality, there is a general trend of increasing water temperature with increasing aquifer depth.

Selective water temperature values for the Woodbine are plotted with respect to depth (fig. 88) and, as expected, the plot shows a positive correlation between temperature and depth. However, the plot of Woodbine temperature values shows considerably more scatter among data points than is seen for the other aquifers investigated. This scatter of values may result from the diverse facies that compose the Woodbine near its outcrop belt. It might also be due to mixing of waters from various stratigraphic horizons, or it might be a result of contamination from surface waters containing a high content of dissolved solids.

#### Geothermal Potential of the Woodbine

There are several towns in North-Central Texas that use ground water from the Woodbine aquifer for public water supply (table 3). However, most of these towns use water that contains dissolved solids in concentrations greater than 1,000 mg/l (fig. 89). The zone of optimum geothermal potential for Woodbine ground water, that is, where

TDS(mg/l)



PLOTTED VALUES -

445

EXCLUDED VALUES -

1

MISSING VALUES -

3

Figure 85. Total dissolved solids/depth scattergram for the Woodbine.

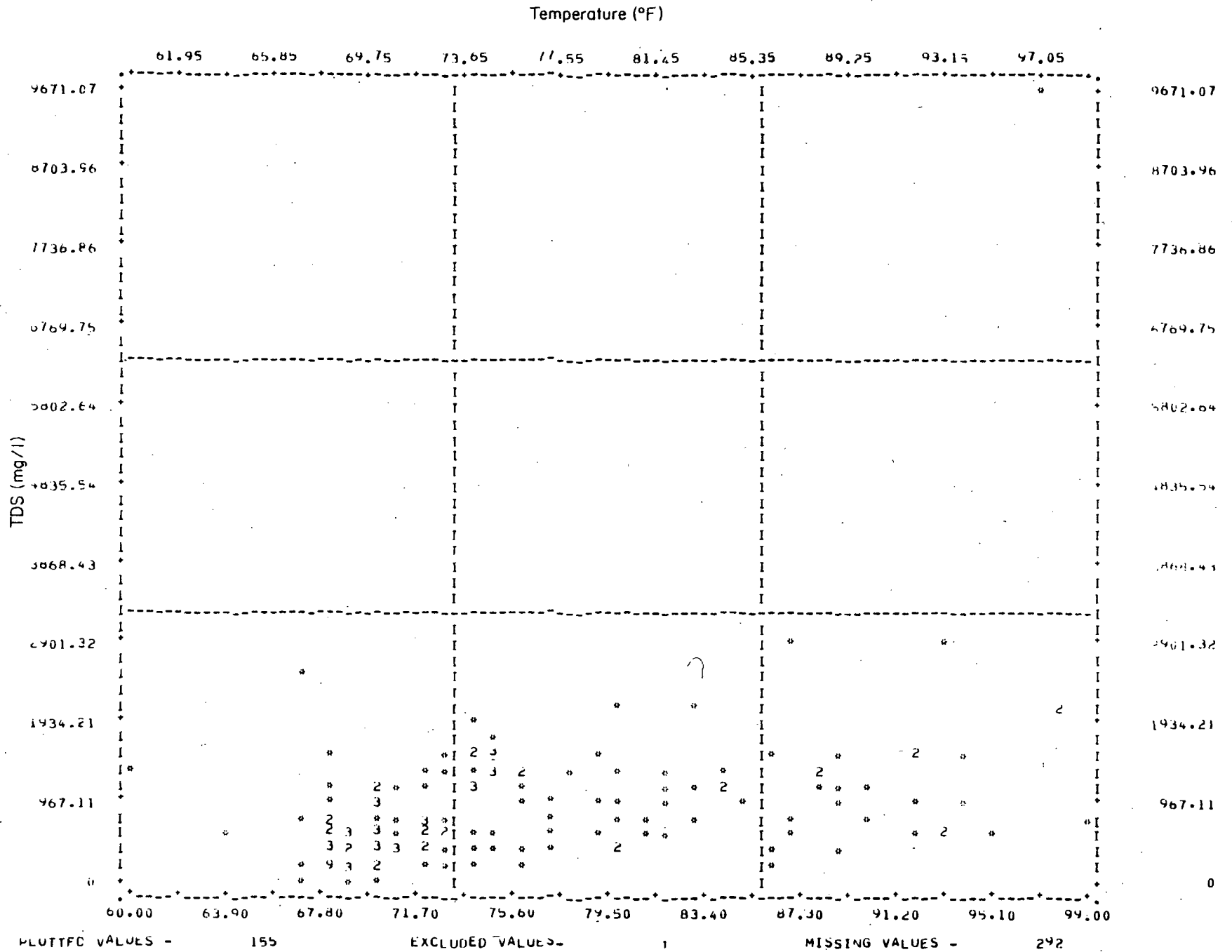


Figure 86. Temperature/total dissolved solids scattergram for the Woodbine.

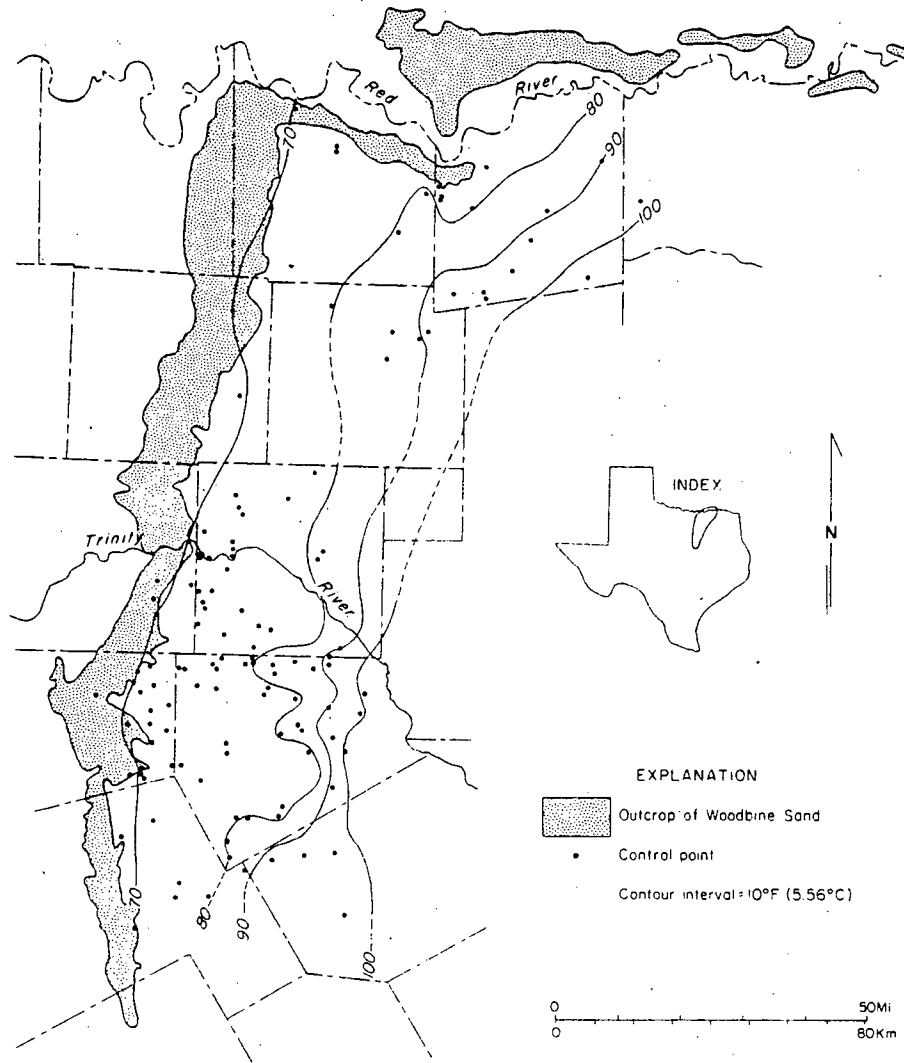
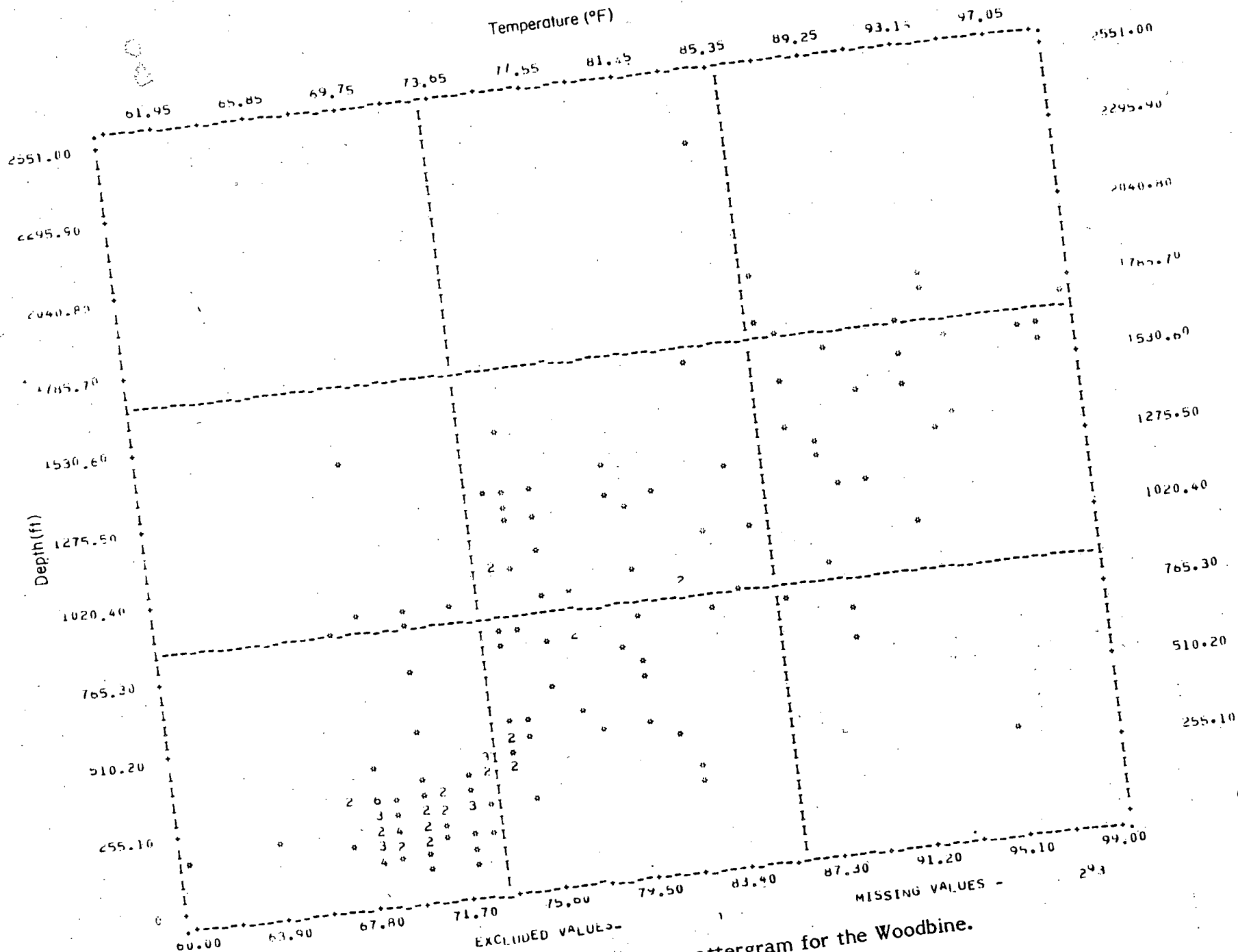


Figure 87. Water temperature contours for the Woodbine.

137



Temperature/depth scattergram for the Woodbine.

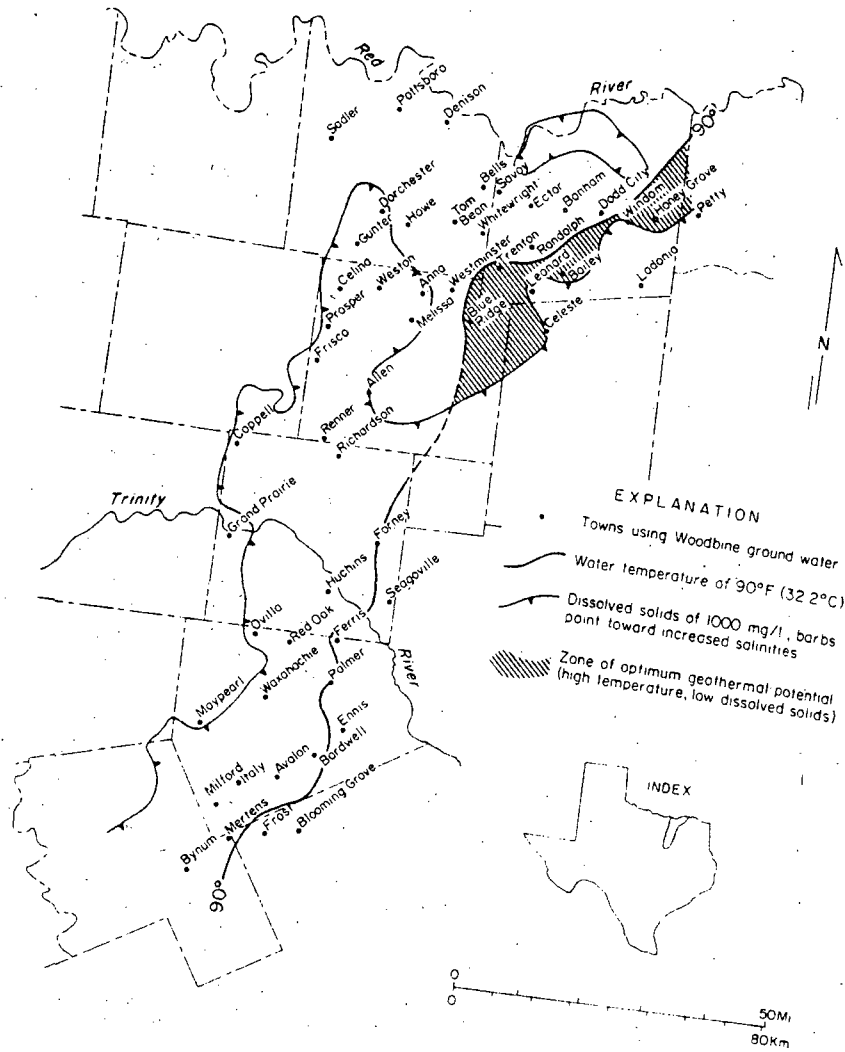


Figure 89. Municipalities using Woodbine ground water compared to areas of optimum geothermal potential.



Table 3. Selected municipal ground-water withdrawals--Woodbine aquifer  
(data from Texas Department of Water Resources).

County	Municipality	Mean January Pumpage (1972-1976)	Mean Yearly Pumpage (1972-1976)
Collin	Allen	5,806,400	73,170,200
Collin	Anna	1,684,333*	20,212,000
Collin	Blue Ridge	720,596	10,275,220
Collin	Celina <sup>⊕</sup>	3,445,420	44,923,840
Collin	Frisco <sup>⊕</sup>	7,540,000	102,232,000
Collin	Melissa	663,300*	13,346,340
Collin	Prosper	680,540	11,202,509
Collin	Renner	929,000*	11,148,000
Collin	Westminster	858,678	20,720,465
Collin	Weston	194,056	3,491,315
Dallas	Coppell <sup>⊕</sup>	3,847,733*	35,005,267*
Dallas	Seagoville <sup>+</sup>	2,548,250*	48,507,671
Dallas	Grand Prairie <sup>⊕</sup>	140,509,440	1,870,745,220
Dallas	Hutchins	7,114,020	79,342,180
Dallas	Mesquite	2,293,890	28,918,060
Dallas	Richardson	403,820	7,837,260
Ellis	Avalon	287,571*	3,450,850*
Ellis	Bardwell	457,846	6,060,783
Ellis	Waxahachie	998,063	14,388,541
Ellis	Ennis	700,000*	10,900,000*
Ellis	Ferris	5,388,800	70,093,000
Ellis	Italy	2,337,300	32,642,500
Ellis	Maypearl	595,000	7,301,000
Ellis	Milford	1,426,000	21,246,860
Ellis	Ovilla	600,450	8,457,860
Ellis	Palmer	3,843,040	50,342,220
Ellis	Red Oak	1,853,148	26,017,240
Fannin	Bailey	189,625*	5,590,460
Fannin	Bonham	20,622,000*	312,722,000*
Fannin	Dodd City	334,300	4,053,000
Fannin	Ector	668,500*	9,147,750*
Fannin	Honey Grove	6,734,000	85,706,800
Fannin	Ladonia <sup>+</sup>	1,496,000*	28,226,750
Fannin	Leonard	4,419,320	54,397,940
Fannin	Randolph	205,464	2,736,300
Fannin	Savoy	2,009,400	25,848,000
Fannin	Trenton	2,238,980	24,555,690
Fannin	Windom	331,400*	4,090,800

- \* indicates less than 5 years of measurements
- ⊕ draws from both Hosston/Trinity and Woodbine aquifers
- + draws from both Paluxy and Woodbine aquifers

Table 3 (cont'd)

County	Municipality	Mean January Pumpage (1972-1976)	Mean Yearly Pumpage (1972-1976)
Grayson	Bells	2,118,820	26,167,640
Grayson	Denison	2,763,379	34,458,032
Grayson	Gunter	2,060,600	26,200,000
Grayson	Howe	5,661,860	72,847,144
Grayson	Pottsboro	1,104,648*	14,549,033
Grayson	Sadler	445,450*	6,750,475*
Grayson	Tom Bean	1,695,228	22,173,377
Grayson	Van Alstyne	3,457,918	40,734,162
Hill	Whitewright	5,974,100	77,170,872
Hill	Bynum	197,067*	2,364,800
Hill	Itasca <sup>⊕</sup>	6,124,600	90,406,484
Hunt	Mertens	180,000*	4,239,300
Lamar	Celeste	174,420	22,021,520
Navarro	Petty	385,020	5,071,120
Navarro	Blooming Grove	2,029,302*	21,173,130
	Frost	1,500,000*	18,000,000

\* indicates less than 5 years of measurements  
<sup>⊕</sup> draws from both Hosston/Trinity and Woodbine aquifers  
+ draws from both Paluxy and Woodbine aquifers

TDS values are less than 1,000 mg/l and water temperature is greater than 90° F (32° C), occurs only within a narrow zone in Collin, Fannin, and Hunt Counties.

Within the "optimum zone" the town of Blue Ridge during January pumps an average of 720,596 gal (2,727,672 l) of water at 93° F (34° C) from 385 ft (117.4m). The energy expended in obtaining this water during an "average" January equals  $2.97 \times 10^6$  Btu ( $7.5 \times 10^5$  kg-cal), and the heat value of the water consumed equals  $4.16 \times 10^7$  Btu ( $1.05 \times 10^7$  kg-cal). The net energy gain of  $3.8 \times 10^7$  Btu ( $9.6 \times 10^6$  kg-cal) is worth only \$95, assuming a (conservative) dollar value per Btu of  $\$2.5 \times 10^{-6}$ . As mentioned in the context of the other geothermal aquifers, this caloric asset is a maximum value; it does not account for heat-exchange efficiencies or other factors that result in a loss of energy. Nonetheless, this warm water is presently consumed regardless of its energy values, and people should be aware of its potential.

Despite elevated TDS concentrations, ground water produced from the other towns that lie outside the optimum geothermal zone still has a potential for supplying warm water for space heating and other purposes. For example, a current project is underway to obtain 126° F (52° C) water from a depth of approximately 2,200 ft (670 m) at Corsicana in Navarro County. The dissolved solids content of this water is roughly 5,000 mg/l, but the water is to be used solely for its heat content and not for drinking purposes. When a heat exchange system is employed, the water need not meet drinking-quality standards. But in these instances the heat value alone must justify drilling the well and pumping the water. The many towns that presently use high-TDS Woodbine ground water for drinking and for other purposes as well; this results in an added credit in terms of amortizing drilling and pumping costs.

The area not presently tapped for water supply but which is of greatest future potential for producing geothermal ground waters from the Woodbine is in Hopkins County along the thick sand trends that make up the fluvial and deltaic systems there. These sands are deep enough (greater than 3,000 ft, or 915 m) to have elevated water temperatures comparable to those of the deep parts of the Hosston aquifer in Central Texas. But despite the depth, the orientation of sand trends indicates that there might be direct hydrologic communication with the Woodbine outcrop (recharge area) approximately 50 mi (80 km) to the north. Similar thick sand bodies occur in Franklin, Titus, and Morris Counties; these areas also warrant study for their geothermal resource potential.

## CONCLUSIONS

The area delineated by the Balcones and Luling-Mexia-Talco Fault Zones is a low-grade geothermal province. It is denoted by a convergence of structural and stratigraphic features that define a major tectonic hinge zone. The normal faults expressed at the surface form a graben across part of the region, and these surface structures are superjacent to the buried Ouachita structural belt. The Ouachita belt contains zones of thrust faulting and progressively higher grades of metamorphism as dip increases precipitously into the Gulf Coast Basin. The Jurassic subcrop begins near the downdip extent of recognizable Paleozoic rocks, and this indicates that the hinge zone delineates one locus of initial rifting of the Gulf of Mexico.

The Balcones/Ouachita structural trend is an area of anomalously high geothermal gradient, and there several aquifers contain waters with elevated temperatures. The source of this heat is conjectural, but it may be a result of (1) deep circulation of meteoric waters along faults, (2) upwelling of connate waters from the deep subsurface, either from deformed Ouachita rocks or from Jurassic strata, (3) stagnation of deep ground waters owing to faults that retard circulation, (4) local hot spots, such as high radiogenic heat sources (felsic plutons) within the basement complex, or (5) other loci of high heat flow.

Of the various aquifer systems that we initially recognized as yielding ground water in Central Texas, the Hosston/Trinity Sands show the most promise as a geothermal resource. These sands occur across the largest area and exhibit some of the best developed fluvial and deltaic trends of any aquifer investigated during this project. The Hosston/Trinity strata are extensively faulted in the Balcones and Luling-Mexia-Talco Fault Zones, and most displacement occurs in a down-to-the-coast direction. The Hosston/Trinity occurs directly above much of the Ouachita structural belt, and farther downdip these sands are in contact with (and are locally indistinguishable from) underlying Jurassic strata. Hence, because of downfaulting and because the Hosston/Trinity compose the basal Cretaceous sands, these aquifers occur at greater depths than others studied. All of these attributes--areal extent, sand geometry, faulting, stratigraphic position--have contributed to the geothermal potential of the Hosston/Trinity. Geographic extent and orientation of sand trends combine to mediate such aquifer properties as sustainable well yield and water quality, whereas depth and structural configuration enhance the elevated temperature of ground water. In sum, a combination of factors, some fortuitous, some interrelated, has resulted in

aquifer systems that yield a large amount of potable water at temperatures that are locally high with respect to aquifer depth. Moreover, these warm-water-bearing strata occur beneath one of the major population trends in Texas, and the many institutions and other energy consumers along the Balcones-Blackland belt constitute a large potential market for the low-temperature geothermal waters.

Of the other Cretaceous aquifers investigated, only the Paluxy and Woodbine Sands show promise for multiple use. That is, these warm-water-bearing sands, also yield enough water to supply domestic, municipal, and industrial needs and have water quality suitable for drinking. In both instances, however, the heat content is less in comparison with the Hosston/Trinity, and commonly, the dissolved solids content of the Paluxy and Woodbine is higher than that of the deeper basal Cretaceous sands. Excluding use of the water for human consumption, deep reaches of these aquifers show further promise as geothermal resources. Thick deltaic sands occur deep beneath the Talco Fault Zone in northeast Texas. These sands should possess hydrologic properties conducive to high well yields, yet they are deep enough to have some of the highest water temperatures of any within the study region. However, dissolved solids content will probably also be high, and the exact composition of solutes within these waters must be tested to ascertain the engineering problems associated with the operation of heat-exchange systems.

The other two aquifers, the Hensel Sand and the Edwards Limestone, do not appear promising as geothermal resources. The Hensel is unacceptably limited in its downdip extent because of facies changes; sand deposits end and lime or mud deposits begin in the very areas where the aquifer is deep enough to consistently possess elevated water temperatures. The Edwards Limestone is sufficiently hot in its "bad-water zone" to serve as a low-temperature geothermal resource, but water quality attributes there pose severe problems. Much of this deep Edwards water is a hydrothermal brine, and locally, fluorite is precipitating and clogging well bores. These geochemical attributes are intriguing in context of economic geology, but they pose problems for design of a heat exchange system. For multiple use for providing energy and drinking water the Edwards might have potential in its phreatic zone, where large volumes of water at less than 75° F (24° C) supply a population of more than one million people. This resource, however, demands an altogether different kind of technology (a ground-water heat pump that extracts heat from the air during summer and from the water during winter), hence the hydrogeologic and climatic assessments are entirely different from those presented here. That avenue, however, does have potential that warrants further study.

## REFERENCES

- Abbott, P. L., 1974, Calcitization of Edwards Group dolomites in the Balcones Fault Zone aquifer, south-central Texas: *Geology*, v. 2, no. 7, p. 356-362.
- , 1975, On the hydrology of the Edwards Limestone, south-central Texas: *Journal of Hydrology*, v. 24, no. 3/4, p. 251-269.
- Allen, P. M., 1975, Urban geology of the Interstate Highway 35 growth corridor from Hillsboro to Dallas County, Texas: Waco, Baylor Geological Studies Bulletin 28, 36 p.
- Arbingast, S. A., Kennamer, L. G., Ryan, R. H., Buchanan, J. R., Hezlep, W. L., Ellis, L. T., Jordan, T. G., Granger, C. T., and Zlatkovich, C. P., 1976, *Atlas of Texas: The University of Texas at Austin, Bureau of Business Research*, 179 p.
- Baldwin, E. E., 1974, Urban geology of the Interstate Highway 35 growth corridor between Belton and Hillsboro, Texas: Waco, Baylor Geological Studies Bulletin 27, 39 p.
- Bebout, D. G., and Loucks, R. G., 1974, Stuart City Trend, Lower Cretaceous, South Texas: The University of Texas at Austin, Bureau of Economic Geology Report of Investigations 78, 80 p.
- Bebout, D. G., 1977, Sligo and Hosston depositional patterns, subsurface of South Texas, in D. G. Bebout and R. G. Loucks (eds.), *Cretaceous carbonates of Texas and Mexico, applications to subsurface exploration: The University of Texas at Austin, Bureau of Economic Geology Report of Investigations 89*, p. 79-96.
- Bedinger, M. S., Pearson, F. J., Reed, J. E., Sniegocki, R. T., and Stone, C. G., 1974, The waters of Hot Springs National Park, Arkansas--their origin, nature, and management: United States Geological Survey, Open File Report, 102 p.
- Caughey, C. A., 1977, Depositional systems in the Paluxy Formation (Lower Cretaceous), northeast Texas--oil, gas, and ground-water resources: The University of Texas at Austin, Bureau of Economic Geology Circular 77-8, 59 p.
- Fisher, W. L., and Rodda, P. U., 1967, Lower Cretaceous sands of Texas: Stratigraphy and resources: The University of Texas at Austin, Bureau of Economic Geology Report of Investigations 59, 116 p.
- Fisher, W. L., Brown, L. F., Jr., Scott, A. J., and McGowen, J. H., 1969, Delta systems in the exploration for oil and gas, a research colloquium: The University of Texas at Austin, Bureau of Economic Geology Special Publication, 212 p.
- Flawn, P. T., Goldstein, August, Jr., King, P. B., and Weaver, C. E., 1961, The Ouachita System: Austin, The University of Texas Publication 6120, 401 p.
- Geiser, P. A., 1979, Field trip guide to selected thermal springs of western Virginia symposium on geothermal energy and its direct uses in the eastern United States: Geothermal Resources Council, 6 p.

- Hall, W. D., 1976, Hydrologic significance of depositional systems and facies in Lower Cretaceous sandstones, North-Central Texas: The University of Texas at Austin, Bureau of Economic Geology Geological Circular 76-1, 29 p.
- Hayward, C. T., 1978, Structural evolution of Waco region: Waco, Baylor Geological Studies Bulletin 34, 39 p.
- Hayward, O. T., Font, R. G., Brigham, M. S., Charvat, W. A., Corwin, R. V., Hazelwood, R. H., Knapp, R. M., and McKnight, C. S., 1979, The geothermal potential of the Cretaceous aquifers of Central Texas, unpublished report, 79 p.
- Hem, J. D., 1970, Study and interpretation of the chemical characteristics of natural waters: United States Geological Survey Water-Supply Paper 1473, 358 p.
- Henningsen, E. R., 1962, Water diagenesis in Lower Cretaceous Trinity aquifers of Central Texas: Waco, Baylor Geological Studies Bulletin 3, 37 p.
- Hill, R. T., 1901, Geography and geology of the black and grand prairies, Texas: United States Geological Survey, 21st Annual Report, Part VII, 646 p.
- Klemt, W. B., Perkins, R. D., and Alvarez, H. J., 1975, Ground-water resources of part of Central Texas with emphasis on the Antlers and Travis Peak Formations: Texas Water Development Board Report 195, 63 p.
- Loucks, R. G., 1976, Pearsall Formation, Lower Cretaceous, South Texas--depositional facies and carbonate diagenesis and their relationship to porosity: The University of Texas at Austin, unpublished Ph.D. dissertation, 362 p.
- Loucks, R. G., 1977, Porosity development and distribution in shoal-water carbonate complexes--subsurface Pearsall Formation (Lower Cretaceous) South Texas, in D. G. Bebout and R. G. Loucks, (eds.), Cretaceous carbonates of Texas and Mexico--applications to subsurface exploration: The University of Texas at Austin, Bureau of Economic Geology Report of Investigations 89, p. 97-125.
- Oliver, W. B., 1971, Depositional systems in the Woodbine Formation (Upper Cretaceous), northeast Texas: The University of Texas at Austin, Bureau of Economic Geology Report of Investigations 73, 28 p.
- Plummer, F. B., and Sargent, E. C., 1931, Underground waters and subsurface temperatures of the Woodbine Sand in northeast Texas: Austin, University of Texas Bulletin 3138, 175 p.
- Rose, P. R., 1972, Edwards Group, surface and subsurface, Central Texas: The University of Texas at Austin, Bureau of Economic Geology Report of Investigation 74, 198 p.
- Sellards, E. H., and Hendricks, Leo, 1946, Structural map of Texas: Austin, University of Texas, Bureau of Economic Geology Map, Scale 1:500,000.
- ricklin, F. L., Smith, C. I. and Lozo, F. E., 1971, Stratigraphy of Lower Cretaceous Trinity deposits of Central Texas: The University of Texas at Austin, Bureau of Economic Geology Report of Investigations 71, 61 p.